A REINTERPRETATION OF REGIONAL SEISMIC SURVEYS IN NORTHERN ONTARIO AND EASTERN MANITOBA BETWEEN DISTANCES OF 127 KILOMETERS AND 775 KILOMETERS USING SEISMIC MODEL STUDIES OF THE CRUST AND UPPER MANTLE

A Thesis Presented to the
Faculty of Graduate Studies and Research
of
The University of Manitoba

In partial fulfillment
of the requirements for the degree
Master of Science

by
Ralph John Desmarais
May, 1976

"A REINTERPRETATION OF REGIONAL SEISMIC SURVEYS IN NORTHERN ONTARIO AND EASTERN MANITOBA BETWEEN DISTANCES OF 127 KILOMETERS AND 775 KILOMETERS USING SEISMIC MODEL STUDIES OF THE CRUST AND UPPER MANTLE"

by

RALPH JOHN DESMARAIS

A dissertation submitted to the Faculty of Graduate Studies of the University of Manitoba in partial fulfillment of the requirements of the degree of

MASTER OF SCIENCE

TABLE OF CONTENTS

LIST OF TABLES

LIST OF FIGURES

ABSTRACT

Regional seismic refraction and wide-angle reflection surveys conducted in Manitoba and northern Ontario in recent years have resulted in similar but differing interpretations of structure in the Earth's crust and upper mantle. The present work was an attempt to determine, from a modelling study of the kinematic and amplitude characteristics of compressional reflected and refracted waves propagating in a spherically stratified earth, those events bottoming in the Earth's crust and upper mantle which would be most prominent on seismic records and the optimum range of observation distances at which the arrivals of these events could be observed.

It was found that the existence of positive vertical velocity gradients in a crustal layer would severely reduce the maximum observation distance of primary events bottoming in this layer. The loci of arrival-times versus distance of refracted and reflected waves bottoming in the same crustal layer were also found to converge with increasing distance thereby complicating resolution of the two events beyond certain distances. One class of reflection multiples was shown to produce events kinematically similar to primary reflections which could be misinterpreted for

the latter.

The model results were then used to re-interpret the seismic data derived from a short range (127-351 km.) survey by Hall and Hajnal in 1967-69 and a long range (427-775 km.) survey obtained by Gurbuz in 1966 which had resulted in conflicting interpretations.

The two data sets were found to conform to a single consistent crustal model, 34 km. in thickness, having an intermediate discontinuity at 18 km. with constant velocities of 6.05 km/sec. and 6.99 km/sec. respectively above and below the discontinuity. Both surveys led to the interpretation of a first-order discontinuity in the upper mantle at a depth of 50 km. with a compressional velocity of 8.17 km/sec. above the discontinuity. No unique compressional velocity was obtained for the layer below this interface. This may be attributable to lateral velocity variations over the survey area.

ACKNOWLEDGEMENTS

I wish to express my gratitude to Dr. D.H. Hall for his many helpful discussions. His guidance and direction were invaluable to the completion of this endeavour.

I am indebted to Dr. R.F. Mereu for allowing me the use of his computer program XTAMP written by him.

I would also like to thank Mr. M. Bonten for his assistance in drafting the diagrams.

Finally, I wish to thank Ms. K. Cohen for her long work in the preparation and typing of this manuscript and for her continuing support throughout this project.

INTRODUCTION

Since 1961, a number of seismic surveys have been conducted by the University of Manitoba Crustal Studies Group for the purpose of investigating crustal structure in the Churchill and Superior geologic provinces within Manitoba and Northern Ontario. A review of the published results from these surveys has been given by Hall and Hajnal (1973) together with the introduction and a preliminary interpretation of 24 new recordings made between 1967 and 1969.

The energy for these surveys was initiated by underwater explosions and recordings were made using a 12-detector one mile spread and analog tape recording. A complete description of the seismic instrumentation used by the group is given by Hajnal (1970).

With the exception of a long range refraction survey, which was part of Project Early Rise (Gurbuz, 1969, 1970), all of the work has led to an average crustal model containing two layers with bottom depths of 18.25 ± 4.8 km. and 34.28 ± 2.8 km. having constant compressional wave velocities of 6.05 ± 0.05 km./sec. and 6.85 ± 0.05 km./sec. respectively. This horizontally stratified model is based primarily on the travel times of identified primary wide-angle reflections and head waves with confirmation of depths obtained by the converted (head) wave method (Hall, 1966; Hall and Hajnal, 1969).

Gurbuz inferred a three layer, horizontally stratified

crustal model from the travel times of wide angle reflections and primary and converted head waves, whose identifications were supported by spectral amplitude ratios and phase angle spectra. The derived model has layer depths of 18 ± 3 km., 25.5 ± 3.5 km. and 34 ± 3 km. with P-wave velocities of 6.11 ± 0.01 km./sec., 6.81 ± 0.08 km./sec. and 7.10 ± 0.04 km./sec. Both Gurbuz and Hall and Hajnal report a velocity of 7.90 ± 0.05 km./sec. below the Mohorovicic discontinuity at the base of the crust.

A sub-Moho interface was also hypothesized by Gurbuz on the evidence of a primary reflection P_m and a head wave P_n, critically refracted at 46 km. and propagating below this discontinuity at an average velocity of 8.48 km./sec. As a result of this hypothesis, Hajnal's short range (110 km. - 156 km.) continuous refraction profile work was reexamined and events P_m and P_n were found on these records also, yielding a similar depth and velocity. These two events were also tentatively picked on recordings from the above mentioned 1967-69 mid-range regional survey.

The objective of the present thesis is threefold:

1. To investigate further the possibility of identifying events from an upper mantle discontinuity for distances comprising the range of existing deep crustal seismic records.

2. To determine, from a computer predictive modelling approach, those seismic events bottoming in the crust and upper mantle which would theoretically be most prominent on

a seismic trace and an optimum range of distances for which these events would be clearly distinguishable from one another. This knowledge of optimum shot point-receiver distances could be used when planning future refraction surveys to refine crustal and upper mantle structure.

3. Before the first problem can be approached, it is necessary to reconcile the apparently conflicting interpretations of two and three layer crustal models. The fact that Gurbuz does not report a reflection from the second layer at 25.5 km. has led to the suggestion (Hall and Hajnal, 1973) that a gradual increase in velocity with depth may take place between 18 km. and 34 km. and that this possibility may be consistent with both models. A two layer model containing a positive velocity gradient in the lower layer is therefore also considered in the following sections. In addition it has been found (Mereu, 1967; Mereu and Hunter 1969) that when the depth of a refractor exceeds 10 km., the effect of earth curvature becomes significant. Spherically stratified earth models have therefore been employed in the theoretical studies.

CHAPTER 1

DESCRIPTION OF CRUSTAL MODELS

It was recognized that an examination of the theoretical travel times and vertical amplitudes of seismic events associated with the two and three layer crustal models proposed in recent years is necessary. Figures 1a and b illustrate these two models and the ray paths of the compressional reflected and refracted waves produced in each. Model A contains a first order (Intermediate) discontinuity at 18 km. between the surface and the Mohorovicic discontinuity (34 km.) at the crustal base. Model B contains an additional first order discontinuity at 25.5 km. In an attempt to reconcile the conflicting interpretations, Model C (Figure 1), similar to Model A but containing a positive velocity gradient b 0 in the lower layer, is also considered.

The following designation of compressional wave events will be used throughout this study:

For a two layer crust

- P1, P3, P5, etc. refer to <u>refracted</u> waves bottoming in the 1st, 2nd, and 3rd layer respectively.

- P2, P4, P6, etc. refer to <u>reflected</u> waves bottoming in the 1st, 2nd, and 3rd layer respectively.

-P2m, P4m, P6m, etc. are ray paths of waves which bottom and are multiply reflected once within the 1st, 2nd and 3rd layer, respectively.

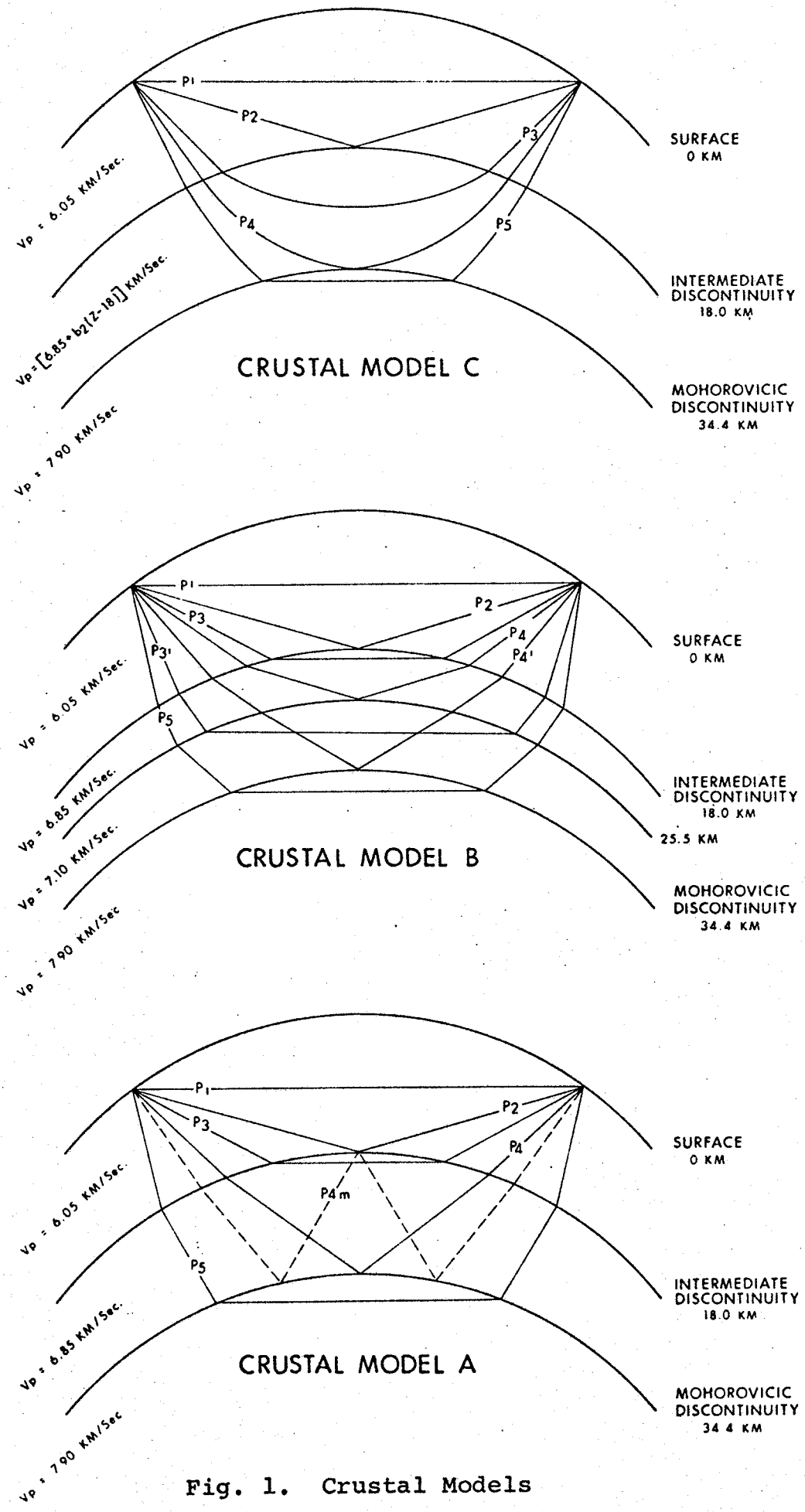

Fig. 1. Crustal Models

For a three layer crust

- the same notation as above will be used; events bottoming in the extra crustal layer, however, will be denoted by P3', P4', etc. (Figure 1 -Model C).

The refracted (body) waves existing in a spherical medium, unlike critically refracted (head) waves which propagate along the top of a constant-velocity layer, penetrate the bottoming layer to a depth dependent on the ray parameter p. As p decreases, the depth of bottoming Z_B and epicentral distance X increase for a refracted ray. The theory of head waves (Cf. Cerveny, 1967), based of the assumption of small distances over which earth curvature is negligible, has not been extended to account for interface curvature. A discussion on the amplitude and travel time characteristics of head waves versus those of body waves is given in Section 1.3.

1.1 Theoretical Time-Distance Curves

A computer program XTAMP (Appendix VII), written by R.F. Mereu, was used to calculate the theoretical travel times of primary events for a range of distances from 0-800 km. The program is based on a numerical solution by Stewart (1968) of the parametric integral equations given by Bullen (1963) for a ray travelling in a spherically stratified earth.

The following aspects of the travel time curves (Figures 2a-d) are common to all three crustal models:

(a) Because of the curvature imposed on the layer

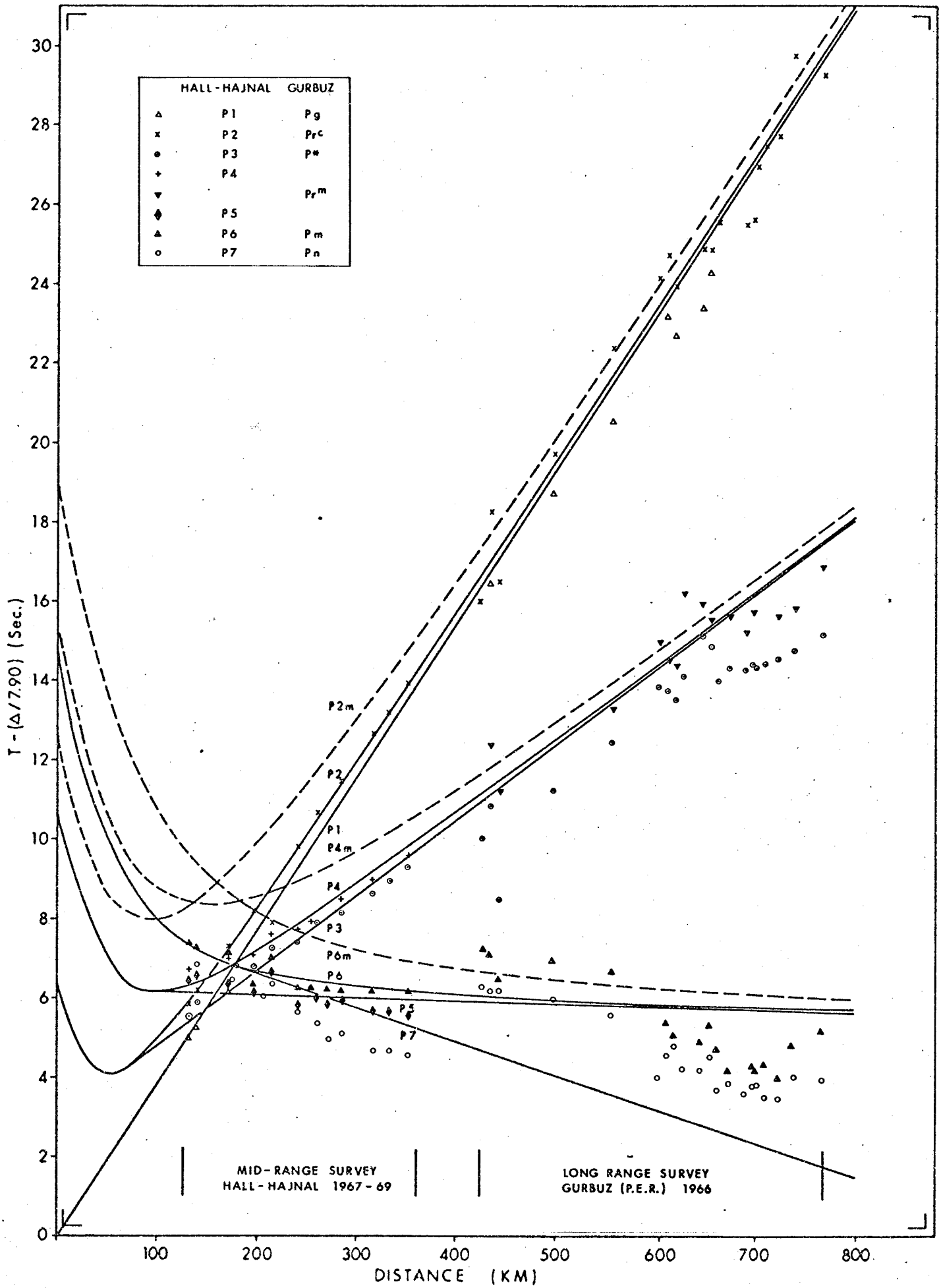

Fig. 2a. Crustal Model A (with upper mantle model 1.1)

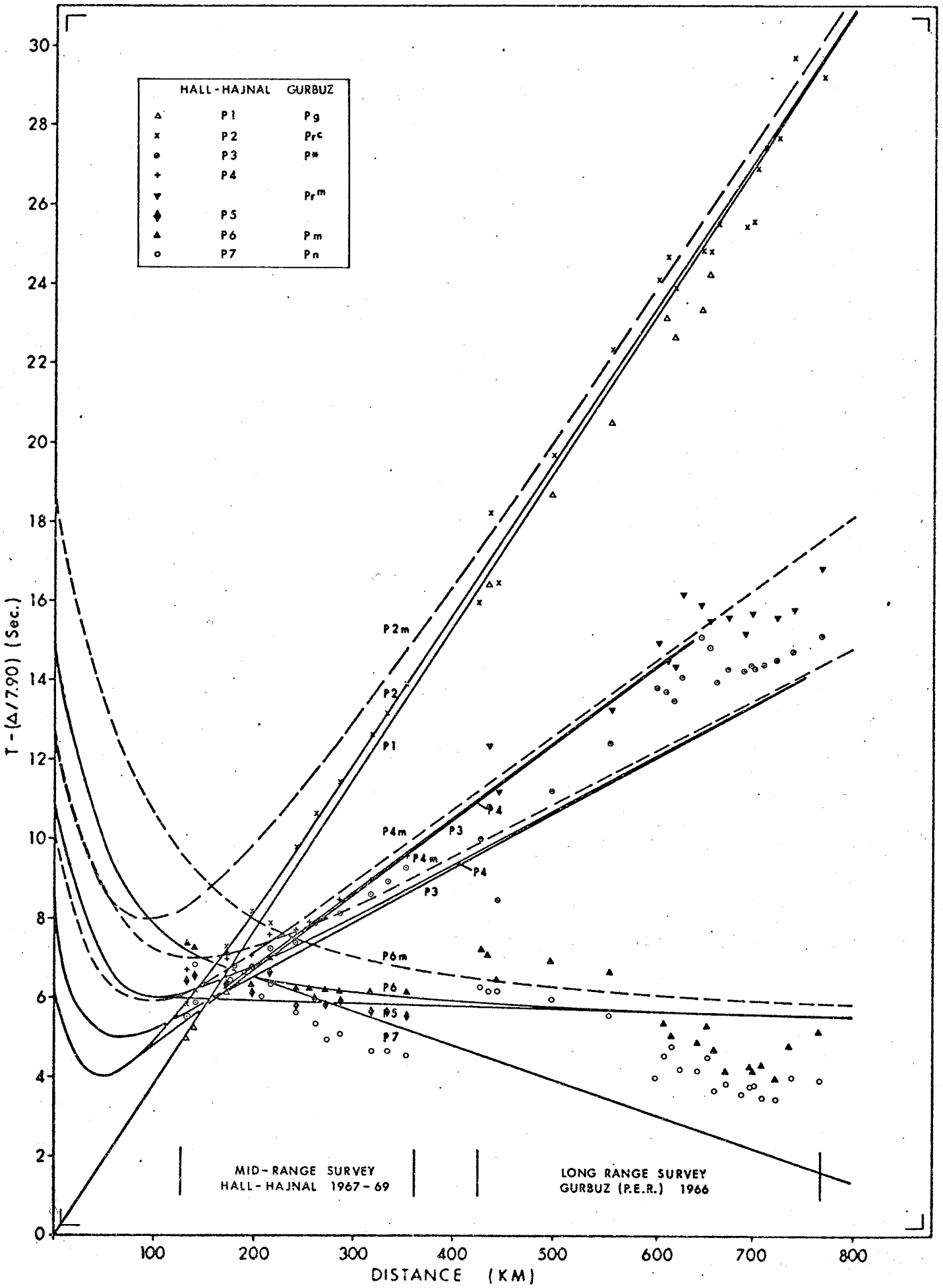

Fig. 2b. Crustal Model B (with upper mantle model 1.1)

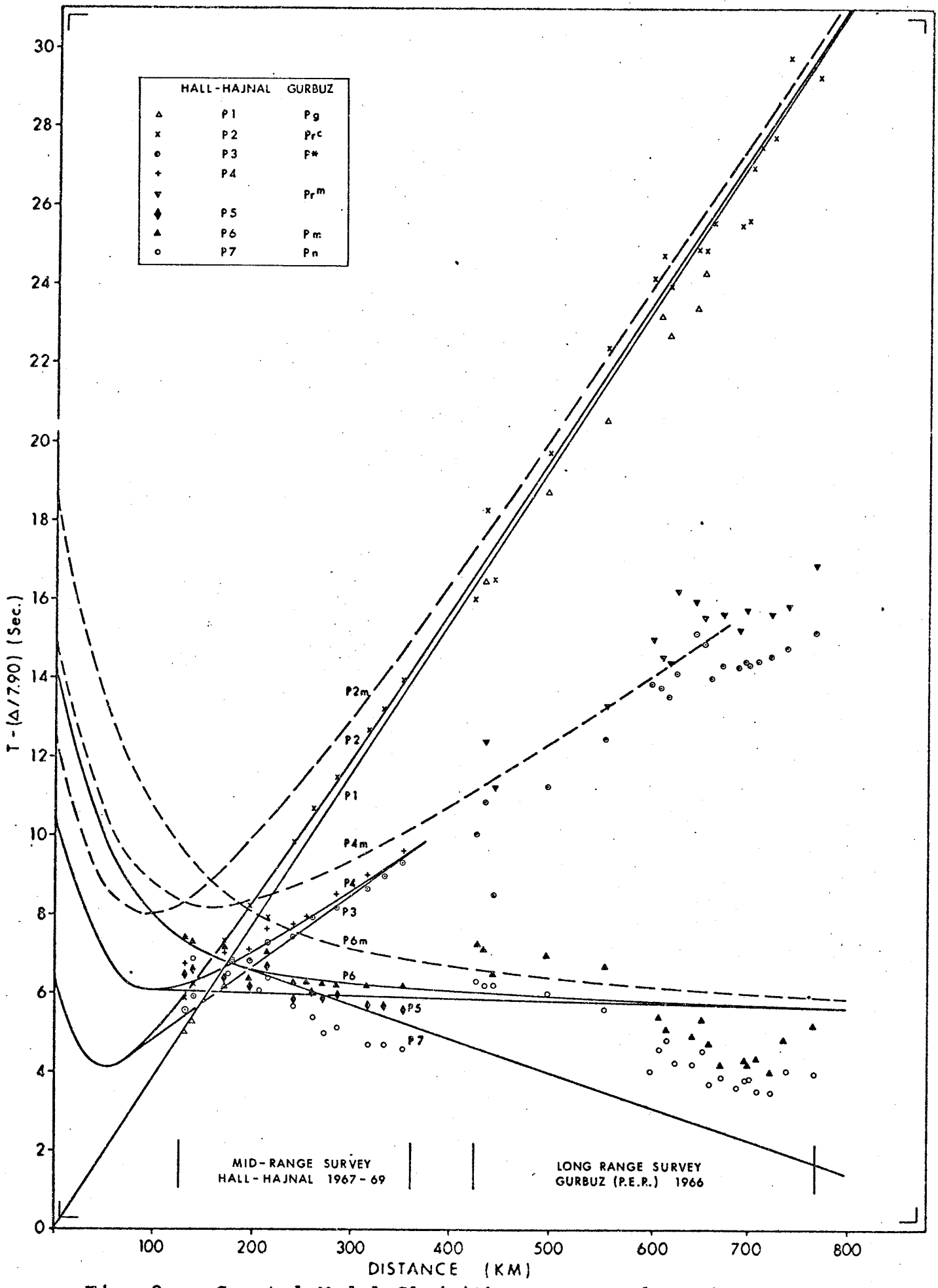

Fig. 2c. Crustal Model C1 (with upper mantle model 1.1)

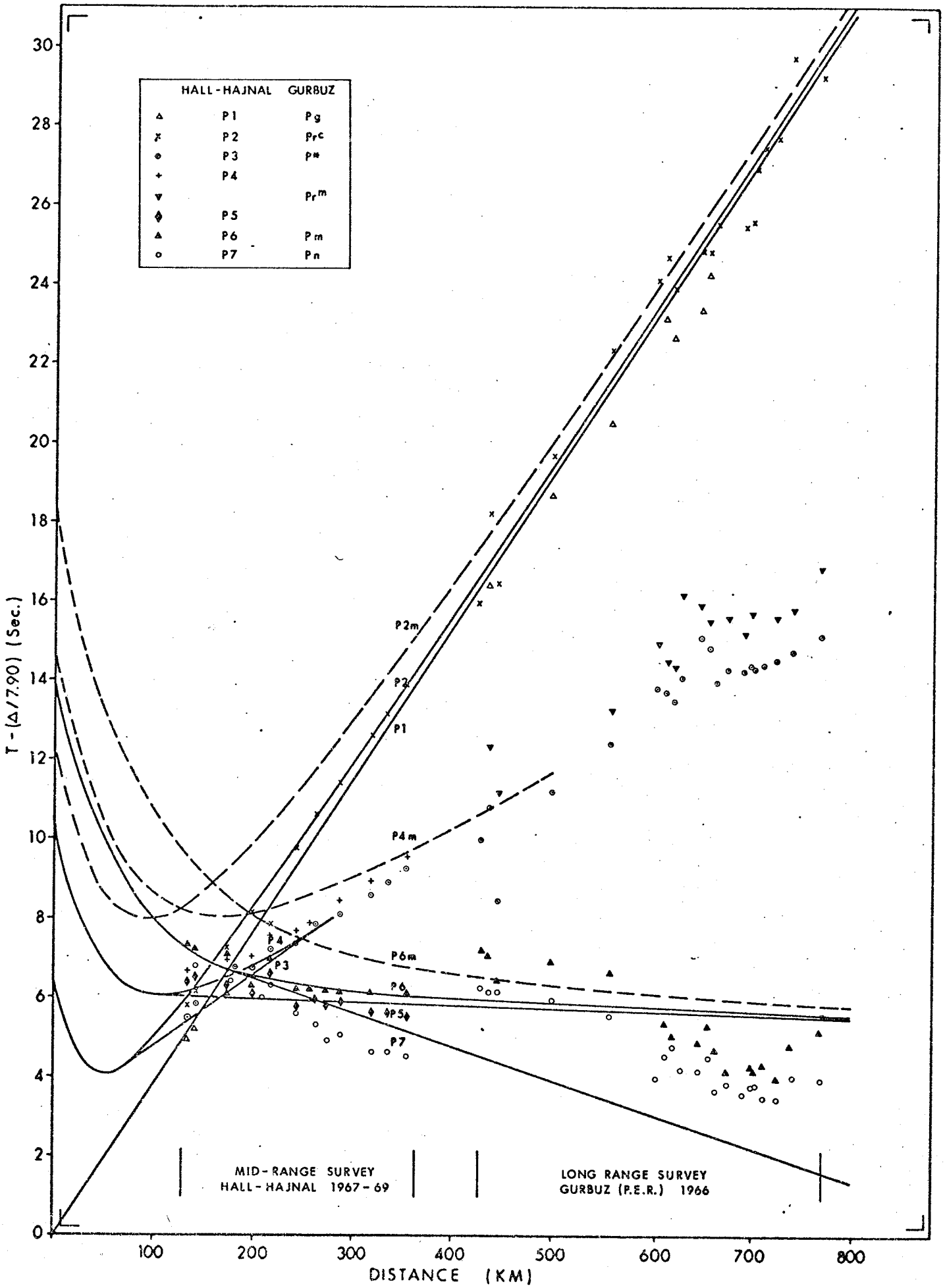

Fig. 2d. Crustal Model C2 (with upper mantle model 1.1)

interfaces, shadow zones are created at relatively short distances beyond which events no longer exist. The maximum distances of observation of all primary events are summarized in Table Ia. The thinning of a layer and/or the presence of a velocity gradient within a layer further reduce the maximum observation distance of events bottoming in it.

(b) For distances less than 60 km., only reflected events and the direct arrival exist. They are well separated in time and consequently their arrival times should be picked on records with relative ease. In the approximate range of 100-280 km. there is difficulty in distinguishing events from one another due to the onset of refracted waves and the convergence of all travel-time curves.

(c) Primary refracted and reflected events bottoming in the same layer (eg. P3 and P4) become asymptotic in time within the range of existing crustal survey distances. Table Ib shows the rate of convergence of these events for each model. This phenomenon has been cited (Lewis and Meyer, 1968) as a source of large error in first arrival measurements at large distances but its effect on later arrivals has largely been ignored. Pakiser and Steinhart (1964) using statistical information theory, conclude that for a S/N ratio of 2:1, first arrivals can be picked to

TABLE Ia

CRUSTAL MODELS A, B, C

RANGE OF OBSERVATION DISTANCES

CRUSTAL MODEL	CRUSTAL EVENTS			UPPER MANTLE EVENTS*		
	Event	Xmin (Km)	Xmax (Km)	Event	Xmin (Km)	Xmax (Km)
A	P1	0	958.2	P5	111.9	987.3
	P2	0	964.3	P6	0	987.3
	P3	85.0	936.6	P7	183.9	———†
	P4	0	936.6			
B	P3	85.0	640.9	P5	117.1	992.4
	P4	0	640.9	P6	0	992.4
	P3'	124.3	753.4	P7	186.8	———
	P4'	0	753.4			
C1 ($b_2 = 0.0072\ sec^{-1}$)	P3	72.28	374.9	P5	113.8	989.2
	P4	0	374.9	P6	0	989.2
				P7	185.0	———
C2 ($b_2 = 0.0156\ sec^{-1}$)	P3	70.05	274.7	P5	116.3	991.6
	P4	0	274.7	P6	0	991.6
				P7	186.4	———

* using average Upper Mantle model 1.1

† maximum distance dependent on possible existence of underlying refractor

TABLE I

CRUSTAL MODELS A, B, C*

ARRIVAL-TIME SEPARATION BETWEEN REFLECTIONS / REFRACTIONS

MODEL	EVENTS	MAXIMUM DISTANCE (Km) FOR T:		
		0.30 sec	0.20 sec	0.10 sec
A	P1:P2	286	354	522
	P3:P4	267	357	503
	P5:P6			
B	P3:P4	131	141	223
	P3':P4'	186	211	373
	P5:P6			
C1 ($b_2 = 0.0072\ sec^{-1}$)	P3:P4	208	240	265
	P5:P6			
C2 ($b_2 = 0.00156\ sec^{-1}$)	P3:P4	172	196	220
	P5:P6			

* using average Upper Mantle model 1.1

an accuracy of ±0.03 sec.; for later arrivals they estimate a time uncertainty of ±0.20 sec. or more. Resolving two events arriving this closely in time on a routinely processed record would therefore be virtually impossible.

Events P1 and P2, bottoming in the uppermost layer, whose properties are common to all crustal models investigated here, terminate at 964 km. The suite of time-distance curves of events bottoming below this layer, however, differs significantly for each model. The slopes of events P3 and P4 for Models A and B are the same since both have a bottoming-layer velocity of 6.85 km./sec.; the pair of events terminate at a much smaller distance (641 km.) in Model B, however, since its second layer is thinner than that of Model A. Furthermore, Model B produces an additional pair of primary events P3' and P4' (having an approximate inverse slope of 7.1 km./sec.), which bottom in the third crustal layer and also terminate at a relatively short distance of 753 km.

Model C, (having $b_2>0$) appears to fail as a compromise between the two- and three-layer constant velocity models. The imposition of a small gradient ($0<b_2<0.001$ sec.$^{-1}$) shortens the termination distance of P3 and P4 but does not noticeably reduce the slope of their travel time curves from those of Model A. Larger gradients of 0.0072 sec.$^{-1}$ and 0.0156 sec.$^{-1}$ (Figures 2c and 2d) produce curves with smaller slopes (and correspondingly higher apparent velocities), but truncation at

very short distances of 375 km. and 275 km.,respectively.

1.2 Theoretical Amplitude-Distance Curves

The theoretical vertical displacement amplitudes of compressional waves impinging on the free surface were calculated using programs XTAMP and HWAMP described in Appendices VII and IV. The former, written by R.F. Mereu, uses Guttenburg's (1944) method for the solution of the Zoepritz equations (Zoepritz, 1919) to calculate the transmission and reflection coefficients along a ray path in a spherical earth model; the latter program calculates the vertical amplitude of head waves as a function of distance for a plane layered medium based on a ray series solution developed by Cerveny (1971) according to the principles of geometrical optics.

The crustal amplitude curves (Figures 3a-d) were generated using an arbitrary source intensity equal to $10R_o^3$ where R_o is the Earth's radius. In general, as expected, the largest amplitudes are exhibited by primary reflections which attain a maximum value at the critical distance X_c and decrease approximately as $X^{-\frac{3}{2}}$ beyond X_c. Amplitudes of refracted body waves, bottoming in a constant velocity medium, however, increase with distance and, in the range of 700-800 km., exceed the amplitudes of reflected waves bottoming at underlying discontinuities.

This knowledge is crucial if amplitude ratios (between reflected and refracted waves) are used to support phase identifications based on arrival times since it was previously shown

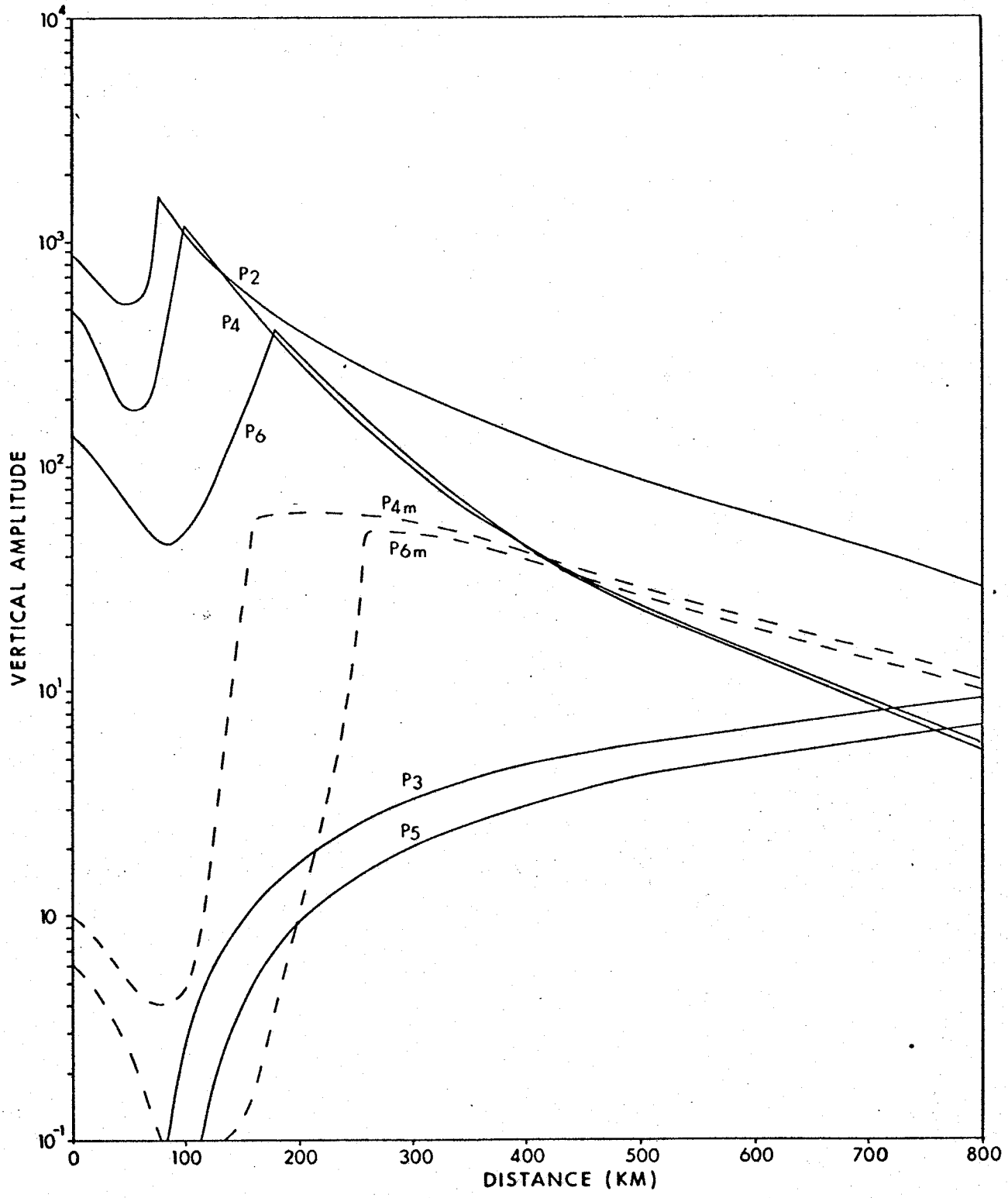

Fig. 3a. Amplitudes vs. distance of principal events: Crustal Model A

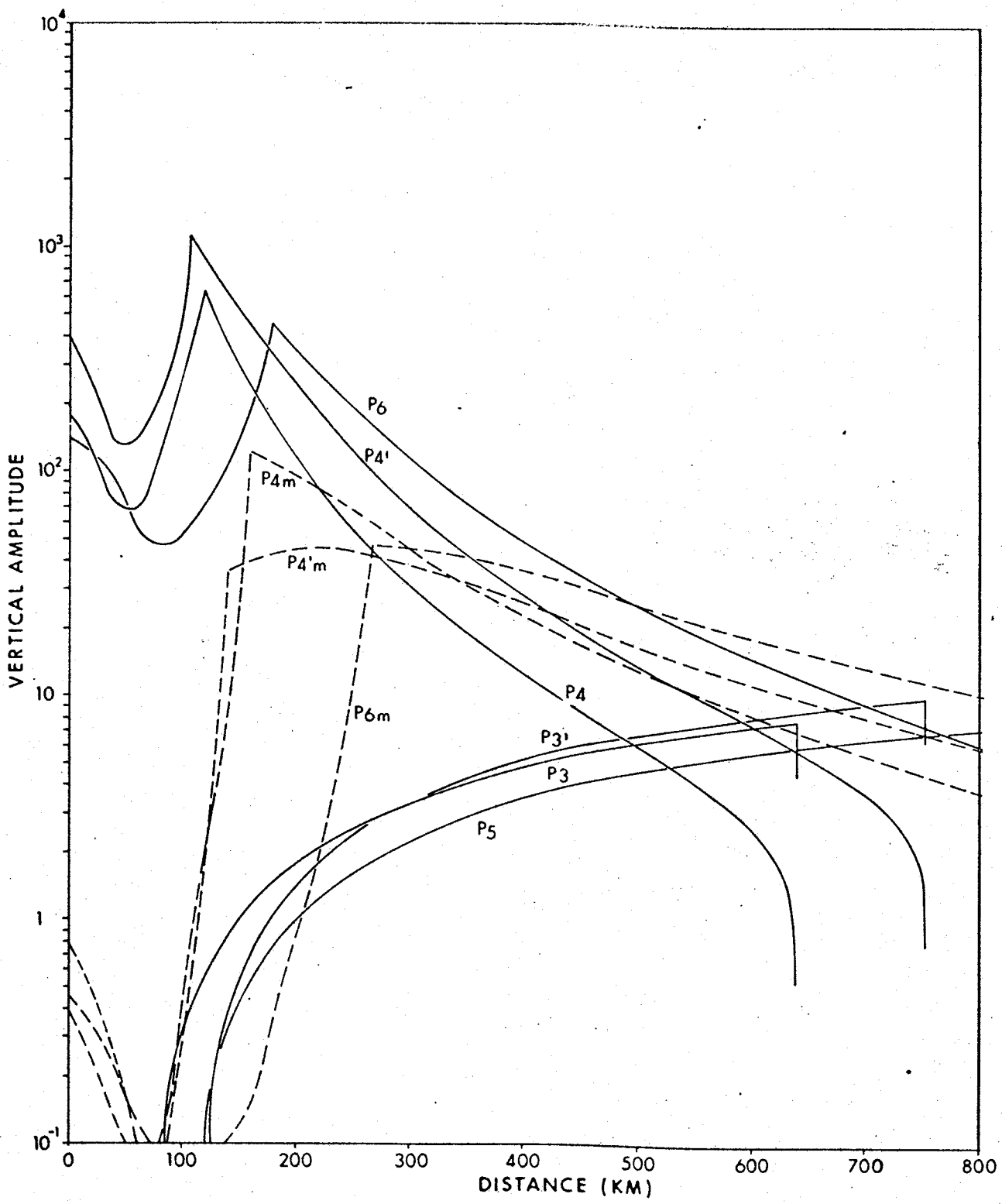

Fig. 3b. Amplitudes vs. distance of principal events: Crustal Model B

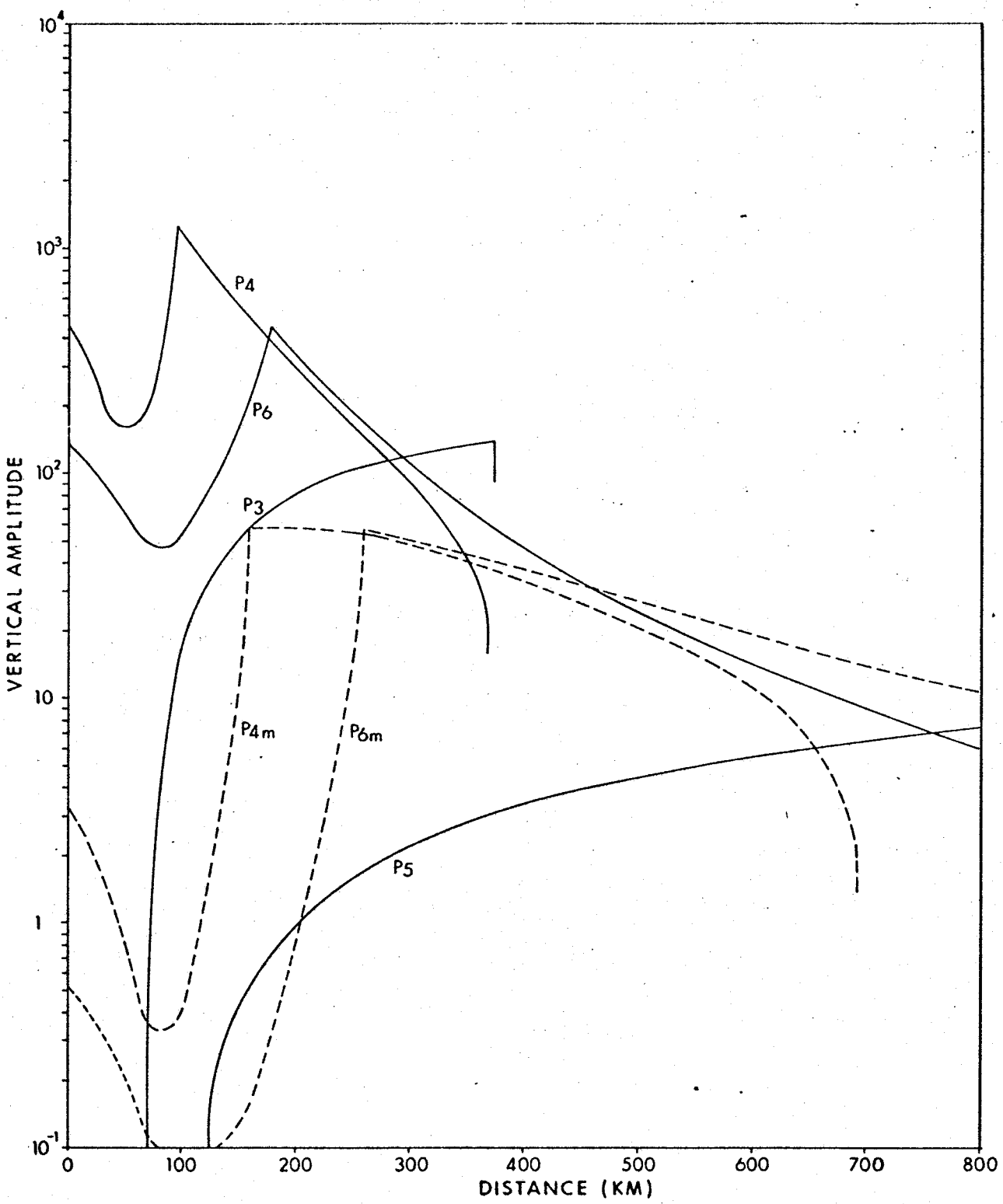

Fig. 3c. Amplitudes vs. distance of principal events: Crustal Model C1

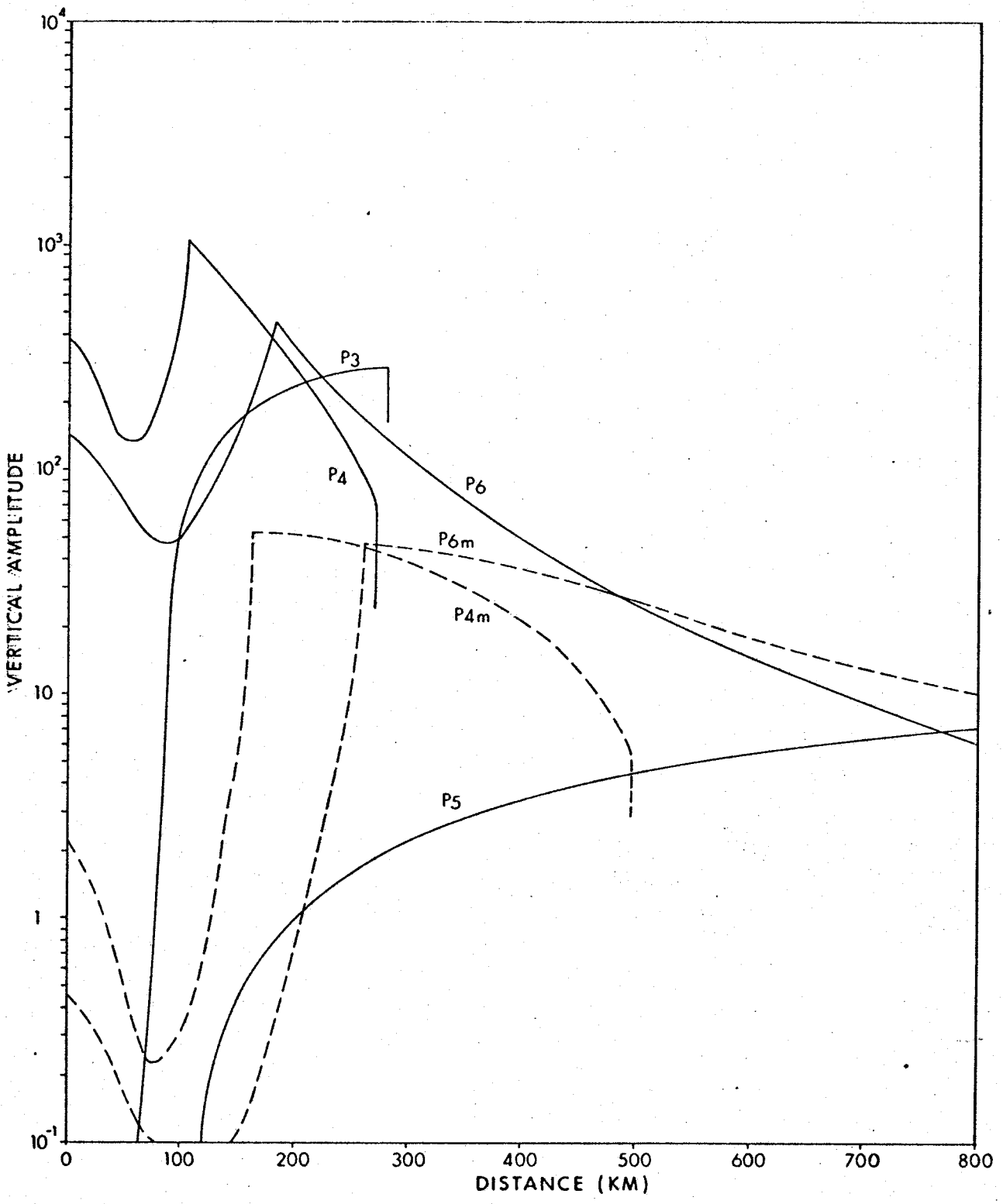

Fig. 3d. Amplitudes vs. distance of principal events: Crustal Model C2

(section 1.1) that travel-times of reflections and refractions bottoming in the same layer become asymptotic at intermediate (300-400 km.) survey distances. Thus the amplitude measurements of a reflected event may, in fact, include a significant contribution from a refraction arriving nearly simultaneously, and vice versa. This problem may be partially alleviated through the combined use of optimum digital filtering and predictive deconvolution (Cf. Robinson and Treitel (1967); Peacock and Treitel (1969)) to resolve the onset of the two events in the time domain; the wavetrains, however, each having similar but not identical theoretical frequency and phase spectra (Gurbuz, 1969) would still interfere with one another, thereby creating a complex composite waveform. Unfortunately, no suitable means of isolating near-simultaneous events such as these in the frequency domain has yet been developed.

Amplitudes of diving waves (eg. P3 in Figures 2c and d), having turning points within the n^{th} layer (b_n 0), increase more sharply with distance than body waves having $b_n=0$, the rate of increase being proportional to b_n. This feature, combined with the kinematic results that

(a) a diving wave together with the nearest underlying reflection terminate at an anomalously short distance

and

(b) these two events are resolvable in time

may provide a useful diagnostic means of verifying a suspected zone of continuous vertical velocity change. A simple approach

would be to conduct a continuous in-line refraction profile beginning at a short distance to delineate the abrupt termination of the two (prominent) events associated with the layer in question.

One important result, which cannot be ignored in future work, is the large amplitude of reflection multiples which attain a maximum value at the distance corresponding to the critical angle $\Theta_n = \sin^{-1} (V_n/V_{n+1})$ (where n is the number of the bottoming layer) and decay gradually beyond this distance. In the zone of intermediate distances (200-500 km.) the amplitudes have magnitudes similar to those of simple reflections. Because the travel time curves of primary and multiple reflections have similar slopes in this distance range, a multiple event could easily be mispicked as a primary reflection and still conform to an acceptable velocity model.

Finally, of use in the comparison of data to the crustal models (Chapter 2), is the fact that the amplitudes of the extra pair of events (P3' and P4') of Model B conform to the same range of values as those of P3 and P4 and should thus be as prominent on survey records if Model B represents true crustal structure.

1.3 Discussion of wavetypes in flat and spherically-stratified Earth models.

1.3.1 Reflected waves

Reflections in a horizontally stratified model are affected by the introduction of interface curvature in the

following ways:

1. Termination of a reflection travel-time segment occurs at infinity in a flat earth model. Truncation at finite distances (as shown in section 1.1) for a curved earth result from a maximum observation distance corresponding to the situation where the ray path in the bottoming layer is a straight line segment, (assuming b=0), tangent to the lower interface.

2. Theoretical $T^2 - X^2$ curves of reflections in a flat earth model are non-linear at large X; interface curvature (as shown in Appendix II and section 1.4) intensifies this non-linearity.

A comparison of the amplitude curves of reflections in plane and spherical models (using programs RDAMP and XTAMP), however, showed the two sets to be nearly identical. This result is anticipated since interface curvature does not affect the coefficients of reflection and transmission and alters the geometrical-spreading factor (Appendix III, equation (3)) negligibly.

1.3.2 Refracted waves

There are two principal types of compressional refracted events associated with a plane layered earth model:

(a) Critically refracted (head) waves which propagate at the top of a layer having a constant velocity.

(b) Diving waves which have a turning point in a layer containing a positive velocity gradient.

The introduction of interface curvature does not affect the theory of diving waves bottoming within a medium having $b>0$; the theory of critically refracted waves in a constant velocity medium, however, appears to break down. Another refracted wave type emerges, having a straight line segment in its bottoming layer for which the depth of bottoming and angular surface distance are uniquely determined by the angle of incidence on the lowest refractor boundary penetrated. This wave type is termed body wave.

All interpretations of crustal surveys in eastern Manitoba and northern Ontario to date, have incorporated a flat earth model and relied extensively on the identification of head wave first-arrivals for velocity and depth determinations. At large distances where curvature effects become significant, the question of the validity of head waves therefore arises.

The bottoming segments of refracted rays, at angles near θ_c, may be reflected one or more times from the top of the bottoming layer before returning to the surface, as in Figure 4. The waves

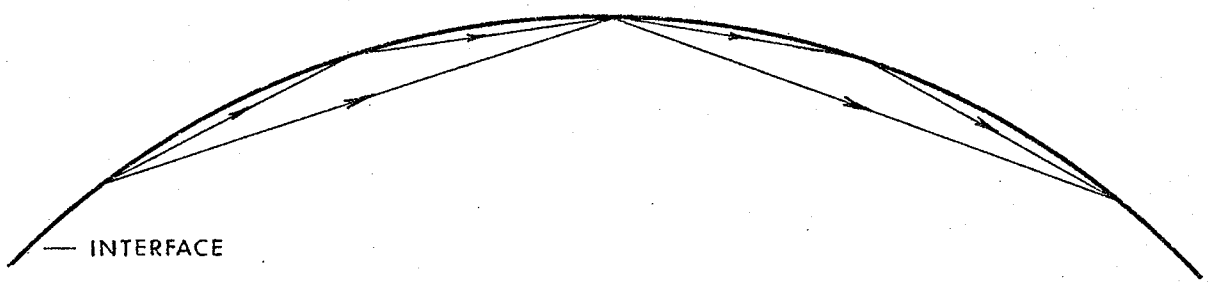

Fig. 4 Generation of interference head waves

corresponding to these multiply reflected ray segments will interfere with one another to form a composite interference head wave (Cerveny and Ravindra, 1971), whose time-distance curve would be indistinguishable from that of a ray propogating along the curved interface. Studies of the amplitude and spectral properties of this interference or diffracted wave have been reported by Buldyrev and Lanin (1965, 1966) and Lanin (1966,1968). Because of the preliminary nature of their results, however, they will not be considered here. For expediency, we shall assume that diffracted waves exist in a spherically stratified medium, that their bottom-segment ray paths follow the curved refractor boundary and that their amplitude variations with distance conform to the head wave theory of Appendix III.

A comparison of the kinematics and amplitudes of diffracted waves versus those of body waves were made using Crustal Model A. Results of the travel-time comparisons, summarized in Table II, show that the arrival times of the two wave types are nearly identical and therefore cannot be distinguished on seismic records. The amplitude-distance curves (Figure 5) of each type, derived for the same source intensity, however, are markedly different. Beyond the range of 300-400 km., the body (P) wave amplitudes surpass those of the head (H) waves, the latter decreasing at a rate proportional to X . Furthermore, although the head wave amplitudes are exceedingly large in the vicinity of X_c, it has been

TABLE III

COMPARISON OF THEORETICAL TRAVEL-TIMES VS. DISTANCE BETWEEN DIFFRACTED (H) WAVES AND BODY (P) WAVES FOR CRUSTAL MODEL A

DISTANCE (Km)	ARRIVAL TIMES (SEC)					
	H3	P3	H5	P5	H7	P7
220	34.95	34.89	33.94	33.90	34.29	34.29
260	40.77	40.70	39.00	38.94	39.00	38.97
300	46.59	46.55	43.95	43.95	43.74	43.75
340	52.41	52.40	49.04	49.03	48.45	48.45
380	50.23	58.22	54.10	54.05	53.21	53.18
420	64.06	64.06	59.10	59.10	57.94	57.91
460	69.88	69.87	64.18	64.12	62.70	62.63
500	75.70	75.68	69.22	69.15	67.40	67.38
540	81.52	81.50	74.26	74.19	72.13	72.08
580	87.34	87.31	79.30	79.24	76.82	76.81
620	93.16	93.13	84.31	84.26	81.57	81.54
660	98.99	98.95	89.39	89.29	86.28	86.25
700	104.81	104.78	94.40	94.34	90.99	90.98
740	110.63	110.57	99.41	99.36	95.68	95.68
780	116.45	116.39	104.43	104.39	100.46	100.42

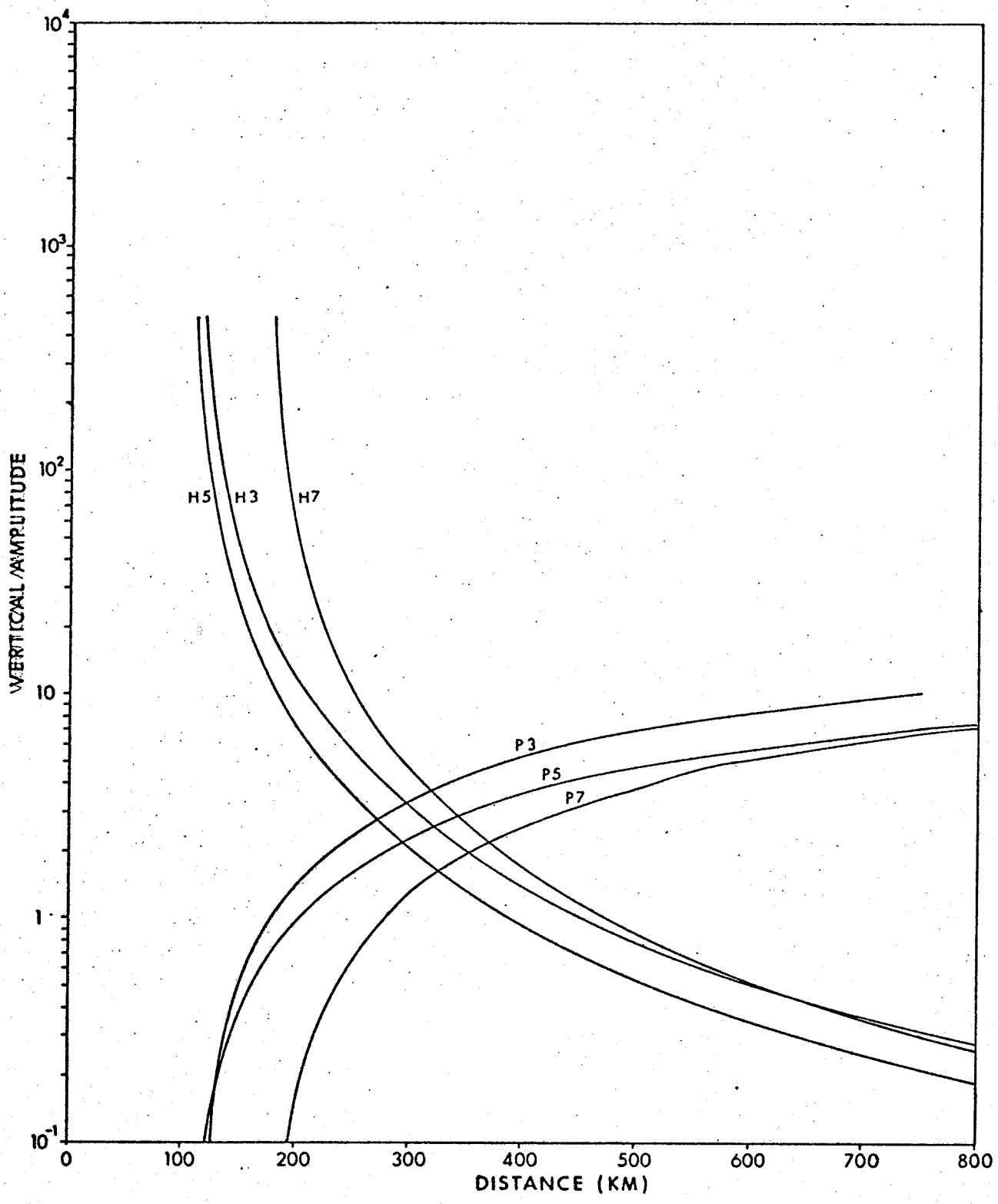

Fig. 5. Amplitudes vs. distance for head waves and body waves: Crustal Model A

noted by previous researchers (e.g. Cerveny (1967)) that theoretical amplitude values within the range of distances known as the "interference zone" do not likely represent the true values.

The foregoing results suggest that, despite an allowance for the existence of diffracted or head waves, their occurence on seismic records acquired at large separations from a source, would be overshadowed by refracted (body) wave events arriving at identical times.

1.4 Effect of Earth curvature on classical velocity-determination methods

1.4.1 Refraction data velocity estimates

To date, most average crustal and upper mantle velocity models have been based on seismic theory derived for a horizontally stratified medium having constant velocity layers. The theory of critically refracted head waves resulting from this type of model is well known (Cf. Dobrin (1960) and Muskat (1933)) and will not be developed here. Head waves have formed the basis of seismic interpretations for the following reasons:

(a) Immediately beyond X_c for a head wave propagating along the boundary of a particular layer, the arrival time of this wave represents the first arrival on seismic records and the event is therefore readily identifiable.

(b) The time-distance curve for a head wave is linear, having an inverse slope equal to the velocity of the medium along whose upper boundary the wave is critically refracted.

When interface curvature is taken into consideration, however, another refracted wave form, termed body wave, emerges whose kinematic characteristics are virtually identical to those of the head wave (as described in Section 1.3).

Mereu (1968), using spherically stratified models, has shown that for refraction depths greater than 10 km., velocity measurements from first arrivals employing a horizontally stratified earth model will be erroneously high; depth measurements for layers in the upper 60 km. of the earth, however, were found to be unaffected by curvature. The relationship derived by Mereu between a measured apparent velocity V' and true velocity V derived from the T-X curve of a compressional refracted wave can be expressed by

$$V = \frac{(R_o - Z)}{R_o} V' \qquad (1\text{-}1)$$

where R_o is the Earth radius and Z is the depth to the refractor. It is important to note that equation (1-1) is independent of source-receiver distance since interpretations of relatively short-range surveys, which hitherto

were assumed to conform to a flat earth model will lead to incorrect velocity results.

1.4.2 Reflection data-velocity estimates

Although a refracted event can be picked with a high degree of accuracy when it appears as a first-arrival on a seismic trace, it becomes more difficult to correlate this event from record to record when it becomes a later arrival at larger distances and its wavetrain interferes with other later events. This difficulty is compounded in the case of regional refraction surveys where the receiver spacing may be very large. Wide-angle reflected waves, as shown in Section 1.2, are the most prominent events on seismic records, and therefore constitute an important secondary source of velocity information.

Unlike head waves, exact velocity values are not readily extractable from the time-distance curves of reflections; in general, time and distance are analytically related in parametric form involving the ray parameter p. Dix (1955) has overcome the difficulty in eliminating this third variable for the restricted case when

(i) X is very small and

(ii) interface curvature is zero.

For this situation, the following relation holds:

$$T_n(X)^2 \simeq T_{o_n}^2 + \frac{X^2}{\overline{V}_{a_n}^2} \qquad (1\text{-}2)$$

$$T_{o_n} = 4Z_n^2/V_{a_n}^2$$

where

T_{o_n} = is the vertical two way travel-time to the n^{th} reflector

Z_n = the depth to the n^{th} reflector

V_{a_n} = the RMS (apparent) velocity of the n^{th} layer

Appendix I gives an explicit derivation of equation (1-2) illustrating the fact that, except for the one-layer case, the formula is only valid when X/Z 1. Its direct applicability to seismic surveys involving large offset distances is therefore questionable. Furthermore, although equation (1-2) is exact for n=1 for any distance (ie. V_a is the true interval velocity) for a plane layered case, it can be shown (Appendix II) that for a reflection in a spherical shell, T^2 and X^2 are related by

$$T_1^2 = T_{o_1}^2 + \frac{X^2}{V_1^2} - \frac{X^2}{V_1^2}\left[\frac{Z_1}{R_o} + \frac{X^2}{48R_o^2} - \frac{Z_1X^2}{48R_o^3} - \frac{X^4}{5760R_o^4}\right] \quad (1\text{-}3)$$

where R_o is the Earth radius.

Therefore the application of equation (1-2) to crustal reflection data from the first layer will result in erroneously large velocity estimates.

Dix has also shown that, for small X , the interval velocity V_{i_n} for the n^{th} layer is related to the apparent velocity V_{a_n} by the equation

$$V_{i_n}^2 = \frac{V_{a_n}^2 T_{o_n} - V_{a_{n-1}}^2 T_{o_{n-1}}}{T_{o_n} - T_{o_{n-1}}} \quad (1\text{-}4)$$

To determine the magnitude of error in T_o, V_a and V_i derived from equations (1-2) and (1-4), linear fits were applied to the theoretical T^2-X^2 curves of reflections from Crustal Models A and B for three sets of distance ranges: 120-360 km., 420-780 km. and 0-800 km. (Tables IIIa to c). The fitted parameters were then compared with the theoretically known values. While the fits to parameters for the one-layer case (P2) were correct to within 3%, errors in curve fits to deeper reflectors ranged from 12% to 21%, the error being greatest for the curve most removed from the origin (420-780 km.).

Durbaum (1954) has shown that T^2-X^2 reflection curves can be fitted to a higher polynomial,

$$T^2 = \sum_{1}^{n} C_i (X^2) \qquad (1\text{-}5)$$

For a curve which passes through the origin X=0 and has monotonically increasing curvature, the first two coefficients of a polynomial fit having sufficiently large n should equal T_o^2 and $1/V_a^2$ respectively.

Regional seismic surveys however, often do not include recordings acquired near the shot point. Higher order polynomial fits using program POLYFIT (Appendix V) were therefore applied to the same data sets described above with two objectives in mind:

(i) to determine the degree (n) of polynomials required to fit the curves.

(ii) to determine the degree of accuracy attained between coefficients C_1 and C_2 and theoretically

TABLE IIIa

POLYNOMIAL FIT TO THEORETICAL $T^2 - X^2$ REFLECTION CURVES Δ: 120-360 km.

CRUSTAL MODEL A (with average Upper Mantle model 1.1)

Event	Parameter	Linear Fit (n=1) Theoretical	Fit	Ratio	Deg. of Polyn. (n)	Best Fit Fit	Ratio
P2	T_o (sec.)	6.22	6.24	1.003	3	6.19	0.995
	V_a (km./sec.)	6.05	6.06	1.002		6.05	1.00
	V_i (km./sec.)	6.05	6.06	1.002		6.05	1.00
P4	T_o (sec.)	10.56	11.95	1.132	5	10.62	1.006
	V_a (km./sec.)	6.39	6.63	1.037		6.40	1.001
	V_i (km./sec.)	6.85	7.20	1.051		6.85	1.001
P6	T_o (sec.)	14.70	16.28	1.107	5	14.77	1.005
	V_a (km./sec.)	6.85	7.30	1.065		6.90	1.007
	V_i (km./sec.)	7.90	8.89	1.125		8.03	1.017

CRUSTAL MODEL B (with average Upper Mantle model 1.1)

Event	Parameter	Linear Fit (n=1) Theoretical	Fit	Ratio	Deg. of Polyn. (n)	Best Fit Fit	Ratio
P4	T_o (sec.)	8.17	10.56	1.291	5	8.07	0.988
	V_a (km./sec.)	6.25	6.61	1.062		6.22	0.996
	V_i (km./sec.)	6.85	7.33	1.070		6.75	0.985
P4'	T_o (sec.)	10.57	12.34	1.170	5	10.554	0.998
	V_a (km./sec.)	6.45	6.78	1.051		6.451	1.000
	V_i (km./sec.)	7.10	7.71	1.086		7.150	1.007
P6	T_o (sec.)	14.62	16.10	1.101	4	14.62	1.000
	V_a (km./sec.)	6.88	7.32	1.064		6.91	1.004
	V_i (km./sec.)	7.90	8.86	1.122		7.98	1.010

TABLE IIIb

POLYNOMIAL FIT TO THEORETICAL $T^2 - X^2$ REFLECTION CURVES Δ: 420-780 km.

CRUSTAL MODEL A (with average Upper Mantle model 1.1)

Event	Parameter	Linear Fit (n=1) Theoretical	Fit	Ratio	Best Fit Deg. of Polyn. (n)	Fit	Ratio
P2	T_o (sec.)	6.22	6.39	1.028	3	6.21	0.998
	V_a (km./sec.)	6.05	6.06	1.002		6.06	1.001
	V_i (km./sec.)	6.05	6.06	1.002		6.06	1.001
P4	T_o (sec.)	10.56	16.75	1.586	4	13.38	1.267
	V_a (km./sec.)	6.39	6.76	1.058		6.65	1.040
	V_i (km./sec.)	6.85	7.16	1.046		7.12	1.039
P6	T_o (sec.)	14.70	22.86	1.555	5	16.19	1.101
	V_a (km./sec.)	6.85	7.65	1.116		7.14	1.042
	V_i (km./sec.)	7.90	9.66	1.222		9.13	1.155

CRUSTAL MODEL B (with average Upper Mantle model 1.1)

Event	Parameter	Linear Fit (n=1) Theoretical	Fit	Ratio	Best Fit Deg. of Polyn. (n)	Fit	Ratio
P4	T_o (sec.)	8.17	15.76	1.929	2	11.57	1.416
	V_a (km./sec.)	6.25	6.75	1.080		6.63	1.061
	V_i (km./sec.)	6.85				7.23	1.056
P4'	T_o (sec.)	10.57	17.15	1.623	3	12.84	1.215
	V_a (km./sec.)	6.45	6.95	1.078		6.74	1.045
	V_i (km./sec.)	7.10	8.90	1.254		7.73	1.089
P6	T_o (sec.)	14.62	22.49	1.538	5	16.85	1.153
	V_a (km./sec.)	6.88	7.65	1.111		7.24	1.053
	V_i (km./sec.)	7.90	9.55	1.210		8.64	1.095

TABLE IIIc

POLYNOMIAL FIT TO THEORETICAL $T^2 - X^2$ REFLECTION CURVES Δ: = 0-800 km.

CRUSTAL MODEL A (with average Upper Mantle model 1.1)

Event	Parameter	Linear Fit (n=2) Theoretical	Fit	Ratio	Best Fit Deg. of Polyn. (n)	Fit	Ratio
P2	T_o (sec.)	6.22	6.29	1.011	3	6.22	1.001
	V_a (km./sec.)	6.05	6.06	1.002		6.058	1.001
	V_i (km./sec.)	6.05	6.06	1.002		6.058	1.001
P4	T_o (sec.)	10.56	13.83	1.310	5	10.89	1.031
	V_a (km./sec.)	6.39	6.73	1.053		6.48	1.015
	V_i (km./sec.)	6.85	7.24	1.057		7.01	1.024
P6	T_o (sec.)	14.70	18.86	1.283	5	14.95	1.017
	V_a (km./sec.)	6.85	7.56	1.104		6.98	1.020
	V_i (km./sec.)	7.90	9.48	1.200		8.18	1.035

CRUSTAL MODEL B (with average Upper Mantle model 1.1)

Event	Parameter	Linear Fit (n=2) Theoretical	Fit	Ratio	Best Fit Deg. of Polyn. (n)	Fit	Ratio
P4	T_o (sec.)	8.17	11.85	1.450	5	8.62	1.057
	V_a (km./sec.)	6.25	6.69	1.071		6.38	1.021
	V_i (km./sec.)	6.85	7.34	1.071		7.16	1.045
P4'	T_o (sec.)	10.57	14.12	1.336	5	10.88	1.030
	V_a (km./sec.)	6.45	6.91	1.071		6.57	1.021
	V_i (km./sec.)	7.10	7.93	1.117		7.24	1.021
P6	T_o (km./sec.)	14.62	18.61	1.273	5	14.83	1.016
	V_a (km./sec.)	6.88	7.57	1.100		7.02	1.019
	V_i (km./sec.)	7.90	9.36	1.184		8.11	1.027

known values T_o^2 and $1/V_a^2$ for T^2-X^2 curves far removed from X=0.

Results of these fits, summarized in Tables IIIa to c, indicate that polynomials of relatively low n ($n \leq 5$) converge to sufficiently accurate fits; note that nearly exact fits of degree 3 for P2 curves confirm the analytic expansion of equation (1-2). Furthermore, as expected, least accurate fits to correct C1 and C2 are obtained for the greatest extrapolation beyond the data set (ie. from the 420-780 km. curves).

The foregoing analysis suggests that more accurate velocity estimates from reflection data than offered by equation (1-2) should be obtainable by utilizing the first two coefficients of the best fit to the T^2-X^2 data and applying them in equation (1-4). The accuracy of the ensuing interval velocity will be dependent on the error associated with the derived intercept times and apparent velocities which in turn are proportional to the degree of separation of the nearest recording site from the source.

CHAPTER 2

APPLICATION OF MODEL RESULTS TO CRUSTAL DATA

As stated earlier, one objective of this study is the reconciliation of the long range (420-766 km.) regional survey data of Gurbuz (from which a three-layer crustal model was inferred) with data from other, shorter range detailed and regional seismic surveys which produced evidence of a two layer crust in the same geographical area.

To facilitate additional comparisons of upper mantle events from both long and shorter range surveys (Chapters 3 and 4), a group of 24 mid-range recordings, acquired in the years 1967-69 and containing possible upper mantle events, were chosen for the present investigation. Before an interpretation is attempted, the two will first be compared individually.

2.1 Mid-range Survey of Hall-Hajnal

This 24 record regional crustal survey, having distances ranging from 127-351 km., has been interpreted by Hall and Hajnal (1973) and found to conform to the established two-layer crustal hypothesis; the published distances and travel-times of principal arrivals are reproduced in Table IV, in which the wavetype identifications correspond to those of Crustal model A (Figure 1). The subsurface coverage of this survey extends from latitude 49°30' to 52° N. and longitude 93° to 98° W.

TABLE IV

DISTANCES AND TRAVEL TIMES FOR PRINCIPAL ARRIVALS
ON RECORDS RECORDED IN 1967, 1968 AND 1969
(AFTER HALL-HAJNAL, 1973)

Station No.	Distance (km)	Travel Times (sec) P1	P2	P3	P4	P5	P6	P7
46-6	127.20	20.94	21.81	21.47	22.67	22.40	23.34	-
44-6	134.64	22.13	23.08	22.80	23.65	23.31	24.21	23.65
41-6	136.16	22.34	23.28	22.98	23.96	23.62	24.39	23.96
42-6	168.38	27.29	28.53	27.50	28.23	27.53	28.28	27.50
45-6	172.23	27.82	29.15	28.18	28.76	28.00	28.77	28.10
38-6	176.88	-	29.95	29.03	29.40	29.03	29.34	29.05
63-8	194.84	-	32.75	31.32	31.60	30.65	30.86	30.60
62-8	203.43	-	34.16	32.55	32.89	31.78	31.91	31.66
52-7	206.07	-	34.49	32.52	33.12	32.12	32.31	31.79
39-6	213.06	-	34.77	34.13	34.46	33.58	33.84	33.15
60-7	218.97	-	36.75	34.63	35.03	33.38	33.91	33.38
43-6	221.49	-	37.14	35.20	35.70	34.09	34.89	33.66
61-7	238.89	-	39.98	37.51	37.82	35.95	36.38	35.76
47-6	243.47	-	40.74	38.18	38.77	36.79	37.64	36.15
40-6	249.39	-	41.70	38.91	39.61	37.51	38.39	36.85
50-7	253.62	-	42.39	39.46	39.93	37.58	38.22	36.98
59-8	259.81	-	43.51	40.70	-	38.75	-	38.08
51-6	266.06	-	44.43	41.34	42.04	39.54	38.94	38.62
58-8	268.64	-	44.82	41.83	-	39.81	-	39.01
53-7	270.43	-	45.15	41.99	42.34	39.90	40.31	39.02
48-7	284.76	-	47.48	44.10	44.45	41.83	42.10	41.00
57-7	315.06	-	52.45	48.44	48.77	45.38	45.90	44.39
55-8	331.80	-	55.20	50.87	-	47.51	-	46.50
56-7	351.63	-	58.47	53.72	54.04	49.92	50.51	48.89

2.2 Long range survey of Gurbuz

Twenty recordings for this survey, having distances from 420-776 km. were acquired from a single shot point in Lake Superior. Recording sites were located in the area bounded by latitudes 49^0 to $50^030'$ N. and longitudes 92^0 to 98^0 W.; the same subsurface coverage, therefore, is common to both surveys.

Gurbuz (1969, 1970) reports the existence of six crustal and two mantle wavetypes on the records, their identification based on the correlation of amplitudes and waveform character from record to record and the correlation of phase velocity from trace to trace. Travel-times and distances of primary events, as published by Gurbuz, are reproduced in Table V.

The ensuing crustal interpretation (illustrated in Figure 6 together with identified wavetypes) was based on a flat-earth assumption. Layer velocities were obtained from the inverse slopes of refraction T-X curves and reflection T-X curves.

2.3 Comparison of data with crustal models

2.3.1 To test the general agreement of the data with previously proposed models, the reduced travel-times of events from both surveys were superimposed on the reduced travel-time curves of Crustal Models A, B, C1 and C2 (Figures 2a to d) introduced in the preceding chapter. The following comparisons of the data with the models are pertinent to the

TABLE V

PROJECT EARLY RISE JULY, 1966
UNIVERSITY OF MANITOBA RECORDING STATION DATA
(AFTER GURBUZ, 1970)

Shot No.	Distance (km)	Travel Times (sec) P_g	P_r^c	P^*	P_r^m	P_m	P_n
1	426.8	-	69.99	63.96	-	61.12	60.12
3	434.7	71.46	73.35	65.77	67.31	61.95	61.02
2	445.4	72.82	72.87	64.72	67.52	62.70	62.34
4	501.7	82.28	83.27	74.68	-	70.34	69.29
5	559.2	91.40	93.25	83.15	84.00	77.28	76.21
6	606.6	-	101.02	90.57	91.72	-	80.60
7	618.2	101.53	103.07	91.95	92.74	83.44	82.62
8	624.9	101.89	103.17	92.59	93.47	84.01	83.67
9	633.7	-	-	94.30	96.40	-	84.24
10	650.6	105.85	107.33	97.48	98.29	87.08	86.32
11	661.7	108.19	108.71	98.61	99.30	88.90	88.11
12	667.2	-	110.13	98.40	-	88.94	87.99
13	681.0	-	-	100.51	101.80	90.15	89.85
14	696.3	-	113.78	102.40	103.31	-	91.54
18	703.5	-	114.79	103.43	104.77	93.15	92.62
15	709.0	-	116.86	104.07	105.79	93.73	93.36
17	717.6	-	118.48	105.21	-	95.01	94.15
16	731.1	-	120.44	107.06	108.16	96.33	95.83
19	746.2	-	124.42	109.22	110.27	99.12	98.32
20	775.3	-	127.56	114.28	115.08	103.19	101.88

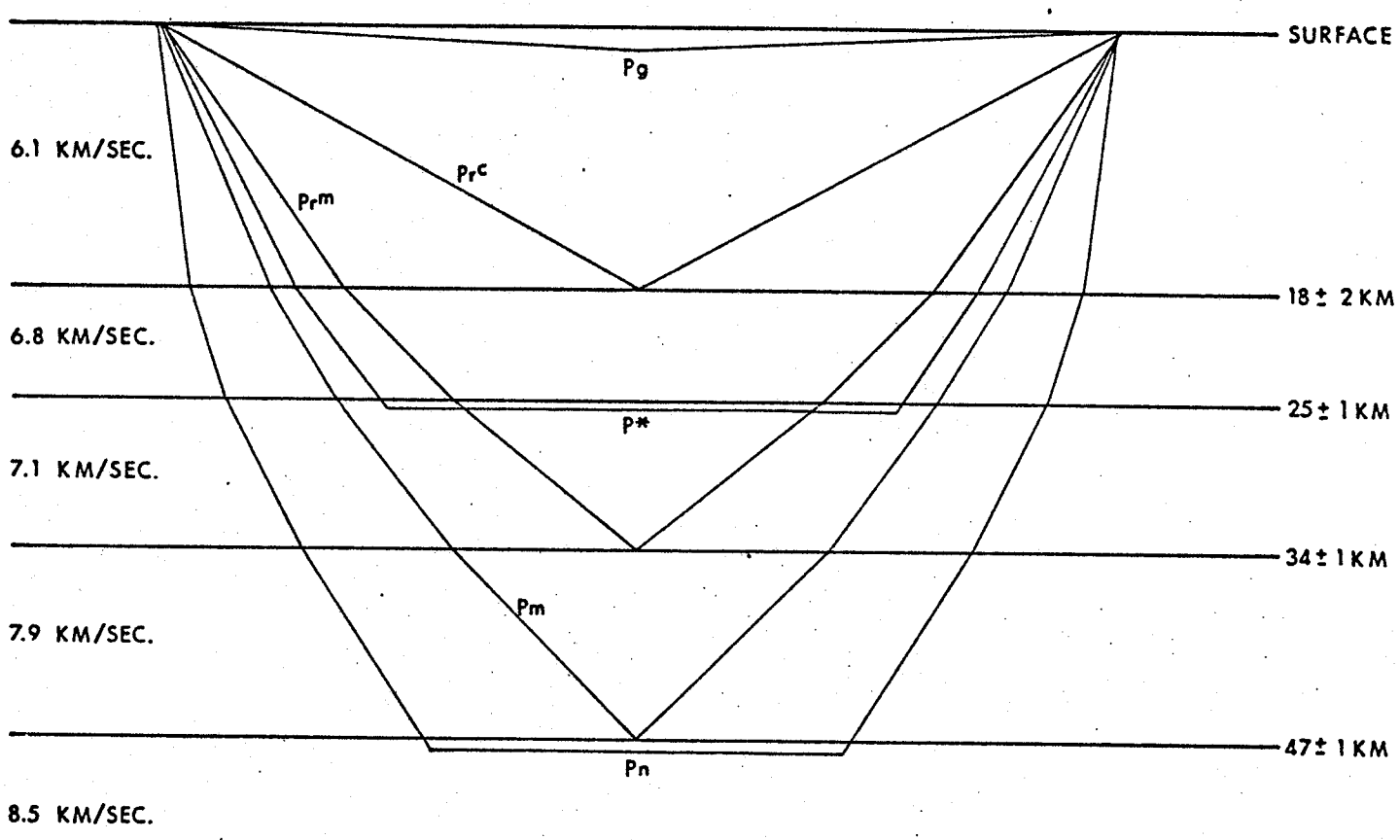

Fig. 6. Average crustal and upper mantle model for Superior geologic province deduced from Project Early Rise records (after Gurbuz 1969, 1970)

ensuing interpretation:

1. The mid-range data most closely matches Model A ($b_2 = 0$) and Model C1 ($b_2 = 0.0072\ sec^{-1}$). The latter is compatible with the hypothesis given by Hall and Hajnal (1973) of a small gradient in the lower crustal layer. Although there is a better fit to Model C1, having a slightly larger apparent V_2, a similar fit to Model A could be achieved by assigning a slightly higher (constant) velocity to the lower crustal layer of the model.

Results of Chapter 1 have shown that the only means of interpreting with certainty the presence of a velocity gradient ($b_2 > 0$) is to detect, on continuous-survey records, an anomalously sharp rate of increase in amplitude of a refracted wave relative to its reflection counterpart, and the termination of both reflected and refracted events at a distance shorter than predicted by the layer thickness and apparent velocity (deduced from T_o and V_a of the refracted event). Because events P3 and P4 have been identified at the longest shot-recorder distance of this survey, we must therefore look to the long range survey data for possible support of the velocity gradient hypothesis.

2. Although the long-range survey data resulted in the postulation by Gurbuz of a three layer crust, a comparison of the data with travel-time curves of Model B

(based on Gurbuz's crustal model) appears to contradict this interpretation for the following reasons:

(a) Whereas a three layer crust must yield four primary events (P3, P4, P3' and P4') bottoming below the Intermediate Discontinuity, which would be resolveable over the shorter distance portion of the Gurbuz survey, only two events (P^* and P_r^m) have been identified.

(b) Event P_r^m, interpreted as a reflection from the Moho discontinuity at the base of the third crustal layer, arrives much later than the corresponding model event P4'; similarly, the arrival times of event P*, interpreted as a wave critically refracted in the third layer, occur mid-way between those of Model B refracted events P3 and P3'.

(c) Although Model B produces termination of events P3 and P4 and events P3' and P4' at distances of 641 km. and 753 km., respectively, all events from the long range survey were identified to the maximum survey range (776 km.).

3. Further comparison with the remaining models suggest that the long range data is most compatible with Crustal Model A (whose events P3 and P4 correspond to events P_r^m and P*, respectively; note that event P* also compares favorably with P3 of the mid-range survey. One feature which appears inconsistent with this conclusion is that,

contrary to prediction, a large time separation exists between P_r^m and P*. We have shown in Chapter 1, however, that one type of reflection multiple becomes a prominent event at large distances and has T-X slopes similar to those of the parent reflections. The possibility that event P_r^m is actually a multiple reflection is examined in greater detail in the following section.

On the basis of the preceding qualitative examination, we are led to the conclusion that both the mid-range and long-range surveys support a two layer crustal interpretation involving no velocity gradient and that events P1, P_g, P2 and P_r^c bottom in the upper layer while events P3, P*, P4, and P_r^m bottom in the second layer.

2.3.2 In order to test the correlation of events from each survey in a quantitative sense, curvature corrections as prescribed by results of Chapter 1 must first be applied to the data:

Refraction data

Linear least squares fits were applied to the refraction T-X values to derive the intercept time T_o and inverse slope V for each separate event and for combined events $P1/P_g$ and P3/P* (Table VIa). The accuracy in T_o and V was calculated using the Student's t distribution theory (described in Appendix VI) for 80% confidence limits; earth curvature corrections were applied to the velocity estimates using Mereu's

TABLE VIa

CRUSTAL REFRACTION T-X DATA
LINEAR LEAST SQUARES FIT

Data Source	Event	Intercept T_o (sec.) Fit	Velocity $V=(\text{slope})^{-1}$ (Km./sec.) Fit	Curv. Corrected*	RMS Dev (sec.)
MID RANGE SURVEY (127-351 Km.)	P1	1.54±0.17†	6.55±.05	6.49±.05	0.023
HALL-HAJNAL 1969 (Recorded 1967-69)	P3	3.54±0.16	7.02±.03	6.97±.03	0.143
LONG RANGE SURVEY (420-776 Km.)	Pg	1.02±1.06	6.18±.07	6.14±.06	0.270
GURBUZ 1970 (Recorded 1966) (PROJECT EARLY RISE)	P*	2.57±	6.95±	6.97±.04	0.314
COMBINED MID RANGE and LONG RANGE SURVEYS	P1/Pg	0.02±0.24	6.02±.02	6.10±.02	0.276
	P3/P*	3.52±0.21	7.02±.02	6.97±.02	0.488

* Curvature corrections applying Mereu's (1967) formula
† All errors calculated for 80% fiducial limits

correction factor (equation 1-1).

In general, the results conform to previously established results based on shorter range surveys over the same area (Cf. Hall and Brisbin (1961, 1965); Hall and Hajnal (1969); Hajnal (1970, 1971)). Whereas T_o and V for P1 are larger than expected, they are based on 5 short-distance values, a statistically unacceptable small number of samples. Note that events P3 and P*, both independently and combined lead to the same velocity of 6.97±.02 km./sec.

Reflection data

It was shown in the preceding chapter that while the method of interval velocity estimation by the application of a linear fit to the T^2-X^2 curve of wide-angle reflection data leads to erroneously high estimates, good fits to theoretical data can be attained through the use of higher degree polynomials. This approach was successful when applied to the mid-range reflection data using the criterion that the highest degree polynomial for which the first two coefficients (corresponding to T_o^2 and $1/V_a^2$) continued to converge to smaller values gave the best estimates of those parameters. The long range reflection data, however, did not lend itself to this method due to the presence of excessively large residuals; (event P_r^c, for example, has a RMS deviation of 0.950 sec. from a linear T^2-X^2 fit). Polynomials of degree greater than one, therefore, attempted to fit oscillations in the data. An additional factor prohibiting reliable estimates of T_o and V_a was

the degree of separation of this data from the origin X=0; in general, the greater the extrapolation of a fit Y(x) to data set $\{x_i, y_i\}$ beyond the range of x_i, the greater is the attendant error.

To overcome this problem, the following approach was taken and applied to both mid-range and long range data sets: Linear least-squares fits were applied to the T^2-X^2 data of the individual reflections and to the combined events $P2/P_r^c$ and $P4/P_r^m$. The resulting T_o and V_a for each curve (Table VIb) were then compared with the parameters derived from the linear fits to the theoretical model curves for the same range of x (given in Tables III a-c). Taking into account slightly higher V_2 values (consistent with those derived from the refraction data), the reflections most closely matched the fits to Crustal Model A. Curvature corrections were then applied using the ratios derived between the linear fits to the model curves and the known theoretical values.

Finally, interval velocities V_i were calculated using equation (I-11) of Appendix I. The error in V_i was obtained through the knowledge that if the interval velocity of the n^{th} layer is given by

$$Vi_n = f(Va'_n, To'_n, Va'_{n-1}, To'_{n-1}) \qquad (2\text{-}1)$$

where $Va'_n = Va_n \pm \alpha$

$To'_n = To_n \pm \beta$

$Va'_{n-1} = Va_{n-1} \pm \gamma$

$To'_{n-1} = To_{n-1} \pm \delta$

TABLE VIb

CRUSTAL REFLECTION T^2-X^2 DATA

LINEAR LEAST SQUARES FIT

Data Source	Event	Intercept T_o(sec) Fit	Intercept T_o(sec) Curv. Correct.	Appar.Vel.(Km/sec) Fit	Appar.Vel.(Km/sec) Curv. Correct.	Int.Vel.(Km/sec) Fit	Int.Vel.(Km/sec) Curv. Correct.	RMS Dev. (sec)
MID RANGE SURVEY (127-351 Km.)	P2	5.56±0.83*	5.54±0.83	6.04±.02	6.03±.02	6.04±.02	6.03±.02	0.202
	P4	12.62±0.26	11.15±0.23	6.68±.02	6.44±.02	7.15±.21	6.81±.20	0.138
LONG RANGE SURVEY (420-776 Km.)	P_r^c	11.65±5.92	11.33±5.76	6.09±.04	6.08±.04	6.09±.04	6.08±.04	0.950
	P_m^r	23.02±3.26	14.51±2.05	6.88±.07	6.50±.05	7.27±4.3	6.95±4.1	0.625
COMBINED MID RANGE and LONG RANGE SURVEYS	$P2/P_r^c$	7.35±1.95	7.27±1.93	6.07±.02	6.06±.02	6.07±.02	6.06±.02	0.871
	$P4/P_m^r$	14.35±1.02	10.95±0.78	6.76±.03	6.42±.03	7.50±.73	7.09±.69	0.600

* All errors calculated for 80% fiducial limits

then, to a first approximation, the maximum error in Vi_n is given by

$$E = \pm \alpha \frac{\partial f}{\partial Va_n}\Big|_{Va_n} \pm \beta \frac{\partial f}{\partial To_n}\Big|_{To_n} \pm \gamma \frac{\partial f}{\partial Va_{n-1}}\Big|_{Va_{n-1}} \pm \delta \frac{\partial f}{\partial To_{n-1}}\Big|_{To_{n-1}} \qquad (2\text{-}2)$$

An explicit representation of equation (2-2) shows that $|E|$ is maximized using $+|\alpha|$, $-|\beta|$, $-|\gamma|$ and $+|\delta|$. The large uncertainty in V_i exhibited by events P4, P_r^m and $P4/P_r^m$ results mainly from the uncertainty inherent in the T_o estimates and serves to illustrate the fact that wide-angle reflections are intrinsically a much less accurate source of interval velocity information than refraction data.

2.4 Reflection multiples

The excessively large intercept times for P_r^m, which would result in unrealistic depth estimates, has led to the suspicion that the event may, in fact, be a multiple reflection of the type examined in Chapter 1.

Original supporting evidence for identification of P_r^m as a primary reflection by Gurbuz came from amplitude and phase spectral analysis. The theoretical amplitude curve of $P4_m$, however, as shown in Figure2a, is nearly identical to that of P4 over the long range survey distances. Furthermore the spectral analysis of supposed individual wavetypes given by Gurbuz (1969, 1970) is inconclusive since it was performed using a 0.50 sec. window within which (as demonstrated earlier) P3 and P4 would exist as a composite waveform. Final proof

that P_r^m corresponds to $P4_m$ of Crustal Model A derives from a comparison of the best linear fits to the $T^2 - X^2$ curves of each, yielding T_o and V_a estimates of 18.95 sec. and 6.79 km./sec. for $P4_m$ and T_o and V_a estimates of 23.02 ± 3.26 sec. and 6.88 ± .07 km./sec. for P_r^m.

Summary of Results

When earth curvature is taken into account, both mid-range and long range survey data substantiate a two layer crustal model similar to Model A but having a slightly higher V_2. Although the Hall-Hajnal survey data is consistent with a small positive velocity gradient in the lower layer, this possibility is not supported by the longer range data. Furthermore, neither data set conforms to the suite of travel-times curves of the three-layer Crustal Model B.

CHAPTER 3

UPPER MANTLE MODELS

3.1 Existing upper-mantle research

Until recently, little was known of the velocity distribution in the upper-mantle within the Canadian Shield. The two major long range refraction surveys conducted in Canada to date are Project Early Rise (1966) and Project Edzoe (1969), the results of which have been reviewed by Berry (1973) and Hales (1972).

Prior to these deep soundings, shorter-distance surveys, including those of Mereu (1965), Berry and West (1966) and O'Brien (1968), have led to an average upper-mantle P-wave velocity of 8.1 km./sec. and crustal thickness of 30-40 km. based on P_n first arrivals. An additional cooperative experiment conducted in the Hudson Bay area in 1965 (Cf. Ruffman (1969), Mereu (1969), Hajnal (1969) and Hall (1969)) suggests an average crustal thickness of 35 km. and a gross average upper-mantle velocity of 8.25 km./sec.

Project Early Rise constitutes the largest available collection of body-wave travel-times in the distance range of 300-3500 km. This long range data has resulted in the identification, at large distances, of first arrivals from sub-Moho discontinuities. Barr (1969) used observed cusps in the travel-time data to identify successive upper-mantle layerings. He concluded that all cusps resulted from

refractions below first order discontinuities and interpreted two sub-Moho interfaces at 126 km. and 366 km. having constant velocities of 8.23 km./sec. and 8.42 km./sec., respectively. Larger intercept-times for a longer distance survey were attributed to significant structural relief within the upper-mantle. Mereu and Hunter (1969) also found evidence for a first-order discontinuity at 84 km. with velocities of 8.10 km./sec. and 8.40 km./sec. above and below the interface respectively. Results of surveys south of Lake Superior (Green and Hales (1968) and Hales (1969)) further support this interpretation.

Project Edzoe, conducted in August, 1969, consisted of twenty shots detonated in Greenbush Lake, B.C. Bates (1971) obtained eight records in southern Saskatchewan and Manitoba with distances ranging from 790 to 1285 km.; his interpretation predicts a velocity gradient below the crustal base with a second order discontinuity in the depth range of 120-150 km. A somewhat contradictory interpretation of data acquired in the Rockies and plains regions has been proposed by Gettrust and Meyer (1971) who found evidence of a low velocity channel in the upper-mantle in the depth range of 90-140 km.

Although the long range refraction survey results described above have been quite variable, they all nevertheless suggest the presence of first or second order discontinuities in the upper 100 km. of the mantle. The question we now wish to examine is whether evidence of upper-mantle structure of

the types hitherto inferred exclusively from long range data (X>700 km.) could also be observed on shorter distance data in the range of the Hall-Hajnal and Gurbuz survey records.

3.2 Effect of crustal structure on upper-mantle events

Results of Chapter 2 have shown that both the mid and long range surveys conform to Crustal Model A, with possible slight differences. To test the effect of crustal variations on upper-mantle events, an average upper-mantle model (Model 1.1 in Fig. 7a), consisting of a first order discontinuity at 50 km. and containing no gradients, was combined with each crustal model previously examined; linear fits were then applied to the theoretical T-X curves of refraction events P5 and P7 and to the $T^2 - X^2$ curves of reflection events P6; results of these fits are summarized in Table VII. The distance range of observation, intercept time and slope of each event were found to be identical (within the normal uncertainty limits of data) for all crustal models. These findings are consistent with the analysis of Dowling (1970) who concluded that velocity uncertainties do not propagate strongly in seismic refraction calculations and that only the roughest estimates of velocities of the overlying layers are required for deducing upper mantle structure from travel-time data. We are therefore justified in employing a single crustal model (Model A) in the following study of upper-mantle models.

TABLE VII

EFFECT OF CRUSTAL MODELS A, B AND C ON UPPER MANTLE EVENTS*

REFRACTIONS: LINEAR FIT TO T - X CURVE

CRUSTAL MODEL	Event	Xmin (Km)	Xmax (Km)	Intercept T_o (sec)	Slope M (Km/sec)	$V_a=1/M$ (Km/sec)
A	P5	111.9	987.3	6.06	0.1261	7.927
	P7	183.9	- †	8.22	0.1182	8.458
B	P5	117.1	992.4	5.82	0.1262	7.922
	P7	186.8	-	8.03	0.1183	8.454
C1 (b_2= 0.0072 sec^{-1})	P5	113.8	989.2	5.98	0.1261	7.927
	P7	185.0	-	8.15	0.1182	8.457
C2 (b_2= 0.0156 sec^{-1})	P5	116.3	991.6	5.90	0.1261	7.928
	P7	186.4	-	8.05	0.1183	8.455

REFLECTIONS: LINEAR FIT TO $T^2 - X^2$ CURVE

CRUSTAL MODEL	Event	Xmax (Km)	Intercept T_o (sec)	$V_a= M^{-\frac{1}{2}}$ (Km/sec)	V_i (Km/sec)
A	P6	987.3	18.86	7.56	9.48
B	P6	992.4	18.61	7.57	9.36
C1 (b_2= 0.0072 sec^{-1})	P6	989.2	18.76	7.56	8.83
C2 (b_2= 0.0156 sec^{-1})	P6	991.6	18.64	7.57	8.85

* using average Upper Mantle model 1.1

† maximum distance dependent on possible existence of underlying refractor

3.3 Examination of upper-mantle models

A thorough study involving all possible upper-mantle structures and the effects of lateral and vertical variations in velocity and depth is beyond the scope of the present work. We have therefore restricted our study to the examination of six mantle models which, based on the findings of others, are most likely to represent true upper-mantle structure and which may give rise to events observable at short distances.

Models 1.1 to 1.3 (Figure 7a) contain a first order discontinuity at 50 km., the first model having no velocity gradients while the remaining two contain positive gradients of 0.002 sec.$^{-1}$ in one or both media. Models 2.1 to 2.3 (Figure 7b) exhibit second order discontinuities at Z=50 km.; the gradients chosen for each are as follows:

Model 2.1 - b_3=0.0 ; b_4=0.002 sec.$^{-1}$

Model 2.2 - b_3=0.002 sec.$^{-1}$; b_4=0.0

Model 2.3 - b_3=0.002 sec.$^{-1}$; b_4=0.003 sec.$^{-1}$

3.3.1 Comparison of travel-time curves

Linear fits to the travel time curves of the primary upper-mantle events are summarized in Table VIII. The following are pertinent characteristics:

(a) The imposition of a velocity gradient of 0.002 sec.$^{-1}$ below the crustal base (within the range of 0-0.003 sec.$^{-1}$ suggested by Bates (1971)) does not affect the slope or intercept time of P5 (commonly termed P_n in the literature); it does, however,

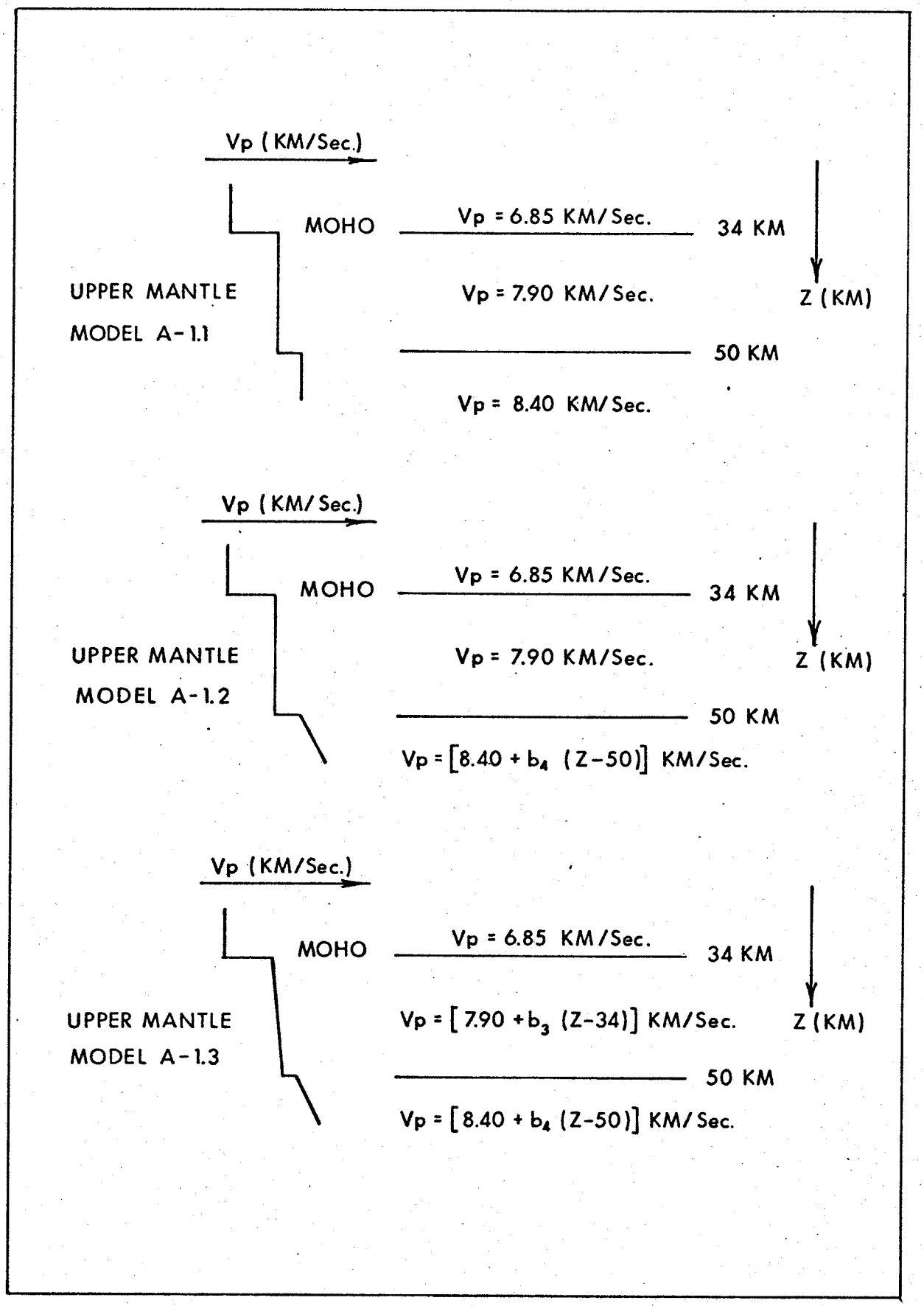

Fig. 7a. Upper mantle models containing first-order velocity discontinuities

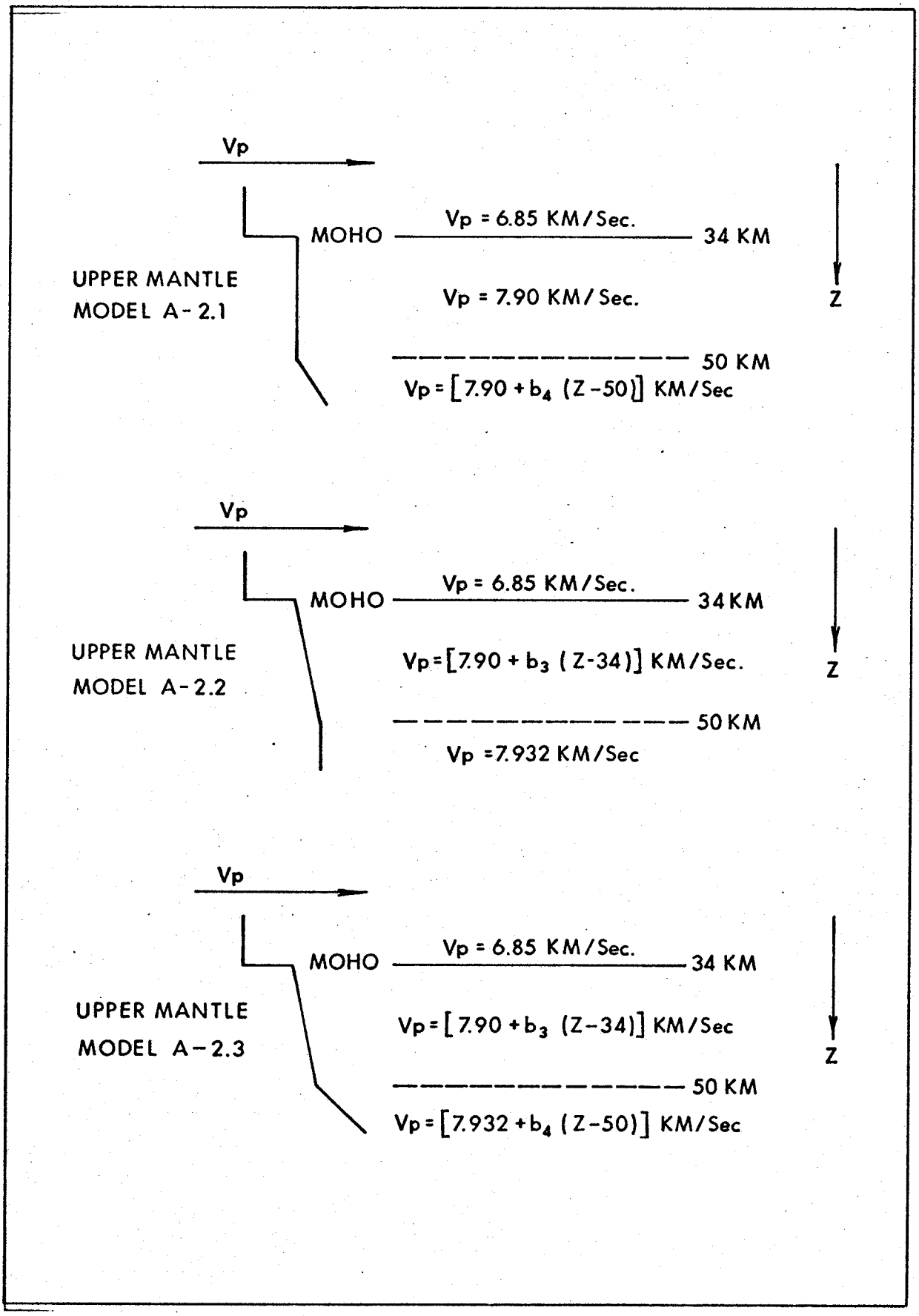

Fig. 7b. Upper mantle models containing second-order velocity discontinuities

TABLE VIII

UPPER MANTLE MODELS

COMPARISON OF TRAVEL-TIME CURVES

OF PRINCIPAL EVENTS

MODEL	REFRACTED EVENTS (T-X CURVES)					REFLECTED EVENTS (T^2-X^2 CURVES)				
	Event	Xmin (Km)	Xmax (Km)	T_x=0 (sec)	Inverse Slope (Km/sec)	Event	Xmax (Km)	T_{x^2}=0 (sec)	V_{app} (Km/sec)	Vint (Km/sec)
A-1.1	P5	112	987	6.23	7.93	P6	987	18.86	7.56	9.48
	P7	184	——†	8.34	8.47					
A-1.2	P5	112	987	6.23	7.93	P6	987	18.86	7.56	9.48
	P7	175	——	8.37	8.48					
A-1.3	P5	103	651	6.27	7.95	P6	651	17.72	7.50	9.76
	P7	177	——	8.33	8.48					
A-2.1	P5	112	987	6.23	7.93					
	P7	988	——	6.53	8.21					
A-2.2	P5	103	651	6.27	7.95					
	P7	665	——	6.48	7.99					
A-2.3	P5	103	651	6.27	7.95					
	P7	671	——	6.55	8.03					

† dependent on underlying structure

appreciably offset the distance of occurence of the travel-time cusp resulting from a lower discontinuity. Note also that the T^2-X^2 curve of event P6, reflected from the upper mantle first-order discontinuity, yields a much larger calculated interval velocity when $b_3>0$ than for $b_3=0$ due to the increased T^2-X^2 curvature at shorter distances.

(b) Event P7 arising from a first-order discontinuity is observable at relatively short shot-receiver separations and, for a fixed discontinuity-depth, the inclusion of velocity gradients above and/or below the discontinuity has little effect on its travel-time curve. In general, however, the following parametric changes reduce the shortest observation (critical) distance:

i. decreasing the depth to the sub-Moho discontinuity

ii. decreasing V_3 and/or increasing V_4

iii. increasing b_4

(c) A second-order discontinuity results in a slight increase in the slope of the first-arrival times at a fairly large distance (650-987 km. for the models chosen). The gradients chosen in Models 2.1 to 2.3 produced only negligible triplication at the onset distance of the event refracted at the discontinuity. Furthermore, no reflections occur at second-order discontinuities due

to the lack of velocity contrast above and below the interface.

3.3.2 Comparison of amplitude-distance curves

The amplitude-distance curves of upper-mantle model events, calculated in the same manner as those of the crustal model events, are depicted in Figures 8a and b. The following aspects of these curves are noteworthy:

(a) In the first three models, containing a first-order discontinuity, the first arrival P7 becomes prominent in the 300-400 km. range and attains the same magnitude as the nearest later arrival P5 beyond these distances. Event P7 should therefore be readily identifiable on short-distance records if this interface exists.

(b) Model 1.3 demonstrates the anomalous rate of amplitude increase with depth of refracted events P5 and P7 together with the sharp rate of decrease of reflected event P6 which occur when velocity gradients are present.

(c) Models 2.1 to 2.3 illustrate the important fact that although second-order discontinuities manifest themselves to a small degree on travel-time curves (producing a slight increase in slope of the first arrival), there is a hiatus between the amplitude-distance curves of the refracted event arriving from above and below the discontinuity. This feature should be diagnostic in the

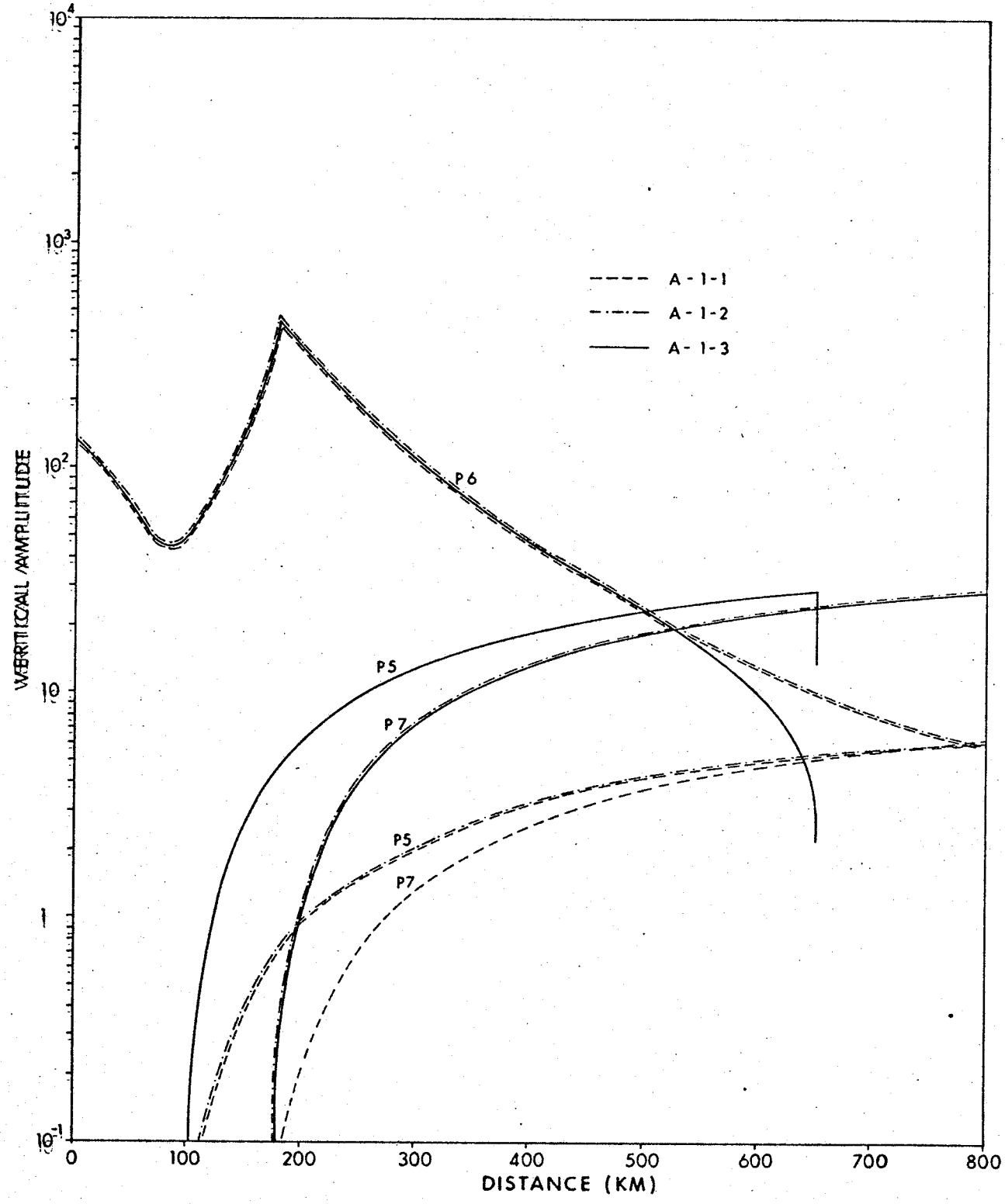

Fig. 8a. Amplitudes vs. distance of principal upper mantle events: Models A-1.1 to 1.3

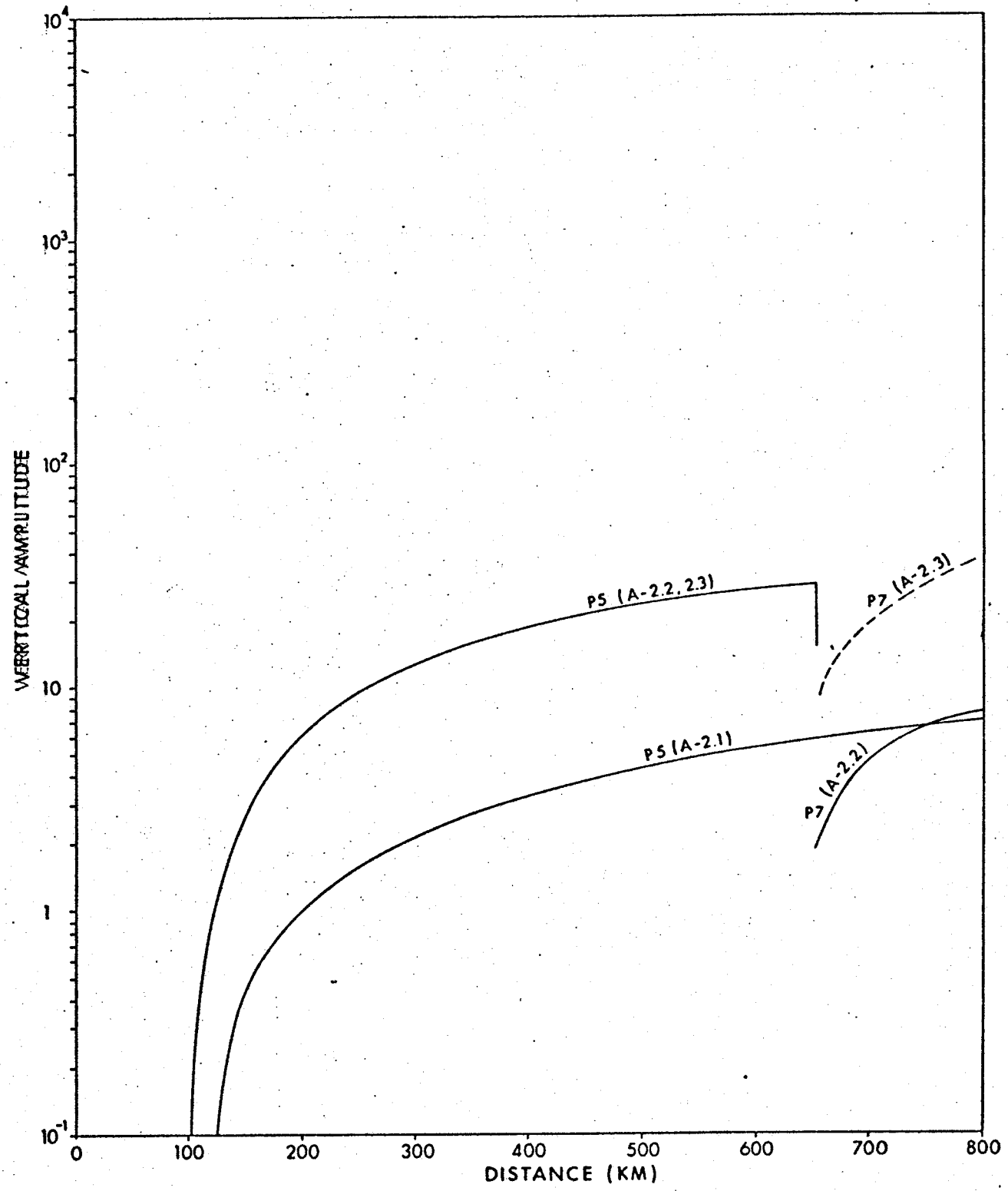

Fig. 8b. Amplitudes vs. distance of principal upper mantle events: Models A-2.1 to 2.3

detection of this type of discontinuity on records from a continuous profile.

CHAPTER 4

INTERPRETATION OF UPPER MANTLE DATA

The 1967-69 mid-range surveys of Hall and Hajnal (1973) and the long range survey of Gurbuz (1969, 1970) presented in Chapter 2 both contain evidence of upper mantle structure. The travel-time curves of events P5, P6 and P7 (Table IV) from the Hall-Hajnal survey have led these authors to interpret a tentative upper mantle model equivalent to that of Model A-1.1 (see preceding chapter), containing a first-order discontinuity at a depth of about 50 km. Gurbuz also found evidence for a sub-Mohorovicic discontinuity within the same depth range based on two events P_m and P_n (whose travel-times are reproduced in Table V); this model is illustrated in Figure 6 of Chapter 2 and the reduced travel-time curves of upper mantle events from both surveys are included with those of the crustal events in Figure 2a-d.

It was shown in Chapter 1 that failure to allow for earth curvature in the analysis of time-distance and amplitude-distance data leads to erroneous interpretations and was subsequently demonstrated that data from both surveys at hand lead independently to a single two-layer crustal model when curvature is included. We now must

determine whether the two sets of sub-Mohorovicic travel time curves, both independently and combined, produce a consistent upper mantle model of the common subsurface when interpreted on the basis of results derived in the preceding chapters.

A qualitative comparison of the upper mantle kinematic data from the surveys with the theoretical model data examined in the preceding chapter does not support the existence of a second-order discontinuity in the upper mantle for the following reasons:

(i) There are no discontinuities in slope of any time-distance curve as theoretically predicted for events penetrating a second-order discontinuity.

(ii) In addition to the P5 event of the mid-range survey, two other prominent events have been picked whose travel-times are consistent with primary events bottoming below a deeper discontinuity. If this discontinuity were of a second-order, however, no additional primary events, distinct from P5, would be produced.

A further comparison of the upper mantle kinematic data with the theoretical curves of Model A-1.1 indicates a favourable agreement in slopes and times, thereby supporting the first-order discontinuity hypothesis. Minor deviations from the theoretical values may be attributable to a greater thickness of the uppermost mantle layer than orig-

inally estinated; velocity functions above and below the lower interface also appear to be greater than first predictions.

4.1 Analysis of Velocities from Upper Mantle Data

Results of the preceding chapters (sections 1.1, 2.1 and 3.3) have demonstrated that small velocity gradients have little effect on the slope and intercept times of refracted events and would be exceedingly difficult to identify on the basis of amplitude variations of traces on regional survey records. Travel-time cusps at anomalously small distances resulting from larger velocity gradients are not evident on either data set. In addition, the inherently large error associated with interval velocity estimates from reflection data (sections 1.4.2 and 2.2) would result in a wide range of theoretical velocity functions which would satisfy the observed data.

As a first approximation, therefore, no gradients in velocity were assumed to exist above and below the discontinuity. Results of linear fits to the refraction time-distance (T-X) data and reflection T^2-X^2 data are summarized in Tables IX a and b. Earth curvature corrections, applied in the same manner as for crustal events, were based on an average upper mantle model A-1.1.

The mid-range data yielded excellent agreement between the velocities derived independently from events P5 and P6, suggesting an average interval velocity of 8.17

TABLE IXa

UPPER MANTLE REFRACTION T-X DATA
LINEAR LEAST SQUARES FIT

Data Source	Event	Intercept T_o (sec.) Fit	Velocity V=(slope)$^{-1}$ (Km./sec.) Fit	Velocity V=(slope)$^{-1}$ (Km./sec.) Curv. Corrected*	RMS Dev (sec.)
MID RANGE SURVEY (127-351 Km.) HALL-HAJNAL 1969 (Recorded 1967-69)	P5	7.01±0.22†	8.20±.07	8.15±.06	0.196
	P7	8.31±0.24	8.73±.07	8.66±.06	0.191
LONG RANGE SURVEY (420-776 Km.) GURBUZ 1970 (Recorded 1966) (PROJECT EARLY RISE	P_n	9.78±0.67	8.48±.07	8.41±.06	0.343
COMBINED MID RANGE and LONG RANGE SURVEYS	$P7/P_n$	6.61±0.25	8.15±.04	8.09±.04	0.570

* Curvature corrections applying Mereu's (1967) formula

TABLE IXb

UPPER MANTLE REFLECTION T^2-X^2 DATA

LINEAR LEAST SQUARES FIT

Data Source	Event	Intercept T_o(sec) Fit	Intercept T_o(sec) Curv. Correct.	Appar.Vel.(Km/sec) Fit	Appar.Vel.(Km/sec) Curv. Correct.	Int.Vel.(Km/sec) Fit	Int.Vel.(Km/sec) Curv. Correct.	RMS Dev. (sec)
MID RANGE SURVEY (127-351 Km.)	P6	16.33±0.53*	14.75±0.48	7.34±.05	6.89±.05	9.22±.77	8.19±.68	0.346
LONG RANGE SURVEY (420-776 Km.)	P_m	28.66±1.67	17.43±1.07	7.90±.06	7.08±.06	11.13±†	9.11±†	0.423
COMBINED MID RANGE and LONG RANGE SURVEYS	$P6/P_m$	19.60±0.90	15.28±0.70	7.67±.03	6.95±.03	9.73±1.40	8.11±1.17	0.408

* All errors calculated for 80% fiducial limits

† Error exceeds physically realizable limits

km/sec. in the uppermost mantle layer; this similarity in the two velocity estimates lends further support to the original premise of a constant velocity in this layer.

The long range survey reflection event P_m, which produced a larger interval velocity of 9.11 km/sec. may be regarded as unreliable due to the excessive scatter in arrival times and attendant error in estimates of intercept time and apparent velocity. It is, in fact, likely that some or all of the time-distance pairs, originally picked and interpreted as event P_m, may actually correspond to reflection multiples similar to those identified in Chapter 2 (ie. whose ray-path in the bottoming layer is twice the length of its primary reflection equivalent). This premise is supported by the apparent velocity and intercept time values deduced from a linear least squares fit of the theoretical time-distance curve derived from model A-1.1 for event $P6_m$. These values (7.75 km/sec. and 24.41 sec., respectively) agree favorably with those obtained from the fit to the P_m data (7.90 ±.06 km/sec. and 28.66 ±1.67 sec., respectively).

Although amplitude studies predict strong sub-Mohorovicic refracted arrivals in the 400-800 km. range when a first-order discontinuity exists at the crustal base, no such event was observed on the Gurbuz seismic records. This may be explained, however, by the nearly simultaneous arrival times of P5 and P6 exhibited by the

upper mantle models 1.1 to 1.3 in the distance range of the Gurbuz survey, which precludes the resolution of the two events.

A confirmation of the sub-Moho discontinuity depth of 50 km. is established by the similarity of the intercept times derived from polynomial fits to the time-distance pairs of P6 from the mid-range survey (Table IXb) and the theoretical model A-1.1 (Table IIIc) for the surface distance range of 120-360 km.

Although the mid-range and long range surveys have independently yielded a consistent crustal model and both support a sub-Mohorovicic velocity discontinuity, the first arrival body waves P7 and P_n produce contradictory evidence of the velocity below this interface. The velocity estimates, when corrected for earth curvature, are 8.66± 0.06 km/sec. and 8.41± 0.06 km/sec. for the mid-range and long range surveys, respectively. Since kinematic data has been shown to be relatively insensitive to vertical velocity gradients, a more likely reason for this discrepancy between the two data sets is a lateral inhomogeneity in both the depth of this interface and the velocity below it. This conclusion is supported both by the large RMS deviation in the linear fit to the long range P_n arrivals and the varied upper mantle interpretations produced by other surveys summarized in Chapter 3.

CONCLUSIONS

Ray-tracing seismic models of a spherically stratified earth demonstrate that compressional reflected and body waves theoretically cannot be detected at the surface beyond a maximum offset distance; this distance is dependent on the compressional velocity for the bottoming layer and its depth. Furthermore, the loci of time-distance pairs for a reflected and a body wave bottoming in the same layer converge with increasing offset distance so that the two events may not be distinguishable on seismic records at large source-receiver distances.

Surface displacement models of seismic waves suggests that events corresponding to refracted body waves, propagating in constant velocity media, increase in distance with increasing offset. Amplitudes of body waves bottoming in crustal layers exceed the amplitudes of crustal reflected waves in the 700-800 km. distance range. This phenomenon is more pronounced when the bottoming layer contains a positive velocity gradient.

The existence of a vertical positive velocity gradient within a given layer is manifested in the termination at anomalously short offsets of both reflected and body wave arrivals bottoming in this layer. This occurence would be most readily observed through the use of a continuous in-line profile having short receiver-to-receiver separations.

Amplitude and kinematic modelling demonstrate that simple reflection multiples are prominent events with travel-

time curves similar to those of primary reflections and could easily be mistaken for the latter, especially on regional profiles having little or no character similarity from record to record.

Model data revealed that body waves bottoming in the uppermost 100 km. below the Mohorovicic discontinuity produce prominent arrivals in the offset range of 100-800 km. This result suggests that, theoretically, upper mantle structural interpretation can be made on seismic records acquired from relatively short-distance range surveys designed for crustal research.

The application of seismic model results to the mid- and long range data of Gurbuz and Hall-Hajnal yields a two layer crustal interpretation; this interpretation suggests an upper crustal layer having a thickness of 18 km. and a 6.05 km/sec. compressional velocity while the lower layer has a thickness and compressional velocity of 16 km. and 6.91 km/sec. respectively. The possibilities of a velocity gradient in the lower layer and existence of a third crustal layer were investigated but are not supported by the observed data when interpreted in conjunction with the ray-tracing models.

Both sets of data are consistent with a single interpretation of an upper mantle first-order discontinuity in the depth range of 50 km., with an intermal compressional velocity of 8.17 km/sec. above the discontinuity. No unique compressional velocity was obtained for the layer below this interface, suggesting the presence of lateral velocity variations.

APPENDIX I

DERIVATION OF DIX'S INTERVAL VELOCITY FORMULA

One Layer

The travel-time T_x for a reflected ray in a single layer of thickness Z and constant velocity V involving no dip or curvature can be expressed as follows:

$$T_x^2 = T_o^2 + \frac{X^2}{V^2} \qquad \text{(I-1)}$$

where $T_o^2 = \frac{4Z^2}{V^2}$ is the intercept time at X = O

and X = the horizontal distance

The velocity therefore is the slope of the $T^2 - X^2$ curve and T_o is the intercept time.

Two Layers

The $T^2 - X^2$ reflection curve for a two layer case will not be a straight line but will curve downwards with increasing X. The effect of the first layer for small X, however, can be removed by considering the angle of incidence Θ, at the base of the upper layer.

We know that

$$\frac{\sin \Theta_1}{V_1} = \frac{dT}{dX}x \qquad \text{(I-2)}$$

A straight line drawn tangent to the $T^2 - X^2$ curve at X = d where $d \ll 1$ will have the form

$$T_x^2 = M + \frac{X^2}{V_a^2(d)} \qquad \text{(I-3)}$$

where $V_a(d)$ is the apparent velocity at X = d. Differentiation of (3) with respect to X gives, at X = d

$$\left.\frac{dT_x}{dX}\right|_{X=d} = \frac{d}{V_a^2(d)T_d} = \frac{\sin\theta}{V_1} \qquad \text{(I-4)}$$

using the relation from (3).

Consider now the ray-path of a down-travelling ray (FIG. A - 1) with very small X and no dip:

let $X_1 + X_2 = d$; $T_1 + T_2 = T_d$

where $T_1 = \frac{2Z}{V_1}$; $T_2 = \frac{2Z_2}{V_2}$

then $d = T_1 V_1 \tan\theta_1 + T_2 V_2 \tan\theta_2 \qquad \text{(I-5)}$

Since d<<1 we can approximate

$$\tan\theta_i \simeq \sin\theta_i \qquad \text{(I-6)}$$

and using Snell's law, equation (5) becomes

$$d \simeq V_1 T_1 \sin\theta_1 + \frac{V_2^2}{V_1} T_2 \sin\theta_2 \qquad \text{(I-7)}$$

Substituting (4) into (7)

$$d \simeq \frac{(V_1^2 T_1 + V_2^2 T_2)\, d}{V_{a_2}^2 (d)\, T_d} \qquad \text{(I-8)}$$

Dividing through by d and taking the limit as d→o (8) becomes

$$\lim_{d\to o} V_{a_2}^2 (d) = \lim_{d\to o} \left(\frac{V_1^2 T_1 + V_2^2 T_2}{T_d} \right)$$

so that

$$V_{a_2}^2(0) = \frac{V_1^2 T_{o_1} + V_2^2 (T_{o_2} - T_{o_1})}{T_{o_2}} \qquad \text{(I-9)}$$

where T_{o_1} and T_{o_2} are the two-way travel-times to the bottom

of the first and second layer, respectively, at X = 0.

Equation (9) can now be solved for the unknown interval velocity in the second layer V_2:

$$V_2 = \left[\frac{V_{a_2}^2 \, T_{o_2} - V_1^2 \, T_{o_1}}{T_{o_2} - T_{o_1}} \right]^{1/2} \qquad \text{(I-10)}$$

N Layers

The two layer result of equation (10) may be generalized to an n-layered medium. The interval velocity in the n^{th} layer is given by

$$V_n = \left[\frac{V_{a_n}^2 \, T_{o_n} - V_{a_{n-1}}^2 \, T_{o_{n-1}}}{T_{o_n} - T_{o_{n-1}}} \right]^{1/2} \qquad \text{(I-11)}$$

where T_{o_i} and $1/V_{a_i}^2$ are the coefficients of the best straight-line fit to the $T^2 - X^2$ curve a reflection from the i^{th} layer.

The preceeding development, following Dix's (1955) derivation, is based on the crucial assumption that X is very near zero, where the angles of incidence are very small and the approximation of equation (6) holds. At larger distances, straight-line fits to $T^2 - X^2$ curves for a given reflection will yield progressively larger erroneous intercept times and apparent velocities with correspondingly high interval velocities.

Deviations from the small-angles-of-incidence approximation at relatively short distances also occur for reflections from the n^{th} layer when n becomes large. Dix's inter-

val velocity formula using apparent velocities derived from inverse slopes of straight line fits to $T^2 - X^2$ data is therefore valid only when X is very near zero and the number of layers is small.

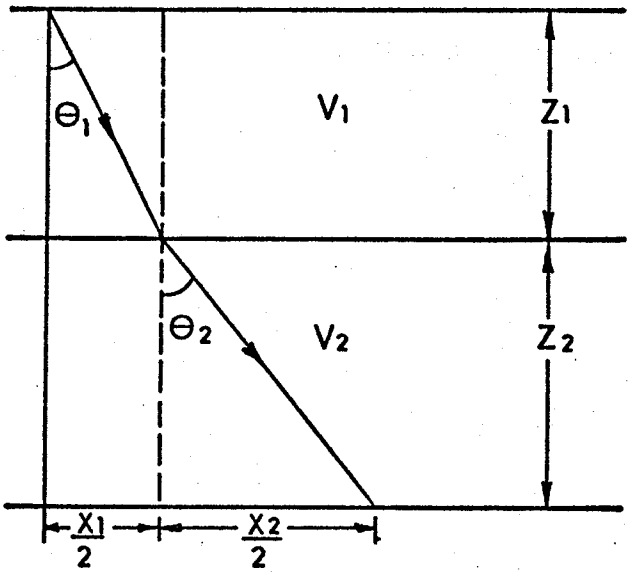

FIGURE A-1 Ray-path geometry for two layer horizontally stratified media

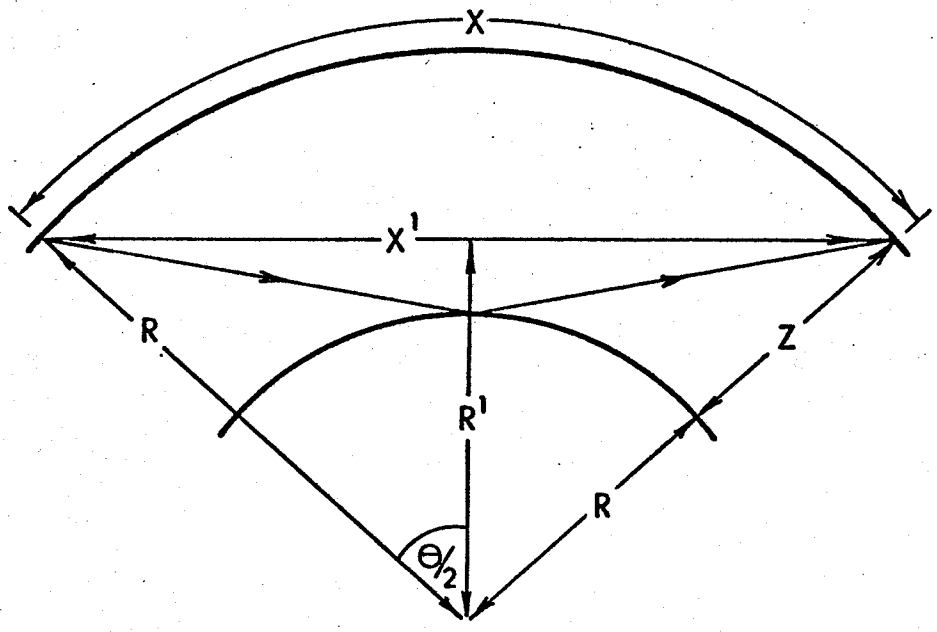

FIGURE A-2 Ray-path geometry for two layer spherically stratified media

APPENDIX II

DEVIATION OF $X^2 - T^2$ FROM STRAIGHT LINE FOR SPHERICAL EARTH - ONE LAYER CASE

The $T^2 - X^2$ curve for a ray reflected from a single layer involving no dip or curvature is exactly a straight line having the form

$$T^2 = \left(\frac{2Z}{V}\right)^2 + \frac{X^2}{V^2} \qquad \text{(II-1)}$$

as shown in equation (1) of Appendix I. At large X, however, the effect of earth curvature becomes significant and the $T^2 - X^2$ curve is no longer a straight line.

Consider the geometry (Figure A-2) for a reflected ray in a single-layer spherically-stratified earth where

R_o = Earth radius

$Z = R_o - R$ = thickness of layer

$Z' = R' - R$ = apparent thickness of layer

$X = \theta R_o$ = source-receiver distance at surface

X' = apparent source-receiver distance

We can relate Z' and Z as follows:

$$Z' = R' - R = R_o \cos(\theta/2) - R_o = Z \qquad \text{(II-2)}$$
$$= Z - R_o\,(1 - \cos(X/2R_o))$$

Similarly, by straightforward geometry,

$$X' = \frac{R_o \sin\theta}{\sin\,(\pi/2 - \theta/2)} = 2R_o \sin\theta/2 \qquad \text{(II-3)}$$

or $$X' = 2R_o \sin(X/2R_o)$$

Expanding cos $(X/2R_o)$ and sin $(X/2R_o)$ with Taylor series expansions and retaining only the first 3 terms of each, equations (2) and (3) become

$$Z' \simeq Z - \frac{X^2}{8R_o} + \frac{X^4}{384R_o^3} \qquad \text{(II-4)}$$

$$X' \simeq X - \frac{X^3}{24R_o} + \frac{X^5}{1920R_o^4} \qquad \text{(II-5)}$$

Equations (4) and (5) represent the depth and horizontal distance corresponding to the equivalent flat earth geometry for which equation (1) holds.

Substituting equations (4) and (5) into equation (1), we have

$$T'^2 = \frac{1}{V^2}\left[\left(X - \frac{X^3}{24R_o^2} + \frac{X^5}{1920R_o^4}\right)^2 + 4\left(Z - \frac{X^2}{8R_o} + \frac{X^4}{384R_o^3}\right)^2\right]$$

$$= \frac{4Z^2}{V^2} + \frac{X^2}{V^2} - \frac{X^2}{V^2}\left[\frac{Z}{R_o} + \frac{X^2}{48R_o^2} - \frac{ZX^2}{48R_o^3} - \frac{X^4}{5760R_o^4}\right] \qquad \text{(II-6)}$$

The first two right-side terms of equation (6) represent the total T^2 for a single plane layer of thickness Z while the last term represents the difference ΔT between the plane and spherically layered $T^2 - X^2$ reflection curves.

APPENDIX III

THEORETICAL VERTICAL AMPLITUDE DISPLACEMENTS FOR WAVES IN A PLANE LAYERED MEDIUM

The amplitude formulae described herein are based on a time-series solution (Cerveny and Ravindra,1971) to the plane wave equation (expressed in inverse powers of frequency) having the form

$$W = \exp\{i\omega\ (t - \tau)\} \sum_{0}^{\infty} (i\omega)^{-k} W_k \qquad \text{(III-1)}$$

where W is the particle displacement vector. Equation (1) is a ray series where τ is a phase function and W_k are the amplitude coefficients.

III.1 Reflected and refracted (diving) waves

The zero-order solution, obtained according to the principles of geometric optics, employs only the leading terms of eq'n. (1) and has been found to be sufficiently accurate for reflected and refracted waves.

Restricted versions of the generalized amplitude formulae given by Cerveny (op cit) were developed to satisfy the following conditions:

a. A multilayered (horizontally stratified) medium exists and contains no lateral inhomogeneities.

b. The source and receiver both lie at the top of the first layer (ie. at or near the free surface).

c. The compressional-wave velocity in the j^{th} layer can be

expressed by $v = v_j\{ 1 + b_j(z - z_j)\}$ where v_j is the velocity at the top of the layer having a depth z_j, and $b_j>0$ is a constant positive velocity gradient.

Note that refracted or diving waves (as distinguished from head waves) are those waves which have a turning point in the bottoming layer due to a positive gradient ; the ray therefore penetrates the bottom layer to a depth dependent on the ray parameter.

The amplitude formulae of the vertical component of displacement for reflected and refracted waves are as follows:

$$A_z^r = \frac{1\{}{|L|} \prod_{1}^{l-1} |R_j| \times |R_{21-j}| \} \; R_1 q_z \qquad \text{(III-2a)}$$

for a ray reflected in the j^{th} layer (ie. at the $(j+1)^{th}$ interface and

$$A_z^r = \frac{1\{}{|L|} \prod_{1}^{l-1} |R_j| \times | R_{21-j}| \} \; q_z \qquad \text{(III-2b)}$$

for a refracted ray bottoming in the j^{th} layer (ie. below the j^{th} interface)

The variables in the RHS of 2(a) and 2(b) are defined as follows:

$$L = \left\{ 2r \left(\sum_{1}^{l} \frac{\partial r_j}{\partial \phi_o} \right) \frac{1-p^2v_1^2}{pv_1} \right\}^{\frac{1}{2}}$$

is the spreading function where

$p \equiv \sin \phi / v$ is the ray parameter

ϕj, $\phi j'$= angles of incidence and transmission respectively at the j^{th} interface

r_j = distance travelled by a wave in the j^{th} layer where

$$\underline{b_j>0}: \quad r_j=\{(1-p^2v_j^2)^{\frac{1}{2}}-\{1-p^2v_j^2(1+b_j(z_{j+1}-z_j))^2\}^{\frac{1}{2}}\}/\!/ \; pv_jb_j \tag{III-5a}$$

$$\frac{\partial r_j}{\partial \phi_o}=\frac{r_j(1-p_2^2v_1^2)^{\frac{1}{2}}(1-p^2v_j^2)^{\frac{1}{2}}}{pv_1\{1-p^2v_j^2(1+b_j(z_{j+1}-z_j))^2\}^{\frac{1}{2}}} \tag{III-5b}$$

$$\underline{b_j=0}: \quad r_j = (z_{j+1}-z_j)pv_j/(1-p^2v_j^2)^{\frac{1}{2}} \tag{III-6a}$$

$$\frac{\partial r_j}{\partial \phi_o} = \frac{(z_{j+1}-z_j)v_j(1-p^2v_1^2)^{\frac{1}{2}}}{v_1(1-p^2v_j^2)^{3/2}} \tag{III-6b}$$

For reflected waves: $r = 2\sum^{l} r_j$

For refracted waves: $r = 2\sum^{l-1} r_j + \frac{1}{|b_l|}\frac{(1-p^2v_l^2)^{\frac{1}{2}}}{pv_l}$

The R-coefficients of equations (2a) and (2b) are the coefficients of reflection and transmission at layer interfaces. General equations for these coefficients were first derived by Knott (1899) and Zoeppritz (1919); the analytic expressions, however, are excessively cumbersome for numerical calculations and approximate solutions have been derived by Gutenburg (1944), Steinhart and Meyer (1961), Tooley et. al (1965), Berry and West (1965), and others.

The present treatment follows that of Cerveny and Ravindra (1971) where R_{mn} is the solution of a set of four

linear equations:

$$\sum_{1}^{4} a_{in} R_{mn} = (-1)^{i} a_{im} \quad (i=1,2,3,4) \qquad \text{(III-9)}$$

where a_{in} are elements of matrix A:

$$A = \begin{matrix} \sin\theta_1 & \cos\theta_2 & -\sin\theta_3 & -\cos\theta_4 \\ \cos\theta_1 & -\sin\theta_2 & \cos\theta_3 & -\sin\theta_4 \\ \rho_1\alpha_1\cos 2\theta_2 & -\rho_1\alpha_1\gamma_1\sin 2\theta_2 & -\rho_2\alpha_2\cos 2\theta_4 & \rho_2\alpha_2\gamma_2\sin 2\theta_4 \\ \rho_1\alpha_1\gamma_1^2\sin 2\theta_1 & \rho_1\alpha_1\gamma_1\cos 2\theta_2 & \rho_2\alpha_2\gamma_2^2\sin 2\theta_3 & \rho_2\alpha_2\gamma_2\cos 2 \end{matrix}$$

The ordered subscripts m and n of the R coefficient define the ray on the upper and lower sides of an interface where

m,n = 1 corresponds to P wave ray segment above interface
m,n = 2 " " SV " " " " "
m,n = 3 " " P " " " below "
m,n = 4 " " SV " " " " "

so that, for example, R_{13} diagramatically, corresponds to

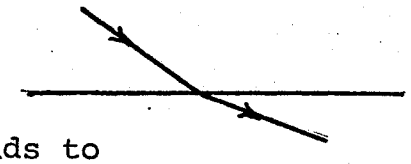

and R_{11} corresponds to

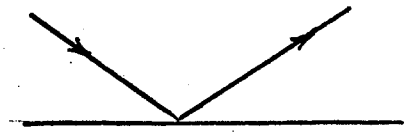

α_i, β_i (i=1,2) = P wave and SV wave velocities respectively above (i=1) and below (i=2) the interface

ρ_i (i=1,2) = density of media above and below the interface

$\gamma_i = \alpha_i/\beta_i$ and

q_z = conversion coefficient for a receiver on the earth's surface.

1.2 Head Waves

Head waves are defined as waves whose ray paths are critically refracted at a plane interface and which travel at the top of the medium below the interface provided the medium contains n velocity gradient. Original theoretical solutions of the wave equation were based on integral methods (Cf. Cagniard, 1962; Petrashen, 1964) it was later shown, however, that for non-interfering head waves, all results deduced by wave methods could be derived through geometric optics by the ray method which produces an asymptotic (ray) series solution given by equation (1). The following vertical amplitude formula (Cerveny and Ravindra, 1971) is based on a first order (second term) solution for a symmetric, non-converted head wave having both source and receiver at the free surface and bottoming in the 1^{th} layer

$$A_z^* = \frac{v_1 v_1}{r^{\frac{1}{2}}(v_1^2-v_1^2)^{\frac{1}{2}}(r-r^*)^{3/2}} \left| \Gamma_{1-1} \prod_{j=1}^{1-2} R_j R_{21-1-j} \right| q_z \qquad \text{(III-11)}$$

where $r^* = 2 \sum_{1}^{\ell-1} r_j^*$ is the critical distance (III-12)

$$r_j^* = \frac{(z_{j+1}-z_j)(v_j(1+b_j(z_{j+1}-z_j))+v_j)}{(v_\ell^2-v_j^2)^{\frac{1}{2}}+(v_\ell^2-v_j^2(1+b_j(z_{j+1}-z_j))^2)^{\frac{1}{2}}} \quad \text{(III-13)}$$

Γ_k = head wave coefficient for the interface at which the ray is critically refracted.

The remaining variables in equation (11) are defined in equations (4) to (10).

Computer programs RWAMP and HWAMP (Appendix II) were written to calculate the amplitudes of symmetric reflected waves, diving waves and head waves using the preceding thecry for a horizontally stratified medium.

APPENDIX IV

PROGRAMS: HWAMP and RDAMP

A. IDENTIFICATION

Title: Vertical amplitude variations with distance for head waves, diving waves and reflected waves in a horizontally stratified earth model.

Programmer: R. Desmarais

Date: January, 1973

Language: FORTRAN IV

B. PURPOSE

To calculate the amplitude-distance curves of compressional reflected and refracted waves using the classical plane-wave theory derived for horizontally stratified media.

C. USAGE

1. Operational Procedure: Program RDAMP calculates amplitudes for reflected waves and diving waves; program HWAMP calculates head wave amplitudes. Program MAIN of each reads the input parameters defining the earth model and calculates the theoretical times and distances for the rays bottoming in a specified layer. The amplitudes for each distance are calculated using the reflectivity coefficients derived from subroutine RCOEFF.

2. Input Parameters:

M = number of layers + 1

Z(I),(I=1,M) = depth to top of each layer

VP(I),(I=1,M) = compressional wave velocity for each layer

VS(I),(I=1,M) = shear wave velocity for each layer

B(I),(I=1,M) = linear velocity gradient for each layer

RO(I),(F=1,M) = density of each layer

3. Output Parameters:

Program HWAMP

RC = critical distance

TC = critical time

G131 = transmissivity coefficients for interface at which head wave is critically refracted

Programs HWAMP and RDAMP

R13(I),(I=1,M-1) = transmissivity coefficients for down-going ray path

R31(I),(I=1,M-1) = transmissivity coefficient for up-going ray path

R11 = reflectivity coefficient for reflecting interface (where applicable)

RCOF = product of transmissivity and (where applicable) reflectivity coefficients for all interfaces encountered by ray

RI = surface distance of ray

RR = travel-time at distance RI

RT = reduced travel-time

AMP = vertical amplitude displacement at distance RI

4. Space Requirements: 84K for each program
5. Temporary Storage: none
6. Input Tape: none
7. Output Tape: none
8. Time: 3.6 sec. for 40 distance-points
9. Reference: Cerveny and Ravindra (1971)
10. Remarks: The mathematical equations used in the programs are given in Appendix III. Due to the simplicity of the programs, no detailed descriptions follow.

```
C  PROGRAM HWAMP                          PROGRAMMER: R.J. DESMARAIS
C  HEAD WAVE AMPLITUDE VARIATIONS WITH DISTANCE
      COMPLEX*16 G131
      DOUBLE PRECISION VP(6),VS(6),Z(7),RO(6),B(6),P,RCOF,Q3Z,AMP,T,R(7
     1,ZB,RR,VPB,DLOG,DABS,CDABS,RI,RC,TC,DELTA,AMP1,TN,TT
      COMMON IND,NL,VP,VS,Z,RO,B,P,RCOF,Q3Z,ZB,G131
  100 READ(1,10) M
      READ(1,11) (Z(I),I=1,M)
      NL=M-1
      READ(1,11) (VP(I),I=1,M)
      READ(1,11) (VS(I),I=1,M)
      READ(1,11) (B(I) ,I=1,M)
      READ(1,11) (RO(I),I=1,M)
      WRITE(3,12)
   12 FORMAT(1H ,'DEPTH',5X,'P-VELOCITY',5X,'S-VELOCITY',5X,'GRADIENT',
     15X,'DENSITY')
      WRITE(3,13) (Z(I),VP(I),VS(I),B(I),RO(I),I=1,M)
   13 FORMAT(1H ,F5.2,8X,F4.2,11X,F4.2,8X,F8.6,6X,F5.2)
   10 FORMAT(I2)
   11 FORMAT(7F10.2)
C
C CALCULATE CRITICAL DISTANCE AND TIME
      RC=0.D0
      T=0.D0
      P=1.D0/VP(M)
      DO 1 I=1,NL
      IF(B(I)) 3,2,3
    2 R(I)=(Z(I+1)-Z(I))*P*VP(I)/(1.D0-P*P*VP(I)**2.D0)**.5D0
      T=T+ (Z(I+1)-Z(I))/(((1.D0-P*P*VP(I)*VP(I))**.5D0)*VP(I))
      GO TO 1
C DETERMINE WHETHER RAY BOTTOMS IN ITH LAYER
    3 ZB=(1.D0/(P*VP(I))+B(I)*Z(I)-1.D0)/B(I)
      IF(ZB.GT.Z(I).AND.ZB.LT.Z(I+1)) GO TO 4
      R(I)=((1.D0-P*P*VP(I)*VP(I))**.5D0-(1.D0-P*P*VP(I)*VP(I)*(1.D0+B
     1)*(Z(I+1)-Z(I)))**2.D0)**.5D0)/(P*VP(I)*B(I))
      VPB=VP(I)*(1.D0+B(I)*(Z(I+1)-Z(I)))
      T=T+(Z(I+1)-Z(I))*DLOG((VPB*(1.D0+(1.D0-P*P*VP(I)*VP(I))**.5D0))
     1VP(I)*(1.D0+(1.D0-P*P*VPB*VPB)**.5D0)))/(VPB-VP(I))
      GO TO 1
    1 RC=RC+2.D0*R(I)
      TC=2.D0*T
      TN=P*VP(1)/((1.D0-P*P*VP(1)*VP(1))**.5D0)
      DELTA=1.D0
      WRITE(3,21) RC,TC
      WRITE(3,51)
      CALL RCOEFF
   61 FORMAT(1H ,6(E14.5,2X))
      AMP1=RCOF*VP(M)*DELTA*(DABS(Q3Z))*TN*CDABS(G131)/10.D0
      AMP1=AMP1/6.29
      WRITE(3,61) RCOF,G131,Q3Z,TN,AMP1
      RC1=SNGL(RC/10.D0)
      II=IFIX(RC1+1.)
      RI=II*10
      DO 50 I=1,70
      AMP=AMP1/((RI**.5D0)*((RI-RC)**1.5D0))
      TT=TC+(RI-RC)/VP(M)
      RT=TT-(RI/7.90)
      WRITE(3,52) RI,TT,AMP,RT
```

```
   50  RI=RI+10.00
       GO TO 100
    4  WRITE(3,53) I
   53  FORMAT(1H ,'RAY BOTTOMS IN LAYER ',I2)
   21  FORMAT(1H ,'CRITICAL DIST. =',F6.2/1H ,'CRITICAL TIME =',F5.2)
   51  FORMAT(1H ,'DISTANCE',10X,'TIME',10X,'AMPLITUDE'//)
   52  FORMAT(3X,F6.2,9X,F6.2,10X,E14.5,F6.2)
   60  STOP
       END
```

```
      SUBROUTINE RCOEFF
      COMPLEX*16  P1,P2,P3,P4,R13(6),R31(6),D,A1,A2,B1,B2,CDSQRT,G131
      DOUBLE PRECISION VP(6),VS(6),Z(7),RO(6),B(6),RCOF,Q3Z,ZB,RO1,RO2,
     1Q,X,Y,ZZ,P,CDABS
      COMMON IND,NL,VP,VS,Z,RO,B,P,RCOF,Q3Z,ZB,G131
C  CALCULATE THE CONVERSION COEFF Q3Z FOR RECEIVER AT SURFACE
      P1=(1.DO-VP(1)*VP(1)*P*P)**.5DO
      P2=(1.DO-VS(1)*VS(1)*P*P)**.5DO
      D=(1.DO-2.DO*VS(1)*VS(1)*P*P)**2.DO+4.DO*P1*P2*P*P*(VS(1)**3.DO)/
     1P(1)
      Q3Z=2.DO*P1*(1.DO-2.DO*VS(1)*VS(1)*P*P)/D
C  CALCULATE THE R-COEFFICIENTS AND THEIR PRODUCT
      RCOF=1.DO
      DO 1 I=1,NL
    4 A1=VP(I)*(1.DO+B(I)*(Z(I+1)-Z(I)))
      A2=VP(I+1)
      B1  =VS(I)*(1.DO+B(I)*(Z(I+1)-Z(I)))
      B2  =VS(I+1)
      RO1=RO(I)
      RO2=RO(I+1)
      Q=2.DO*(RO2*B2*B2-RO1*B1*B1)
      X=RO2-Q*P*P
      Y=RO1+Q*P*P
      ZZ=RO2-RO1-Q*P*P
      P1=CDSQRT(1.DO-A1*A1*P*P)
      P2=CDSQRT(1.DO-B1*B1*P*P)
      P3=CDSQRT(1.DO-A2*A2*P*P)
      P4=CDSQRT(1.DO-B2*B2*P*P)
      D=A1*A2*B1*B2*P*P*ZZ*ZZ+A2*B2*P1*P2*X*X+A1*B1*P3*P4*Y*Y+RO1*RO2*(
     1B1*A2*P1*P4+A1*B2*P2*P3)+Q*Q*P*P*P1*P2*P3*P4
      IF(I.EQ.NL) GO TO 2
      R13(I)=2.DO*A1*RO1*P1*(B2*P2*X+B1*P4*Y)/D
      R31(I)=2.DO*A2*RO2*P3*(B1*P4*Y+B2*P2*X)/D
      WRITE(3,88) R13(I),R31(I)
   88 FORMAT(1H ,2(E14.5,2X,E14.5))
      RCOF=RCOF*CDABS(R13(I))*CDABS(R31(I))
      GO TO 1
    2 G131=2.DO*A1*A2*RO1*RO2*P1*((B2*P2*X+B1*P4*Y)**2)/(D*D)
    1 CONTINUE
    3 RETURN
      END
```

```
C  PROGRAM RDAMP                    PROGRAMMER  R.J. DESMARAIS
C REFLECTION AND DIVING WAVE AMPLITUDE VARIATIONS WITH DISTANCE
      COMPLEX*16 CDSQRT,L,DR
      DOUBLE PRECISION VP(6),VS(6),Z(7),RO(6),B(6),P ,RCOF,Q3Z,AMP,T,R(
     1),ZB,RR,VPB,DLOG,DABS,CDABS
      COMMON IND,NL,VP,VS,Z,RO,B,P,RCOF,Q3Z,ZB
      READ(1,10) M
      READ(1,11) (Z(I),I=1,M)
      NL=M-1
      READ(1,11) (VP(I),I=1,M)
      READ(1,11) (VS(I),I=1,M)
      READ(1,11) (B(I) ,I=1,M)
      READ(1,11) (RO(I),I=1,M)
      WRITE(3,12)
   12 FORMAT(1H ,'DEPTH',5X,'P-VELOCITY',5X,'S-VELOCITY',5X,'GRADIENT',
     15X,'DENSITY')
      WRITE(3,13) (Z(I),VP(I),VS(I),B(I),RO(I),I=1,M)
   13 FORMAT(1H ,F5.2,8X,F4.2,11X,F4.2,8X,F8.6,6X,F5.2)
   10 FORMAT(I2)
   11 FORMAT(7F10.2)
      WRITE (3,7)
    7 FORMAT(1HO,'RAY PARM-P',5X,'DISTANCE',5X,'TIME',5X,'AMPLITUDE')
      P=0.0
   99 P=P+0.001
C
C CALCULATE TRAVEL TIMES AND DISTANCES
      RR=0.D0
      DR=0.D0
      T=0.D0
      IND=0
      DO 1 I=1,NL
      IF(B(I)) 3,2,3
   2  R(I)=(Z(I+1)-Z(I))*P*VP(I)/(1.D0-P*P*VP(I)**2.D0)**.5D0
      T=T+ (Z(I+1)-Z(I))/(((1.D0-P*P*VP(I)*VP(I))**.5D0)*VP(I))
      DR=DR+((Z(I+1)-Z(I))*VP(I)*(1.D0-P*P*VP(1)*VP(1))**.5D0)/(VP(1)*(
     1.D0-P*P*VP(I)*VP(I))**1.5D0)
      GO TO 1
C DETERMINE WHETHER RAY BOTTOMS IN ITH LAVER
   3  ZB=(1.D0/(P*VP(I))+B(I)*Z(I)-1.D0)/B(I)
      IF(ZB.GT.Z(I).AND.ZB.LT.Z(I+1)) GO TO 4
      R(I)=((1.D0-P*P*VP(I))**.5D0-(1.D0-P*P*VP(I)*VP(I)*(1.D0+B(I)*(Z(
     1+1)-Z(I)))**2.D0)**.5D0)/(P*VP(I)*B(I))
      VPB=VP(I)*(1.D0+B(I)*(Z(I+1)-Z(I)))
      DR=DR+(R(I)*((1.D0-P*P*VP(1)*VP(1))**.5D0))/(((1.D0-P*P*VP(I)*VP(
     1))**.5D0)*((1.D0-P*P*VPB*VPB)**.5D0)*P*VP(1))
      T=T+(Z(I+1)-Z(I))*DLOG((VPB*(1.D0+(1.D0-P*P*VP(I)*VP(I))**.5D0))/
     1VP(I)*(1.D0+(1.D0-P*P*VPB*VPB)**.5D0)))/(VPB-VP(I))
      GO TO 1
   4  IF(I .NE.NL) GO TO 5
      R(I)=((1.D0-P*P*VP(I)*VP(I))**.5D0)/(B(I)*P*VP(I))
      DR=DR-((R(I)*(1.D0-P*P*VP(1)*VP(1))**.5D0))/(P*VP(1)*(1.D0-P*P*VP
     1I)*VP(I))*2.D0)
      T=T+DLOG((1.D0+(1.D0-P*P*VP(I)*VP(I))**.5D0)/(P*VP(I)))/(DABS(B(I
     1)*VP(I))
      IND=1
 1    RR=RR+2.D0*R(I)
      T=2.D0*T
C  CALCULATE SPREADING FUNCTION L
```

```
      ER=1.DO-P*P*VP(1)*VP(1)
      L=CDSQRT(2.DC*RR*DR*(ER**.5DO)/(P*VP(1)))
C  CALCULATE R-COEFFICIENTS
      CALL RCOEFF
      WRITE(3,81) RCOF
   81 FORMAT(1H ,'RCOF=',E14.5)
      AMP=RCOF*Q3Z/(CDABS(L))
      IF(IND .EQ. 1)GO TO 101
      GO TO 102
  101 WRITE(3,8) ZB
  102 CONTINUE
      WRITE(3,9)P,RR,T,AMP
    8 FORMAT(1H ,'DIVING WAVE FROM Z= ',F5.2,'KM')
    9 FORMAT(1H ,2X,Fo.4,8X,F6.2,6X,F6.2,5X,E12.5)
      IF(RR .GT. 1000.) GO TO 100
      GO TO 99
    5 WRITE(3,14) I
   14 FORMAT(1H ,'RAY BOTTOMS ABOVE ANTICIPATED DEEPEST LAYER')
  100 CONTINUE
      STOP
      END
```

```
      SUBROUTINE RCOEFF
      COMPLEX*16  P1,P2,P3,P4,R13(6),R31(6),D,A1,A2,B1,B2,CDSQRT
      DOUBLE PRECISION VP(6),VS(6),Z(7),RO(6),B(6),RCOF,Q3Z,ZB,RO1,RO2,
     1Q,X,Y,ZZ,P,CDABS
      COMMON IND,NL,VP,VS,Z,RO,B,P,RCOF,Q3Z,ZB
C  CALCULATE THE CONVERSION COEFF Q3Z FOR RECEIVER AT SURFACE
      P1=(1.D0-VP(1)*VP(1)*P*P)**.5D0
      P2=(1.D0-VS(1)*VS(1)*P*P)**.5D0
      D=(1.D0-2.D0*VS(1)*VS(1)*P*P)**2.D0+4.D0*P1*P2*P*P*(VS(1)**3.D0)/
     1P(1)
      Q3Z=2.D0*P1*(1.D0-2.D0*VS(1)*VS(1)*P*P)/D
C  CALCULATE THE R-COEFFICIENTS AND THEIR PRODUCT
      LL=NL-1
      IF(LL .EQ. 0.AND.IND.EQ.1) GO TO 3
      RCOF=1.D0
      DO 1 I=1,NL
    4 A1=VP(I)*(1.D0+B(I)*(Z(I+1)-Z(I)))
      A2=VP(I+1)
      B1  =VS(I)*(1.D0+B(I)*(Z(I+1)-Z(I)))
      B2  =VS(I+1)
      RO1=RO(I)
      RO2=RO(I+1)
      Q=2.D0*(RO2*B2*B2-RO1*B1*B1)
      X=RO2-Q*P*P
      Y=RO1+Q*P*P
      ZZ=RO2-RO1-Q*P*P
      P1=CDSQRT(1.D0-A1*A1*P*P)
      P2=CDSQRT(1.D0-B1*B1*P*P)
      P3=CDSQRT(1.D0-A2*A2*P*P)
      P4=CDSQRT(1.D0-B2*B2*P*P)
      D=A1*A2*B1*B2*P*P*ZZ*ZZ+A2*B2*P1*P2*X*X+A1*B1*P3*P4*Y*Y+RO1*RO2*(
     1B1*A2*P1*P4+A1*B2*P2*P3)+Q*Q*P*P*P1*P2*P3*P4
      IF(LL.EQ.0) GO TO 6
      IF(I .EQ.NL) GO TO 6
      R13(I)=2.D0*A1*RO1*P1*(B2*P2*X+B1*P4*Y)/D
      R31(I)=2.D0*A2*RO2*P3*(B1*P4*Y+B2*P2*X)/D
   88 FORMAT(1H ,2(E14.5,2X,E14.5))
      RCOF=RCOF*CDABS(R13(I))*CDABS(R31(I))
      IF(I-LL) 1,5,5
    5 IF(IND)1,1,3
    6 RCOF=RCOF*CDABS(-1.D0+2.D0*P1*(A2*B2*P2*X*X+B1*A2*RO1*RO2*P4+Q*Q*
     1P*P*P2*P3*P4)/D)
    1 CONTINUE
    3 RETURN
      END
```

APPENDIX V

PROGRAM: POLYFIT

A. IDENTIFICATION

Title: Least squares fit of an n^{th} degree polynomial to data

Programmer: R. Desmarais

Date: May, 1975

Language: FORTRAN IV

B. PURPOSE

To compute the set of n+1 coefficients of an n^{th} degree polynomial which best fits a discrete set of squared time and distance values for a reflected event.

C. USAGE

1. Operational Procedure: Program MAIN reads the data sets and the highest desired degree of polynomial fit. It then creates the required system of normal linear equations in matrix form. Subroutine GAUSS calculates the solution vector.

2. Input Parameters:

NSETS = number of input data sets

NP = number of ordered pairs per data set

N = maximum number of polynomial coefficients

DEL(I), (I=1,NP) = distance values

T(I,J), (I=1,NP), (J=1,NSETS) = time values

3. Output Parameters:

   AA(I,J), (I,J=1,N) = matrix elements of A where AX=B

   BB(I), (I=1,N) = elements of matrix B

   X(I), (I=1,N) = elements of solution vector X corresponding to least squares fitted polynomial coefficients

   NSETI = data set number

   RMS = root-mean-square deviation of polynomial fit to data set NSETI

   DEL2(I), (I=1,NP) = squares DEL(I)

   T2(I), (I=1,NP) = squares of T(I)

   ET(I), (I=1,NP) = values of polynomial at DEL(I)

   ET1(I), (I=1,NP) = squares of ET(I)

4. Space Requirement: 96K

5. Temporary Storage: none

6. Input Tape: none

7. Output Tape: none

8. Time: 52.24 seconds for three 40 point data sets and highest fitted polynomial of degree 5

9. Reference: P.W. Williams (1972) p. 58-64

POLYFIT PROGRAM DESCRIPTION

The purpose of this program is to calculate the coefficients X_i, i=1, n for an n-1 degree polynomial $p(d^2)$ which best fits a discrete set of m $t^2 - d^2$ values. Minimization, in a least squares sense, of the error between the data and $p(d^2)$ leads to a set of n normal linear equations which determine the coefficients x_i:

$$a_{11}\, x_1 + a_{12}\, x_2 + \ldots\ldots\ldots\ldots + a_{2n}\, x_n = b_1$$

$$a_{21}\, x_1 + a_{22}\, x_2 + \ldots\ldots\ldots\ldots + a_{2n}\, x_n = b_2$$

$$\ldots\ldots\ldots\ldots\ldots\ldots\ldots\ldots\ldots\ldots\ldots\ldots$$

$$a_{n1}\, x_1 + a_{n2}\, x_2 + \ldots\ldots\ldots\ldots + a_{nn}\, x_n = b_n$$

where $a_{ij} = (d_k^2)$

$b_i = t_k^2 (d_k^2)^{i-1}$

Program MAIN reads the data and calculates the elements of A and B. The solution of the matrix equation AX=B for the polynomial coefficients $X = \{x, x, \ldots, x_{n+1}\}$ is accomplished by subroutine GAUSS using the method of Gaussian reduction. This method performs operations on the system to convent matrix A into upper triangular form; elements of X are then solved by back substitution.

The accuracy of X is in part a function of the degree of ill-conditioning of the original matrices. Numerical analysis has shown, however, that first approximations to the solution can be improved upon by using the residuals $R=\{r_i\}$ defined by AX-B=R where X is the first approximation. Because

$AX^{O}-B=0$ represents the true solution, then $A(\Delta X)=R$ where $\Delta X=X^{O}-X$ is the difference between the first approximation and the true solution. A solution for ΔX is obtained by the same method as above. This record approximation is used in GAUSS only when the magnitude of the residuals $ER\equiv |r_i|$ exceeds a predetermined value after the first iteration.

Once the desired accuracy in X has been achieved for the $(n-1)^{th}$ degree polynomial fit, the values are returned to MAIN and the remaining output parameters are calculated. The order of the polynomial to be fitted is then reduced by one, the matrices re-initialized and the process repeated. This procedure is continued until all polynomial fits from degree 2 to n-1 have been calculated, after which another data set is read and the entire procedure repeated.

It should be noted that the method of Gaussian reduction is very sensitive to round-off error and its application is therefore limited to low $n(n<10)$. For higher order polynomial fits, the method of orthogonal projection (Cf. Sheid(1968), p.236-37) is recommended.

```
      PROGRAM  POLYFIT
      PROGRAMMER:  R.J. DESMARAIS
  THIS PROGRAM FITS 1ST TO 5TH O DEGREE POLYNOMIALS IN A
  LEAST SQUARES SENSE TO THEORETICAL T2-DEL2 REFLECTION TRAVEL
  TIME CURVES

  NSETS=NO. OF INPUT REFLECTION CURVES
  NP= NO. DATA PTS PER CURVE
  N-1= ORDER OF FITTED POLYNOMIAL
      DOUBLE PRECISION AA(6,6),BB(6),RM(6),R(6),DX(6),X(6),DEL(50),
     1T(50,7),RN1,RN2,AT,DIF,RJ,SQAT,RMS,DABS,DSQRT,B,RA(6,6),RB(6)
      DOUBLE PRECISION ET(50),ET2(50),T2(50),RT(50),RET(50),DEL2(50)
      DOUBLE PRECISION RNP
      COMMON RA,RB,X,N,NSETI
  98  READ(1,1) NP,NSETS
  1   FORMAT(2I5)
      NSETI=C
      DO 3 I=1,NP
  3   READ(1,2) DEL(I),(T(I,J),J=1,NSETS)
  2   FORMAT(8F10.C)
   INITIALIZE MATRICES TO ZERO
  102 NSETI=NSETI+1
      IF(NSETI .GT. NSETS) GO TO 98
      N=6
      DO 4 I=1,N
      DO 4 J=1,N
  4   AA(I,J)=0.DO

      DO 5 K=1,NP
      DO 5 I=1,N
      DO 5 J=1,N
      RN2=2*(I+J)-4
  5   AA(I,J)=AA(I,J)+DEL(K)**RN2
      WRITE(3,10)
  10  FORMAT(1H ,'COEFFICIENT MATRIX')
      DO 11 I=1,4
  11  WRITE(3,12)(AA(I,J),J=1,N)
  12  FORMAT(1H ,6(E15.7,2X))
      N=6
      DO 7 I=1,N
  7   BB(I)=C.DO
      DO 6 I=1,N
      RN1=2*I-2
      DO 6 K=1,NP
  6   BB(I)=BB(I)+(T(K,NSETI)**2.DO)*(DEL(K)**RN1)
      WRITE(3,13)
  13  FORMAT(1H ,'DATA MATRIX B')
      WRITE(3,14)(BB(I),I=1,N)
  14  FORMAT(1H ,6(E15.7,2X))
  101 DO 55 I=1,N
      NI=N+1-I
      DO 55 J=1,N
      NJ=N+1-J
  55  RA(I,J)=AA(NI,NJ)
      DO 67 I=1,N
      NI=N+1-I
  67  RB(I)=BB(NI)
      CALL GAUSS
```

```
      CALCULATE RMS DEV OF FIT TO CURVE
          B=0.D0
          DO 17 I=1,NP
          AT=0.DC
          DIF=0.D0
          DO 16 J=1,N
          RJ=2*J-2
          JJ=N+1-J
       16 AT=AT+X(JJ)*DEL(I)**RJ
          ET2(I)=AT
          AT=DABS(AT)
          SQAT=DSQRT(AT)
          ET(I)=SQAT
          T2(I)=T(I,NSETI)**2.D0
          RT(I)=T2(I)-(DEL(I)**2.D0)/62.41
          RET(I)=ET2(I)-(DEL(I)**2.DC)/62.41
          DEL2(I)=DEL(I)**2.D0
          DIF=T(I,NSETI)-SQAT
          DIF=DABS(DIF)
       17 B=B+DIF*DIF
          RNP=NP
          B=DABS(B/RNP)
          RMS=DSQRT(B)
          WRITE(3,18) N,NSETI,RMS
       18 FORMAT(1H ,'POLYN OF ORDER ',I2,'FIT TO CUVVE ',I2,' HAS RMS DEV='
         1,E15.7//)
          WRITE(3,19)
          DO 25 I=1,NP
       25 WRITE(3,20)(DEL(I),DEL2(I),T(I,NSETI),ET(I),T2(I),ET2(I),RT(I),RET(I
         1(I))
       19 FORMAT(1H ,'DISTANCE',6X,'DIST2',6X,'TTHEOR',2X,'T-EST',2X,'TSQ',2X,'TESQ
         1X,'TESQ',2X,'REDT',2X,'RTEST')
       20 FORMAT(1H ,F6.2,2X,E14.5,2X,2(F6.2,2X),4(E12.5,2X))
      103 IF(N.EQ.2) GO TO 102
          N=N-1
          GO TO 101
       99 STOP
          END
```

```
      SUBROUTINE GAUSS
C  SOL'N OF SET OF LINEAR EQN'S BY GAUSSION ELIMINATION WITH RESIDUAL
C  APPROXIMINATION
      DOUBLE PRECISION AA(6,6),BB(6),RM(6),R(6),X(6),DX(6),DABS,DSQRT
      DOUBLE PRECISION TA(6),TB(6),PP,SC(6)
      COMMON AA,BB,X,N,NSETI
C  SCALE ROWS OF MATRIX AA
      DO 3 I=1,N
    3 SC(I)=0.D0
      DO 6 I=1,N
      DO 4 J=1,N
    4 IF(DABS(SC(I)).LT. DABS(AA(I,J))) SC(I)=AA(I,J)
      DO 6 J=1,N
    6 AA(I,J)=AA(I,J)/SC(I)
C
  100 CONTINUE
      DO 5 I=1,N
    5 BB(I)=BB(I)/SC(I)
   23 FORMAT(1H ,6(E15.7,2X))
  102 CONTINUE
C  FIND LARGEST ELEMENT IN COLUMN LL & INTERCHANGE THIS ROW WITH ROW LL
      NN=N-1
      DO 8 LL=1,NN
      PP=0.D0
      DO 66 J=LL,N
C KEEP VALUES OF ROW LL
      TA(J)=AA(LL,J)
      TB(LL)=BB(LL)
      IF(DABS(PP) .LT. DABS(AA(J,LL)))GO TO 55
      GO TO 66
   55 LJ =J
      PP=AA(J,LL)
   66 CONTINUE
C  INTERCHANGE ROWS LL & LJ
      DO 7 K=LL,N
      AA(LL,K)=AA(LJ,K)
    7 AA(LJ,K)=TA(K)
      BB(LL)=BB(LJ)
      BB(LJ)=TB(LL)
C  ELIMINATE COLUMN LL FOR I=LL+1 TO N
      L1=LL+1
      DO 8 L=L1,N
      LM=L-1
C CALCULATE MULTIPLIER M(L) & APPLY
      RM(L)=AA(L,LL)/AA(LL,LL)
      DO88 K=LL,N
   88 AA(L,K)=AA(L,K)-RM(L)*AA(LL,K)
      BB(L)=BB(L)-RM(L)*BB(LL)
    8 CONTINUE
      DO 22 I=1,N
   22 WRITE(3,23)(AA(I,J),J=1,N),SC(I),BB(I)
      WRITE(3,23)(RM(I),I=1,N)
C  CALCULATE COEFFICIENTS X(N) BY BACK SUBSTUTITUTION
      X(N)=BB(N)/AA(N,N)
      N1=N-1
        DO 10 J=1,N1
      K=N-J
      X(K)=BB(K)
```

```
      DO 11 L=K,N1
      L1=L+1
   11 X(K)=X(K)-AA(K,L1)*X(L1)
   10 X(K)=X(K)/AA(K,K)
      WRITE(3,26)(X(I),I=1,N)
   26 FORMAT(1H ,'X(I):',6(E15.7,2X))
C
C  CALCULATE RESIDUALS R(N)=AA*X(N) -BB
      ER=0.D0
      DO 14 I=1,N
      R(I)=-BB(I)
      DO 33 J=1,N
   33 R(I)=R(I)+AA(I,J)*X(J)
   14 ER=ER+DABS(R(I))
      WRITE(3,18) (R(I),I=1,N),ER
   18 FORMAT(1H ,'RESIDUALS AFTER 1ST APPROX:',6(E15.7,2X)/1H ,'ER= ',E1
     15.7)
      IF(ER .LT. 1.D-06) GO TO 16
C  SOLVE AA*DX=-R BY BACK SUBS. & COMPUTE FINAL X
      X(N)=X(N)-RM(N)*R(N)/AA(N,N)
      N1=N-1
      DO 12 J=1,N1
      K=N-J
      NJ=N+1-J
      DX(K)=-R(K)*RM(NJ)
      DO 13 L=K,N1
      L1=L+1
   13 DX(K)=DX(K)-AA(K,L1)*DX(L1)
      DX(K)=DX(K)/AA(K,K)
   12 X(K)=X(K)+DX(K)
      GO TO 17
   16 WRITE (3,19)
   19 FORMAT(1H ,'CONVERGENCE ATTAINED IN 1ST APPROX')
   17 WRITE(3,26) (X(I),I=1,N)
      RETURN
      END
```

APPENDIX VI

PROGRAM: LSTSQR

A. IDENTIFICATION

Title: Linear least squares fit to data

Programmer: R. Desmarais

Date: May, 1975

Language: FORTRAN IV

B. PURPOSE

To compute the coefficients a, b of a linear curve which best fits a discrete set of time, distance data points; also to compute the error in a and b for a prescribed set of fiducial limits.

C. USAGE

1. Operational Procedure: Program MAIN reads the input data and calculates the coefficients of the best straight line fit to the data using the least squares criterion. It then calculates the error in the coefficients which are correct to a factor (called "Student's t") dependent on the desired fiducial (or confidence) limits.

2. Input Parameters:

NP = number of ordered pairs (X(I),T(I)) of data

REVNT = alphanumeric title of data

X(I),I=1,NP = distance values

T(I),I=1,NP = time values

3. Output Parameters:

TO = intercept time of linear fit

TA = error in TO correct to "Student's t" factor

RM1 = slope of linear fit

TB = error in RM1 correct to "Student's t" factor

V = inverse of RM1

RMS = root-mean-square deviation of fit to data

NS = NP-2 is the number of degrees of freedom for the "student's t" factor used to obtain the fiscal errors TA and TB

4. Space Requirements: 96K
5. Temporary Storage Required: none
6. Input Tape: none
7. Output Tape: none
8. Time: 10.13 seconds for six 35 point data sets
9. Reference: R.G. Stanton (1961)pp.52-62

LSTSQR PROGRAM DESCRIPTION

The purpose of this program is to calculate the best linear fit to a discrete set of refraction time-distance values using the well-known method of least squares minimization. The two linear equations whose solution yields the unknown coefficients a and b (corresponding to the intercept time and slope, respectively) are:

$$\sum t_i = na + b\sum x_i \qquad \text{(VI-1)}$$

$$\sum x_i t_i = a\sum x_i + b\sum x_i^2 \qquad \text{(VI-2)}$$

where n is the number of data points. The output variable RMS represents the root-mean-square deviation σ expressed by:

$$\sigma^2 = \sum\{t_i - (a + b_{xi})\}^2/n \qquad \text{(VI-3)}$$

Assuming that the error in $y_i = a + b_{xi}$ follows a normal distribution, the errors T_α and T_β in a and b respectively have been calculated in the following manner:

$$T_\alpha = \left(\tau_{n-2}\left[\frac{n\sigma^2}{n-2}\left(\frac{1}{n} + \frac{\bar{x}^2}{(x_i-\bar{x})^2}\right)\right]\right)^{\frac{1}{2}}$$

$$T_\beta = \tau_{n-2}\left[\frac{n\sigma^2}{(n-2)\ \{\Sigma(x_i-\bar{x})^2\}}\right]^{\frac{1}{2}}$$

where σ^2 is given by equation (3),

$$\bar{x} = \frac{1}{n}\Sigma x_i$$

and τ_{n-2} is a numerical constant tabulated as "Student's t", it is dependent on the percentage fiducial limits and the number of degrees of freedom (n).

```
C     PROGRAM   LSTSQR
C    PROGRAM CALCULATES LEAST SQUARES FIT TO DATA POINTS X(I),T(I), I=1,NP
C     OUTPUT   INTERCEPT TIME,SLOPE,VELOCITY,RMS DEV., AND ERRORS IN LINEAR
C    1COEFFS. USING STUDENT'S T DISTRIBUTION
      DOUBLE PRECISION X(50),T(50),S(3),R(3),XB,RI,RM1,V,TO,RN,XB,T2,RM,
     1SIG,STU,TA,TB,RMS,TT(50)
   99 READ(1,30) NP,REVNT
   30 FORMAT(I2,2X,6A2)
      WRITE(3,32) REVNT
   32 FORMAT(1H ,'EVENT',2X,6A2)
      READ(1,31)(X(I),T(I),I=1,NP)
   31 FORMAT(2F10.0)
      DO 1 I=1,3
      S(I)=0.DO
    1 R(I)=0.DO
      XB=0.DO
      DO 2 I=1,3
      RI=I-1
      DO 2 J=1,NP
      S(I)=S(I)+X(J)**RI
    2 R(I)=R(I)+T(J)*X(J)**RI
C   CALCULATE COEFFS
      RM1=(S(1)*R(2)-S(2)*R(1))/(S(1)*S(3)-S(2)*S(2))
      V=1.DO/RM1
      TO=(S(3)*R(1)-S(2)*R(2))/(S(1)*S(3)-S(2)*S(2))
C   CALCULATE ERRORS IN COEFFS
      RN=NP
      T2=0.DO
      RM=0.DO
      DO 5 I=1,NP
      TT(I)=TO+RM1*X(I)
      RM=RM+(T(I)-TT(I)) *(T(I)-TT(I))
      XB=XB+X(I)
    5 T2=T2+T(I)*T(I)
      XB=XB/RN
      SIG=0.DO
      DO 6 I=1,NP
    6 SIG=SIG+(X(I)-XB)*(X(I)-XB)
      NS=NP-2
      STU=NS
      TA=((RM/STU)*((1.DO/RN)+(XB*XB/SIG)))**0.5DO
      TB=(RM/(STU*SIG))**0.5DO
      RMS=(RM/RN)**0.5DO
      WRITE(3,10)NP
      WRITE(3,33) (X(I),T(I),TT(I),I=1,NP)
   33 FORMAT(1H ,3(E15.7,5X))
      WRITE(3,13)
      WRITE(3,11) TO,TA,RM1,TB,V
      WRITE(3,12) RMS,NS
   10 FORMAT(1H ,'NMBER DATA PTS= ',I2//)
   13 FORMAT(1H ,5X,'TO',5X,'ERROR',5X,'SLOPE',5X,'ERROR',5X,'VEL'//)
   11 FORMAT(1H ,5(E15.7,2X))
   12 FORMAT(1H ,'STD DEV= ',E15.7/1H ,'CONVERT ABOVE ERRORS USING STUDENT
     1NTS T(',I2,')')
      GO TO 99
   98 STOP
      END
```

APPENDIX VII

PROGRAM: XTAMP

A. IDENTIFICATION

Title: Calculation of travel-times, distances and amplitudes for a specified ray type in a spherically stratified earth model

Programmer: R.F. Mereu, University of Western Ontario

Date: 1972-73

Language: FORTRAN IV

B. PURPOSE

To compute the times, distances and amplitudes of primary compressional wave events which would arise in realistic models of the earth's crust and upper mantle.

C. USAGE

1. Operational Procedure: Subroutine LAYPAR calculates all the necessary model values required by the remaining subroutines. Subroutine VELBOT calculates apparent velocity, depth of bottoming and bottoming velocity. Subroutine DELTA calculates distances prescribed by the input parameters for any ray segment; subroutine TIME then calculates the corresponding time for the ray segment. The total distance, time and amplitude for an entire ray path are then calculated by subroutine DISTM. The horizontal and vertical amplitude components are calculated by subroutine ZOEPP and GELG.

2. Input Parameters: These variables are defined in the comment statements at the beginning of the listing of program XTAMP.

3. Output Parameters: These variables are defined in the comment statements preceding subroutine DISTM in the listing of program XTAMP.

4. Space Requirements: 196K

5. Temporary Space: none

6. Input Tape: none

7. Output Tape: none

8. Time: 18.47 sec. for a two segment ray sampled at 40 distance-points

9. References: travel-time calculations - Bullen (1963), Stewart (1968); Julian and Anderson (1968)

amplitude-distance calculations - Gutenberg (1944); Steinhart and Meyer (1961)

XTAMP PROGRAM DESCRIPTION

Input parameters defining the earth model and the ray tape for which time and amplitude versus distance calculations are desired are read by program MAIN. The times and distances are calculated by subroutines DELTA and TIME using formulae resulting from the closed form solutions of Bullen's (1961) equations for a spherically stratified earth (Cf. Stewart (1968) and Bates (1971). If triplications or shadow zones are suspected, the user is advised to first run the program calculating times for a large number of rays before attempting to iterate the distances.

The theoretical amplitudes are calculated by subroutine ZOEPP using the formula (Gutenburg (1944)):

$$A = \left[\frac{cB}{f} \quad (F_1F_2 \cdots F_n)\ \gamma \left|\frac{d\ \cos\alpha_1}{d\Delta}\right| \frac{1}{\sin\Delta\cos\phi_1}\right]^{\frac{1}{2}}$$

where c is a constant depending upon the source energy

f is the frequency of the arriving waves

B is the ratio of ground displacement to incident amplitude at the free surface

F_i are the ratios of transmitted or reflected energy to incident energy at each discontinuity encountered by the ray path

γ is the absorption factor

α_1 is the angle of incidence at the source

ϕ_1 is the angle of emergence at the receiving point

Δ is the angular distance between source and receiver

The F_i are calculated by the matrix solution (using Gaussian reduction) of Zoeppritz' equations (Zoeppritz (1919)).

```
//JOB  WATFIV
      PROGRAM XTAPE(INPUT,OUTPUT,PUNCH,TAPE1=INPUT,TAPE3=OUTPUT,TAPE7=
     1 PUNCH,TAPE11)
      THIS A RAY TRACING TIME DISTANCE AMPLITUDE PROGRAM BY R.MEREU
C     THIS PROGRAM CALCULATES THE TIMES DISTANCES AND RELATIVE AMPLITUDE
     FOR ANY RAY TYPE THROUGH A SPHERICALLY LAYERED EARTH
      RAY THEORY IS ASSUMED
      DIRECT WAVES REFLECTED WAVES CONVERTED WAVES AND MULTIPLE WAVES
      CAN BE HANDLED
      THE PROGRAM WILL CALCULATE THE VARIOUS QUANTITIES
      FOR ANY RAY PARAMETER P ON ANY. BRANCH
      OR FOR ANY GIVEN DISTANCE
      AT THE END ONE HAS THE OPTION OF SORTING ALL THE ARRIVALS AT ANY
      DISTANCE INTO A SEQUENCE BASED ON EXPECTED ARRIVAL TIMES
      THE PROGRAM SOLVES ZOEPPRITZ EQUATIONS AT EACH DISCONTINUITY ALONG
      THE PATH AND TAKES INTO ACCOUNT THE FREE SURFACE EFFECT AS WELL AS
      GEOMETRICAL SPREADING


      INPUT CARD 1 ----NMOD,IDIP1,IDIP2,IDIP3,IDIP4,LAYCH,IDIPS,KKSORT
        NMODD=NUMBER OF MODELS TO BE STUDIED
        IDIP1=OUTPUT OPTION    IDIP1=0 OR =1
           IF IDIP1=0 DETAILED OUTPUT OF STRUCT AND TRDSTS SUBROUTINES
           WILL NOT BE PRINTED
      IDIP2=OUTPUT OPTION    IDIP2=0 OR 1
        IF IDIP2=0 DETAILED OUTPUT FROM SUBROUTINEZOEP WILL NOT BE PRINTRINTED
        IDIP3=OUTPUT OPTION    IDIP3=0 OR 1
        IF IDIP3=1    OUTPUT CARDS WILL BE PRINTED FROM SORT
      KCARD=IDIP3
      IDIP4=OUTPUT OPTION    IDIP4=0 OR 1
      IF IDIP4=0 RESULTS OF RAY SEGMENT CODING WILL NOT BE PRINTEDD
      LAYCH = LAYER CHANGE OPTION LAYCH = 1 OR 0
      IF LAYCH =1 LAYERS MAY BE CHANGED AFTER A RAY CARD IS READ
      IDIPS = A STRUCTURE OPTION
      NORMALLY IDIPS =0
      IF IDIPS=1 DIFFERENT STRUCTURES SHOULD BE READ IN AFTER
      A RAY CARD IS READ IN
      KKSORT= A SORTING AND PRINTING OPTION
      IF KKSORT=0 NO SORTING IS DONE
      IF KKSORT=2 OUTPUT FROM SORT IS GIVEN

      INPUT CARD 2----PNUMB,DMMN,DMMX,DGAP,REDV,RADUS,IKM
      PNUMB= NUMBER OF RAY PARAMETERS TO BE EVALUATED PER RAY TYPE
      NORMALLY THIS VALUE IS SET AT 1. THE PROGRAM THEN COMPUTES
      DISTANCE WHICH OCCUR FOR THE MAX AND MIN VALUE OF THE RAY
      PARAMETER WHICH CAN BE USED WITH EACH RAY TYPE
      DMMN=THE MINIMUM DISTANCE TO BE USED IN THE WHOLE PROGRAM
      DMMX = MAXIMUM DISTANCE TO BE USED IN THE WHOLE PROGRAM
      DGAP = DISTANCE INCREMENT TO BE USED
      IF DMMN=100.0,DMMN=225.0 ,AND DGAP=25.0 THEN THEPROGRAM
      WILL EVALUATE TIMES DISTANCE AND AMPLITUDES OF RAYS
      ARRIVING AT THE DISTANCE 100, 125, 150, 175, 200, 225
      REDV= TH REDUCING VELOCITY
      RADUS = RADIUS OF THE EARTH
      IKM=1 IF DISTANCE CONTROLS ARE GIVEN IN KM
      IKM=0 IF DISTANCE CONTROLS ARE GIVEN IN DEGREES
```

```
INPUT CARD 3---- FOCD
FOCD EQUALS THE FOCAL DEPTH

THE NEXT SET OF INPUT CARDS ARE THE EARTH MODEL CARDS
READ IN THE MODEL PARAMETERS USING ONE CARD FOR EACH LAYER
MDL = THE MODEL IDENTIFYING NUMBER
N=LAYER NUMBER
VT=P VELOCITY AT TOP OF LAYER
VB=PVELOCITY AT BOTTOM OF LAYER
THICK = THICKNESS OF THE LAYER
POISS=POISSONS RATIO FOR THE LAYER
IF VST IS GREATER THAN 0 THE COMPUTER WILL USE THE VALUES OF
VST AND VSB FOR THE TOP AND BOTTOM S VELOCITIES
IF VSB IS LESS THAN ONE VSB=VST
IF VST IS LESS THAN ONE THE COMPUTER WILL CALCULATE
THE S VELOCITIES USING A VALUE OF 0.25 FOR POISSONS RATIO
IF POISSONS RATIO=0.0 THE COMPUTER WILL CALCULATE THE VALUES
OF THE S VELOCITIES AT THE TOP AND BOTTOM OF THE LAYER
USING A VALUE OF 0.25
DENST = THE DENSITY AT THE TOP OF THE LAYER
IF NO VALUES ARE GIVEN TO DENST, THE PROGRAM WILL ASSIGN A VALUE
DENSB= THE DENSITY AT THE BOTTOM OF THE LAYER
IF NO VALUES ARE GIVEN TO DENSB, THE PROGRAM WILL ASSIGN A VALUE
DENSITIES ARE CALCULATED FROM A LINEAR DENSITY VELOCITY
RELATIONSHIP UNLESS OTHERWISE SPECIFIED
RTOP = THE RADIUS OF THE EARTH AT THE TOP OF THE LAYER
IF NO VALUE IS GIVEN TO RTOP THE PROGRAM WILL ASSGN A VALUE
= TO THE RADIUS OF THE PREVIOUSLY READ IN LAYER
PUT A BLANK CARD AT THE END OF THE SET OF LAYER CARDS
MIXIMUM NUMBER OF LAYERS THAT CAN BE USED = 20
IF MORE LAYERS ARE REQUIRED THE PROGRAM WILL HAVE TO BE REDIMENSIONED

THE NEXT INPUT CARD IS THE RAY CARD
INPUT CARD 5----RX,RY,RZ,NLY,NS,KTEST,NDEX,(ID(M),M=1,16),(NL(7)8M=1,16)
RAY CARD CODE IS AS FOLLOWS
RX,RY,RZ THIS IS THE RAY TYPE IDENTIFIER
ONE MAY USE UP TO 16 LETTERS TO IDENTIFY A RAY TYPE
NLY= THE NUMBER OF LAYERS NEEDED TO CALCULATE THE TOTAL RAY PATH
NS= THE NUMBER OF RAY SEGMENTS
KTEST IS AN OPTION CARD
IF KTEST=0 ONLY ONE CARD WILL BE USED TO IDENTIFY A RAY AND ITS CODES
IF KTEST =1 AT LEAST ONE MORE RAY CODE CARD MUST BE USED FOR THAT RAY
IF RAY HAS TRIPLICATION ON IT SET KTEST TO BE NEGATIVE
THIS WILL CAUSE THE COMPUTER TO READ ANOTHER CARD
THIS NEW CARD HAS THE PREDETERMINED LIMITS ON IT FOR THE
RANGE OF VALUES OF THE RAY PARAMETER STPTT= UPPER LIMIT STPBR=LOW
TO PREDETERMINE THE RANGES OF VALUES OF P FOR EACH BRANCH
RUN A SOLUTION THROUGH WITH THE VALUE OF PNUMB SET AT 100.0
NY= NUMBER OF THE LAYER TO WHICH A SEGMENT BELONGS
NDEX = 1 IF RAY IS NOT A REPETATIVE MULTIPLE
NDEX = 2 IF RAY REPEATS ITSELF 2 TIMES ETC
ID = THE SEGMENT IDENTIFIER USING THE FOLLOWING CODE
0 SECOND PORTION OF ARCUY WAVE WHICH HAS BOTTOMED
1 DOWN GOING REFRACTED WAVE
2 UP GOING REFRACTED WAVE
```

```
C     3 DOWN GOING REFLECTED WAVE
C     4 UP GOING REFLECTED WAVE
C     6 DOWN GOING REFRACTED SV WAVE
C     7 UP GOING REFRACTED SV WAVE
C     8 DOWN GOING REFLECTED SV WAVE
C     NY=LAYER NUMBERS FOR EACH OF THE GIVEN RAY SEGMENTS
C     PUT A BLANK CARD AT END OF THE RAY CARD SET
C     THE MAXIMUM NUMBER OF RAYS TO BE HANDLED IS MXRAY
C     MAXIMUM NUMBER OF RAY SEGMENTS (NOT COUNTING REPETATIVE SEGMENTS
C     IS 32
C
      DIMENSION PV(20),PU(20),SV(20),SU(20),R(20),RHO(20),BP(20),BS(20),
     1 THK(20),POIS(20),NN(20),RHOT(20),RHOB(20),PTTP(20),PBBP(20),
     1 PTTS(20),PBBS(20),PTP(20),RBT(20),POIST(20),POISB(20),
     1 ID(50),NL(50),U(50),V(50),B(50),CPR(50),CPT(50),CSR(50),CST(50),
     1 PT(50),PB(50),PWV(50),SWV(50),CTR(50),DIST(100),
     1RAX(100),RAZ(100),RAY(100),DISMN(100),DISMX(100)
     1,DD(100), DIPP(50),ARRZ(50),APPZ(50),PO(50),DELTTA(50)
     1,TYME(50)
      DIMENSION PTT(40),TTT(40)
      COMMON B,U,V,PU,PV,SU,SV,RHO,CPR,CPT,CSR,CST,COEF,PW,SW,RADUS,P,
     1 NLY, NS,NL,IPFL,D,PWV,SWV,CTR,RTP,RBT
     1,EMT,APEM,EDELT,AMDEL,KR,RHOT,RHOB,ANDEX,NSS,PHASE
     1,PO,ARRZ,APPZ,DIPP,DELTTA,TYME,TAZCOR,GIVAZ
     1, IDIP1,IDIP2,IDIP3,IDIP4,IMP,ID
     1,QQ,AQ,AMPG,FREQC
      MAXSEG= MAXIMUM NUMBER OF SEGMENTS
      MAXLAY = MAXIMUM NUMBER OF LAYERS
      MAXSEG=32
      MAXLAY=20
      DTR=3.14159265/180.0
2000  FORMAT(8I5)
      INPUT CARD 1
      READ (5,2000) NMODD,IDIP1,IDIP2,IDIP3,IDIP4,LAYCH,IDIPS,KKSORT
      KCARD=IDIP3
      INPUT CARD 2
      READ (5,2001) PNUMB,DMMN,DMMX,DGAP,REDV,RADUS,IKM
2001  FORMAT (6F10.2,I5)
      IPAD= RADUS
      IF (IPAD.EQ.0) RADUS=6371.028
      IF (IKM.EQ.0) DGAP=DGAP*DTR*RADUS
      IF (IKM.EQ.0) DMMN=DMMN*DTR*RADUS
      IF (IKM.EQ.0) DMMX=DMMX*DTR*RADUS
      RAD=RADUS
      PNUMB1=PNUMB
      PNUMB2=PNUMB
      MXRAY=200
      JMAX=100
      MXM=40
      GIVAZ=0.0
      DO 50 NMODEL=1,NMODD
      NTAP=0
      R(1)=RADUS
555   FORMAT(F6.1)
      INPUT CARD 3
      READ (5,555) FCCD
```

```
      NLAY=0
      INPUT CARD 4
      READ IN THE MODEL LAYER PARAMETERS HERE
      READ (5,157)RMDL
157   FORMAT(3A2)
      IINDEX=0
      CONTINUE
55    FORMAT(I4,8F7.2,F10.3)
      READ (5,155) N,VT,VB,THICK,POISS,VST,VSB,DENST,DENSB,RTOP
      IF (N.EQ.0) GO TO 3
      IF (RTOP.GT.0.0) GO TO 156
      IF (N.EQ.1) RTOP=RADUS
      IF (N.GT.1) RTOP=RBT(N-1)
      R(N)=RTOP
56    CONTINUE
      CALL LAYPAR(VT,VB,THICK,POISS    ,DENST,DENSB,RTOP,PU(N),PV(N),
     1SU(N),SV(N),PTTP(N),PTTS(N),PBBP(N),PBBS(N),THK(N),NN(N),BP(N),
     2BS(N),RTP(N),RBT(N),POIS(N),RHOT(N),RHOB(N),VST,VSB,POIST(N),POISB
     3(N))
      NN(N)=N
      IMB=5
      NLAY=NLAY+1
      GO TO 4
      CONTINUE
7     FORMAT (7H1MODEL ,3A2 //114H LAYER P VTOP     P VBOT THICKNESS
     1POISSON     RADIUS     S VTOP     S VBOT          BP          BS TOP DENS
     2  BOT DENS)
      FORMAT (1H,I4,2F10.3,F10.2,2F8.2,F10.2,6F10.3)
      MFOCD=FOCD
      IF (MFOCD.LT.0) NFD=-1
      IF (MFOCD.EQ.0) NFD=0
      IF (MFOCD.EQ.0) GO TO 6
      BP= INDEX FOR THE VELOCITY DEPTH LAW V=V0*RADUS**(-BP)
      BS = THE VELOCITY DEPTH INDEX FOR S WAVES
      CONTINUE
      WRITE (6,17) RMDL
      WRITE (6,9) (NN(N),PU(N),PV(N),THK(N),POIST(N),POISB(N),RTP(N),
     1 SU(N),SV(N),
     2 BP(N),BS(N),RHOT(N),RHOB(N),N=1,NLAY)
15    FORMAT (1H0,10HP SEGMENT ,10X,10HS SEGMENT ,10X,10H LAYER      ,/
     1 5X,10HTOP P      ,10HBOT P      ,10HTOP S      ,10HBOT S      )
      WRITE (6,215)
      WRITE (6,216) (PTTP(N),PBBP(N),PTTS(N),PBBS(N),NN(N),N=1,NLAY )
16    FORMAT (1F ,4F10.3,I5)
      AMBD=1.0
      NFRGV=NFD
      IF(IINDEX .EQ. 1) GO TO 170
      NB=0
9     CONTINUE
      BNUMB1=PNUMB
      DO 300 M=1,32
      ID(M)=0
      NL(M)=0
88    CONTINUE
      IF (NR.EQ.MXRAY) GO TO 21
      INPUT CARD 5
```

```
911   FORMAT (2A4,A4,I4,3I5,1X,16I1,1X,16I1)
      READ (5,911) RX,RY,RZ,NLY,NS,KTEST,NDEX,(ID(M),M=1,16),
     1 (NL(M),M=1,16)
      IF (NLY.EQ.0) GO TO 21
900   FORMAT (2F10.5)
      IF (KTEST.LT.0) READ (5,900) STPTT,STPBB
      IF (KTEST.LT.0) GO TO 211
      IF (KTEST.EQ.0) GO TO 211
      READ (5,911) RX,RY,RZ,NLY,NS,KTEST,NDEX,(ID(M),M=17,32),
     1(NL(M),M=17,32)
211   CONTINUE
912   FORMAT (1H0,5X,2A4,A4,3X,4I5,1X,32I1,7X,32I1)
      WRITE(6,912) RX,RY,RZ,NLY,NS,KTEST,NDEX,(ID(M),M=1,32),
     1(NL(M),M=1,32)
      ANDEX=NDEX
      NSS=NS
      IF (NDEX.GT.1) NSS=NS+1
      NR=NR+1
      PNUMB=PNUMB1
      IF(NR.LT.3) PNUMB=PNUMB2
      RAX(NR)=RX
      RAY(NR)=RY
      RAZ(NR)=RZ
      THE PROGRAM WILL NOT WORK IF STRUCTURE IS CONSIDERED ALONG WITH
      MULTIPLE REFLECTED WAVES
      IF (IDIPS.GT.0) ANDEX=1.0
71    CONTINUE
      READ(5,9008) (PZT(I),I=1,31)
9008 FORMAT(12F6.2)
      IF (LAYCH.EQ.0) GO TO 170
70    CONTINUE
      DO 301 M=1,50
      MSEG=1
      APZ=GIVAZ
      DIP=0.0
      DIPP(M)=0.0
      APPZ(M)=GIVAZ
301   CONTINUE
001   CONTINUE
      INPUT CARD 6
      IF (IDIPS.EQ.1) READ(5,2003) MSEG,DIP,APZ
2003  FORMAT(I5,F10.1,F10.2)
      IF (IDIPS.EQ.1.AND.MSEG.EQ.0) GO TO 1002
      WRITE(6,1003) MSEG,GIVAZ,APZ,DIP
003   FORMAT (1H, 10HSTRUCTURE ,I5,3F10.3)
      DIPP(MSEG)=DIP
      APPZ(MSEG)=APZ
      DO 13 M=1,NSS
      CPR(M)=0.0
      CPT(M)=0.0
      CSR(M)=0.0
      CST(M)=0.0
      CTR(M)=0.0
      IDD=ID(M)
      N=NL(M)
      IF (IDD-5) 51,52,53
```

```
51      U(M)=PU(N)
        V(M)=PV(N)
        B(M)=PB(N)
        PWV(M)=1.0
        SWV(M)=0.0
        GO TO 52
53      U(M)=SU(N)
        V(M)=SV(N)
        B(M)=BS(N)
        SWV(M)=1.0
        PWV(M)=0.0
52      CONTINUE
        IF (IDD-1) 54,55,54
55      CPT(M)=1.0
        GO TO 70
54      IF(IDD-2) 56,57,56
57      CPT(M)=-1.0
        GO TO 70
56      IF (IDD-3) 58,59,58
59      CPR(M)=1.0
        IF (N-1) 70,72,70
72      CONTINUE
        PWV(M-1)=-PWV(M-1)
        SWV(M-1)=-SWV(M-1)
        GO TO 70
58      IF (IDD-4) 60,61,60
61      CPR(M)=-1.0
        GO TO 70
60      IF (IDD-5) 30,31,30
31      CTR(M)=1.0
        IF (B(M).LT.(-1.0)) GO TO 116
C       THIS IS A TEST TO SEE I=RAY BOTTOMS
        CSR(M)=-CSR(M-1)
        CPR(M)=-CPR(M-1)
        CST(M)=-CST(M-1)
        CPT(M)=-CPT(M-1)
         U(M)=U(M-1)
        V(M)=V(M-1)
        B(M)=B(M-1)
        PWV(M)=PWV(M-1)
        SWV(M)=SWV(M-1)
        GO TO 70
62      IF (IDD-6) 62,63,62
63      CST(M)=1.0
        GO TO 70
62      IF (IDD-7) 64,65,64
65      CST(M)=-1.0
        GO TO 70
64      IF (IDD-8) 66,67,66
67      CSR(M)=1.0
        IF(N-1) 70,71,70
71      CONTINUE
        SWV(M-1)=-SWV(M-1)
        PWV(M-1)=-PWV(M-1)
        GO TO 70
66      IF (IDD-9) 68,69,68
```

```
59      CSR(M)=-1.0
58      CONTINUE
70      CONTINUE
13      CONTINUE
        PBB=10000.0
        PTT=10000.00
 9999 CONTINUE
        IREL=1
        DO 16 M=1,NSS
        IDD=ID(M)
        N=NL(M)
        UUU=U(M)
        VVV=V(M)
        BBB=B(M)
        C1=CPT(M)
        C2=CPR(M)
        C3=CST(M)
        C4=CSF(M)
        PW=PWV(M)
        SW=SWV(M)
        KPW=PW
        KSW=SW
        IF(KPW.EQ.0) PTEST=PTTS(N)
        IF(KPW.EQ.0) PBEST=PBBS(N)
        IF (KSW.EQ.0) PTEST=PTTP(N)
        IF (KSW.EQ.0) PBEST=PBBP(N)
        IF (PTT.GT.PTEST) PTT=PTEST
        IF (IREL.EQ.0) GO TO 217
        IF (IDD-0) 218,218,219
218     IREL=0
        MB=M-1
        IF (PTT.GT.PBB) PTT=PBB
        IF (NL(M).EQ.NL(M-1)) PTT=PTEST
        IF (NL(M).EQ.1) PTT=PTEST
        PBB=PBEST
        GO TO 217
219     IF (PBB.LT.PBEST) GO TO 217
        PBB=PBEST
        MB=M
217     CONTINUE
        IF (IDIP4.EQ.0) GO TO 16
105     CONTINUE
        WRITE (6,14) NR,M,N,IDD,UUU,VVV,BBB,C1,C2,C3,C4,PW,SW
14      FORMAT (1H,17HMAIN PART RESULTS,4I5,2F10.2,F10.5,4F5.1,5X,2F5.1)
16      CONTINUE
19      CONTINUE
        IF (KTEST.LT.0) PBB=STPBB
        IF (KTEST.LT.0) PTT=STPTT
        PT(MB)=PTT
        PB(MB)=PBB
        NPT=PNUMB+1.0
        IF (IREL) 24,25,24
24      FACT=(PB(MB)-0.0)/PNUMB
        P=PB(MB)+FACT
        GO TO 26
25      FACT=(PT(MB)-PB(ME))/PNUMB
```

```
      DISMN(NF)=DIST(1)
      DISMX(NF)=DIST(NPT)
      NJ=(DMMX-DMMN)/DGAP+1.)
      NJ=NJ+1
5007  FORMAT (1F ,3HNJ=,I5)
      WRITE (6,5007) NJ
      WRITE (6,177)
      IF (ILEL-1) 90,91,91
91    CONTINUE
      PL1=PBB
      PL2=1.0
      P=PBB/2.0
      GO TO 92
90    CONTINUE
      PL1=PTT
      PL2=PBB
      P=(PTT+PBB)/2.0
92    CONTINUE
      IF (DMX.LT.DMMN) GO TO 37
      IF (DMN.GT.DMMX) GO TO 37
      J=0
      D=DMMN-DGAP
30    CONTINUE
      D=D+DGAP
      J=J+1
      IF (J.GT.JMAX) GO TO 37
      DD(J)=D
34    IF (D-DMN) 32,33,33
32    D=D+DGAP
      J=J+1
      IF (J.GT.JMAX) GO TO 37
      DD(J)=D
      GO TO 34
35    IF (D-DMX) 35,35,37
36    IF (D-DMMX) 36,36,37
37    CONTINUE
      KT=0
      THE ITERATION TO THE DESIRED DISTANCE IS BEGUN HERE
      NIT=0
      Q=P
46    CONTINUE
      KT=KT+1
      TIM=0.0
      DIS=0.0
      DLDP=0.0
      ADEX=1.0
      DO 41 M=1,NS
      IF (M.EQ.1.AND.NL(M).EQ.1) ADEX=ANDEX
      IF (M.EQ.1) GO TO 4615
      IF (NL(M).EQ.1.AND.NL(M-1).EQ.1) ADEX=ANDEX
4615  CONTINUE
      PQ(1)=P
      Q=PQ(M)
      ARRZ(M+1)=0.0
      PQ(M+1)=PQ(M)
      PS=PQ(M)*PQ(M)
```

```
      IF (PER-PTT) 115,116,116
  116 WRITE (6,117) NR
  117 FORMAT (1H0,10HRAY NUMBER,I5,16H  DOES NOT EXIST)
      GO TO 20
  115 CONTINUE
      P=PT(NB)+FACT
  16  CONTINUE
      NH=NL(MB)
      WRITE(6,176) NR,NP,MB,IREL,REDV
  176 FORMAT (1H0,3HNR=,I5,5X,3HNP=,I3,5X,3HMB=,I4,5X,5HIREL=,I2,5X,
     1 18HREDUCING VELOCITY=,F7.2)
      WRITE (6,177)
  177 FORMAT (1H0,4X,9HP        ,8HDPDA     ,10HAMPQ       ,7HCCEF    ,
     1 7HAMDEL   ,7HPHASE  ,7HAMV     ,7HDELTA  ,7HEMT     ,7HAPEM    ,
     1 8HSLOWN    ,7HVBAR   ,7HDPDT   ,7HVBOT   ,7HTIM     ,7HRT      ,
     1 7HDISTT   )
C     THE DO 27 DO LOOP CALCULATES DISTANCE TIMES AND AMPLITUDES ETC
C     AS A FUNCTION OF RAY PARAMETER P
C     THE NUMBER OF CALCULATIONS = PNUMB+1.0
C     ITS PRIMARY PURPOSE IS TO CALCULATE THE MAX AND MIN DISTANCE AT
C     WHICH YOU WILL FIND THE RAY IN QUESTION AS WELL AS THE LIMITS
C     FOR THE RAY PARAMETER WHICH CAN BE USED WITH THAT RAY
C     IF TRIPLICATIONS OR SHADOW ZONES ARE SUSPECTED THE USER IS ADVISED TO DO
C     DO A PRELIMINARY INVESTIGATION IN WHICH A LARGE NUMBER OF RAYS
C     ARE CALCULATED (SET PNUMB TO A LARGE NUMBER). ONE CAN THEN SEE WHAT
C     THE WHOLE T-DELTA CURVE WIL LOOK LIKE BEFORE ATTEMPTS ARE MADE
C     AT ITERATING THE DISTANCES
      DMX=0.0
      DMN=25000.0
      DO 27 K=1,NPT
      KP=K
      P=P+FACT
      IF (P.LT.10.0)P=10.0
      CALL  DISTM(TIM,DISTT,AMV,AMH,DPDA,PHSV,PHSH)
      IF (IMP.EQ.1) GO TO 27
      RAD=RADUS
      Q=PQ(MB)
      DIST(K)=DISTT
      RT=TIM-DISTT/REDV
      CALL VELDCT (MB,NL,N,U,V,RADUS,RTP,E,Q,IREL,SLOWN,VBOT,VBAR,
     1RBT,DBOT)
      VBAR=VBAR*PQ(MB)/PQ(NS)
      SLOWN=SLOWN*PQ(NS)/PQ(MB)
  75  FORMAT (1H ,2X,F9.4,F8.1,F10.4,F7.4,F7.1,5F7.2,F8.4,6F7.2)
      DISTL=DISTT/(RADUS*DTR)
      WRITE (6,175) P,DPDA,AMPQ,CCEF,AMDEL,PHASE,AMV,DISTL,EMT,APEM,
     1 SLOWN,VBAR,DPDT,VBOT,TIM,RT,DISTT
      D=DISTT
      IF (DMX.LT.D) DMX=D
      IF (DMN.GT.D) DMN=D
  20  CONTINUE
  7   CONTINUE
  80  CONTINUE
C     THE NEXT PORTION OF THE PROGRAM CALCULATES TIMES DISTANCE AMPLITU
C     PHASES FOR ALL THE SPECIFIED DISTANCES
      KP=0
```

```
      N=NL(M)
      RT=RTP(N)
      RB=RBT(N)
      VT=U(M)
      VB=V(M)
      B=B(M)
 1101 CALL TIME (G,PS,RT,RB,VT,VB,BB,TM,RCT,RDPDL,DADP)
      CALL DELTA (G,PS,RT,RB,VT,VB,BB,RADUS,AT,DELT,BCD,AJ)
 1103 CONTINUE
      TIM=TIM+ADEX*TM
      DLDP=DLDP+DADP*ADEX
      DIS=DIS+DELT*ADEX
      DELTTA(M)=DELT/DTR
      TYME(M)=TM
      IF(M.EQ.NS) GO TO 41
      KCTR=CTR(M+1)
      IF (KCTR.EQ.1) GO TO 41
      IDT1=0
      IRT1=1
      ARZ=ARRZ(M)
      ARZ=APPZ(M+1)
      DIB=DIPP(M+1)
      UP=CPR(M)+CPT(M)+CSR(M)+CST(M)
      IF (UP.GT.0.0) RADD=RBT(N)
      IF (UP.LT.0.0) RADD=RTP(N)
      UPN=CPR(M+1)+CPT(M+1)+CSR(M+1)+CST(M+1)
      IF (UP.GT.0.0) W1=V(M)
      IF (UP.LT.0.0) W1=U(M)
      FRACT=UPN/UP
      IF (UPN.GT.0.0) W2=U(M+1)
      IF (UPN.LT.0.0) W2=V(M+1)
      BRR=PQ(M)
      ARRZ(M+1)=ARRZ(M)
      B=BRR
      BQ(M+1)=PRR
    1 CONTINUE
      RAD=RADUS
      DST=DIS*RADUS
      BBRX=1.0/(DLDP*RADUS)
      DX=DP-DST
      BR=DP+DX*CX
      IF (KT.GT.20) DP=DP*0.90
    3 FORMAT (1H ,I5,3F10.2,3E15.5,10X,4HDDD )
      IF (KT-40) 160,161,161
   61 WRITE (6,162)
   62 FORMAT (1H ,39H**********************SOLUTION OSCILLATES)
      GO TO 44
   60 CONTINUE
      ADX=ABS(DX)
      IF (ADX-0.1) 44,44,45
    4 CONTINUE
    5 B=B+DP
      QQ=PQ(MSEG)+DP
      IF (QQ-PL2) 80,80,82
   82 IF (PL1-QQ) 80,80,46
   80 B=B-DP
```

```
      DD=DD/2.0
      NIT=NIT+1
      IF (NIT-50) 8,7,7
8     FORMAT (1HO,26HDISTANCE WOULD NOT ITERATE)
7     WRITE (6,8)
      GO TO 40
5     CONTINUE
      GO TO 81
4     CONTINUE
      THE ITERATION TO THE DESIRED DISTANCE ENDS HERE
      K=J
      CALL DISTM(TIM,DISTT,AMV,AMH,DPDA,PHSV,PHSH)
      IF (IMP.EQ.1) GO TO 116
      TOTDST=DISTT
      Q=PQ(MB)
      RT=TIM-DISTT/REDV
      CALL VELRCT (MB,NL,N,L,V,RADUS,RTP,B,Q,IREL,SLOWN,VBOT,VPAR,
     1RHT,DROT)
      SLOWN=SLOWN*PQ(NS)/PQ(ME)
      VBAR=VBAR*PQ(MB)/PQ(NS)
      DISTL=DISTT/(RADUS*DTR)
      AA=90.0-EMT
      WRITE (6,175) P,DPDA,AMPQ,COEF,AMDEL,PHASE,AMV,DISTL,EMT,APEM,
     1 SLOWN,VBAR,DRCT,VBCT,TIM,RT,DISTT
      TTT(J)=TIM
      GO TO 40
      DISTLC=DISTL+DISAC
      DISTTC=DISTT+DISTC
      TMC = TIM+TIMC
      RTC=TMC-DISTTC/REDV
      IF (IDIP1.EQ.0) GO TO 1009
9     FORMAT (1H ,7F8.2)
      WRITE (6,179) DISAC,DISTC,TIMC,DISTLC,DISTTC,TMC,RTC
009   CONTINUE
      DIP=DIPP(MSEG)
      APZ=APPZ(MSEG)
      AJJ=J
      AMSEG=MSEG
      NTAP=NTAP+1
      WRITE (11) NR,RY,RX,P,DPDA,AMPQ,COEF,AMDEL,PHASE,AMV,PHSV,AMH,
     1 PHSH,EMT,APEM,AA,DISTL,SLOWN,VBAR,DRCT,VBOT,TIM,RT,Q,TIMC,DISAC,
     1 DISTC,DIST C,DISTTC,TMC,RTC,J,TOTDST,TRUDST,AZDEV,SAZ
     1,DIP,APZ,AMSEG,PZ
      GO TO 40
7     CONTINUE
      SUM1=0.0
      SUM2=0.0
      DO 9009 I=1,31
      DIF=PZT(I)-TTT(I)
      DIF2=DIF*DIF
      SUM1=SUM1+DIF
9009  SUM2=SUM2+DIF2
      RMEAN=SUM1/31.0
      RDEV=SQRT(SUM2/31.0)
      WRITE(6,9010) RMEAN,RDEV
9010  FORMAT(1H ,'MEAN DELTA T= ',F10.6,'  STD. DEV.= ',F10.6)
```

```
      IF (IDIPS.EQ.1) GO TO 1001
 1002 CONTINUE
      IINDEX=1
      GO TO 4
      GO TO 20
   31 CONTINUE
      THE END OF THE TIME DIST AMPL CALCULATIONS FOR A PARTICULAR RAY
      THE COMPUTER THEN READS A NEW RAY CARD AND REPEATS THE CYCLE UNTIL
      CARD IS REACHED
      THE NEXT STEP IS A SORTING STEP IN WHICH THE VARIOUS RAYS ARRIVING
      AT THE SPECIFIED DISTANCES ARE SORTED IN ORDER OF ARRIVAL TIMES
      THE COMPUTER PRINTS THIS DATA OUT ON A SET OF CARDS SO THAT IT MAY
      IN THE SYNTHETIC SEISMOGRAM PROGRAM
      IF (KKSORT.EQ.0) GO TO 50
 5005 FORMAT (1H , I5,2A6,6F10.3)
      WRITE (6,5005) NR,RY,RX,P,DPDA,AMPO,COEF,AMDEL,PHASE
   50 CONTINUE
      END
      SUBROUTINE DISTM (TIM,DISTT,AMV,AMH,DPDA,PHSV,PHSH)
      SUBROUTINE DISTM WRITTEN BY R MEREU
      THIS SUBROUTINE CALCULATES TOTAL TIMES, TOTAL DISTANCES, AND AMP
      FOR A RAY AS SPECIFIED IN THE X-T-AMP PROGRAM
      THIS PROGRAM GETS ALL RAY DESCRIPTION DATA AND LAYERING DATA FROM
      PROGRAM
      THE OUTPUT RESULTS OF THIS PROGRAM ARE AS FOLLOWS
      EMT = ANGLE OF EMERGENCE = 90.0-ANGLE OF INCIDENCE
      APEM = APPARENT ANGLE OF EMERGENCE
      DISTT=DISTANCE ALONG EARTHS SURFACE
      TIM= TOTAL TRAVEL TIME
      DPDA= DP/D DELTA
      FDELT EQUALS ATERM WHICH DEPENDS ONLY ON GEOMETRICAL SPREADI
      AND THE INTENSITY OF THE SOURCE
      AMV= THE VERTICAL AMPLITUDE
      AMH= THE HORIZONTAL AMPLITUDE
      AMDEL = THE AMPLITUDE BEFORE THE SURFACE
      PHSV= THE PHASE CHANGE OCCURRING ON THE VERTICAL
      PHSH = THE PHASE CHANGE OCCURRING ON THE HORIZONTAL
      PHASE = THE PHASE CHANGE OCCURRING ON TH IMPINGING WAVE
      THE INTENSITY OF THE SOURCE IS ARBITRARILY SET=10.0*RADIUS**3
      THIS VALUE WAS CHOSEN AS THEN THE OUTPUT RESULTS OCCUR IN
     C             CONVENIENTLY SIZED NUMBERS
      DIMENSION
     1R(30),U(50),V(50),PU(20),PV(20),SV(20),SU(20),RHO(20),CPR(50),
     1CBT(50),CSR(50),CST(50),NL(50),PWV(50),SWV(50),CTR(50),RTP(20),
     1 BBT(20),RHOT(20),RHOB(20),PQ(50),ARRZ(50),APPZ(50),DIPP(50),
     1 DELTTA(50),TYME(50),B(50),ID(50)
      COMMON R,U,V,PU,PV,SU,SV,RHO,CPR,CPT,CSR,CST,COEF,Pw,SW,RADUS,P,
     1 NLY,NS,NL,IREL,D,PWV,SWV,CTP,RTP,RBT
     1,EMT,APEM,FDELT,AMDEL,KK,RHOT,RHOB,ANDEX,NSS,PHASE
     1,BQ,ARPZ,APPZ,DIPP,DELTTA,TYME,TAZCOR,GIVAZ
     1, IDIP1,IDIP2,IDIP3,IDIP4,IMP,ID
     1,QQ,AO,AMPO,FREQQ
      IDIP=IDIP4
      DTR=3.14159265/180.0
      TIM=0.0
      DIS=0.0
```

```
      DLDP=0.0
      COFF=1.0
      PHASE=0.0
      PT=1.0
      Q=P
      PQ(1)=P
      ARRZ(1)=GIVAZ
      ADEX=1.0
      AMPQ=1.0
      FREQQ=10.0
      WWW=2.0*3.14159265*FREQQ
      DO 7 M=1,NS
      IF (M.EQ.1.AND.NL(M).EQ.1) ADEX=ANDEX
      IF (M.EQ.1) GO TO 6615
      IF (NL(M).EQ.1.AND.NL(M-1).EQ.1) ADEX=ANDEX
6615  CONTINUE
      Q=PQ(M)
      PS=PQ(M)*PQ(M)
      PQ(M+1)=PQ(M)
      ARRZ(M+1)=0.0
      N=NL(M)
      RT=RTP(N)
      RB=RBT(N)
      VT=U(M)
      VB=V(M)
      BB=B(M)
      PW=PWV(M)
      SW=SWV(M)
 1001 CALL TIME (Q,PS,RT,RB,VT,VB,BB,TM,BCT,RDPDL,DADP)
      CALL DELTA(Q,PS,RT,RB,VT,VB,BB,RACUS,AI,DELT,BOD,AJ)
 1003 CONTINUE
      DELTTA(M)=DELT/DTR
      TYME(M)=TM
      TIM=TIM+ADEX*TM
      DLDP=DLDP+DADP*ADEX
      DIS=DIS+DELT*ADEX
43    CONTINUE
      NSS=NS
      IF (ANDEX.GT.1.0) NSS=NS+1
      IF (M.EQ.NSS) GO TO 2
3     CONTINUE
      FRS=1.0
      IF (N-1) 15,16,15
16    FRS=0.0
15    CONTINUE
      IF (CTR(M+1)) 31,31,2
31    CONTINUE
      UP=CPR(M)+CPT(M)+CSR(M)+CST(M)
      IF(UP.EQ.-1.0 .AND. N.EQ.1) GO TO 666
      IF (UP) 11,2,13
11    CONTINUE
      RADD=RTP(N)
      V1=PJ(N)
      U1=SU(N)
      RHO1=RHOT(N)
      RHO2=RHOB(N-1)
```

```
      V2=PV(N-1)
      U2=SV(N-1)
      V2=V2*FRS
      U2=U2*FRS
      RHO2=RHO2*FRS
      AA=AI/DTR
      GO TO 12
11    CONTINUE
      RHOO=RHOT(N)
      V1=PV(N)
      U1=SV(N)
      RHO1=RHOO(N)
      RHO2=RHOT(N+1)
      V2=PU(N+1)
      U2=SU(N+1)
      AA=AJ/DTR
      GO TO 667
 666  V2=0.0
      U2=0.0
      RHO2=0.0
      AA=AI/DTR
 667  CONTINUE
12    CONTINUE
26    CONTINUE
      PR=0.0
      SR=0.0
      PT=1.0
      ST=1.0
      FAZ=0.0
      AIMP=V1-V2+U1-U2+RHC1-RHC2
      AIMP=ABS(AIMP)
      IF (AIMP.LT.0.0001) GO TO 6
      IDT1=1
      APZ=ARRZ(M)
      DIP=DIPP(M+1)
      ARZ=APPZ(M+1)
      UPN=CPR(M+1)+CPT(M+1)+CSR(M+1)+CST(M+1)
      IF (UP.GT.0.0) W1=V(M)
      IF (UP.LT.0.0) W1=U(M)
      FRACT=UPN/UP
      IF (UPN.GT.0.0) W2=U(M+1)
      IF (UPN.LT.0.0) W2=V(M+1)
      PRR=PQ(M)
      ARRZ(M+1)=ARRZ(M)
      Q=PRR
      PQ(M+1)=PRR
      CALL ZOFP(V1,U1,RHO1,V2,U2,RHC2,AA,PW,SW,PR,PT,SR,ST,PHSPR,
     1PHSPT,PHSSR,PHSST,AMPV,AMPH,PHSAV,PHSAH,PAR,PAT,SAR,SAT,APEM,IDIP)
      FAZ=          PHSPR*ABS(CPR(M+1))+PHSPT*ABS(CPT(M+1))+PHSSR*ABS(CSR(
     1M+1))+PHSST*ABS(CST(M+1))
6     CONTINUE
      CUEG= PR*CPR(M+1)+PT*CPT(M+1)+SR*CSR(M+1)+ST*CST(M+1)
      PHASE=PHASE+FAZ*ADEX
      NOXXX=ADEX
      DO 40 IDX=1,NOXXX
      COEF=COEF*ABS(CUEG)
```

```
      IF (COEF.LT.0.00001) GO TO 41
40    CONTINUE
41    CONTINUE
      IF (IDIP2.EQ.0) GO TO 25
10    FORMAT (1H ,4HZDEP,2I2,4F6.2,5F7.3,F6.1)
      WRITE (6,10) M,N,V1,V2,TIM,AA,PR,PT,SR,ST,COEF,PHASE
25    CONTINUE
2     CONTINUE
7     CONTINUE
1005  FORMAT (1H ,21HTYME DELTTA DIPP ARRZ,F10.2,F10.3,2F10.2)
      IF (IDIP1.EQ.1) WRITE (6,1005) (TYME(M),DELTTA(M),DIPP(M),ARRZ(M),
     1 M=1,NS)
      BBBA=1.0/DLDR
      DISTT=DIS*RADUS
      DISAA=DIS/DTR
      EHR=3.14159265/2.0-ARSIN(P*U(1)/RADUS)
      ETR=3.14159265/2.0-ARSIN(P*U(NS)/RADUS)
      DTR=3.14159265/180.0
      EMH=EHR/DTR
      EMT=ETR/DTR
      ALPHA=PU(1)
      BETA=SU(1)
      SQAB=ALPHA/BETA
      SQAB=SQAB*SQAB
      CETP=SQRT((COS(ETR)*COS(ETR))/SQAB)
      CEHR=SQRT((COS(EHR)*COS(EHR))/SQAB)
      ETR=ARCOS(CETR)
      EHR=ARCOS(CEHR)
      EHM=EHR/DTR
6     LET THE INTENSITY =RADUS**3*10.0
      IF (DIS.LT.0.0000001) EDELT=0.0
      IF (DIS.LT.0.0000001) GO TO 1125
      EDELT=COS(EHR)*DPCA/(SIN(DIS)*SIN(ETR)*SIN(EHR))*U(1)/10.0
1125  CONTINUE
      EDELT=ABS(EDELT)
      IF (ANDEX-1.0) 32,32,33
33    CONTINUE
      COEF=COEF/(ABS(COEG))
      PHASE=PHASE-PAZ
      AMDEL=SQRT(EDELT*COEF)
      GO TO 34
32    CONTINUE
      AMDEL=SQRT(EDELT*COEF)
      M=NS
      V2=0.0
      U2=0.0
      RHO2=0.0
      V1=PU(1)
      U1=SU(1)
      RHO1=RHOT(1)
      PW=PWV(M)
      SW=SWV(M)
      AA=90.0-EMT
      CALL ZOEP (V1,U1,RHO1,V2,U2,RHO2,AA,PW,SW,PR,PT,SR,ST,PHSPR,
     1PHSPT,PHSSR,PHSST,AMPV,AMPH,PHSAV,PHSAH,PAR,PAT,SAR,SAT,APEM,IDIP)
34    CONTINUE
```

```
840   CONTINUE
      IF (PHASE) 834,835,835
835   CONTINUE
      IF (PHASE-360.0 ) 832,833,833
833   CONTINUE
      PHASE=PHASE-360.0
      GO TO 840
832   CONTINUE
      GO TO 836
834   CONTINUE
      IF (PHASE+ 360.0) 837,838,833
837   CONTINUE
      PHASE=PHASE+360.0
      GO TO 834
838   CONTINUE
836   CONTINUE
      AMH=AMDEL*AMPH
      AMV=AMDEL*AMPV
      PHSH=PHASE+PHSAH
      PHSV=PHASE+PHSAV
      IF (IDIP2.EQ.0) GO TO 17
18    CONTINUE
      WRITE (6,8) EMT,APEM,DIS,DPCA,ECELT,CCEF,AMDEL,AMV,PHSV,AMH,PHSH
8     FORMAT (1H ,17HAMPLITUDE RESULTS,2F7.2,F7.4,2E12.4,F8.4,3E12.4,2F8
     1.2)
17    CONTINUE
      RETURN
      END
      SUBROUTINE LAYPAR (VT,VB,THICK,POISS,DENST,DENS3,RTOP,PU,PV,SU,
     1 SV,PTTP,PTTS,PBBP,PBBS,THK,NN,BP,BS,RTP,RBT,  PCIS,RHOT,RHOB
     1,VST,VSB,POIST,PCISB)
C     SUBROUTINE LAYPAR WRITTEN BY R MEREU
C     THIS PROGRAM IS TO BE USED WITH PROGRAM XTAMP
C     THIS PROGRAM CALLECTS TH DATA FROM THE INPUT MODEL CARDS AND
C     CALCULATES ALL THE NECESSARY MODEL VALUES WHICH ARE NEEDED BY
C     PROGRAM XTAMP
      DIMENSION PU(1),PV(1),SU(1),SV(1),RTP(1),RBT(1),BP(1),BS(1),NN(1),
     1 THK(1),PTTP(1),PTTS(1),PBBP(1),PBBS(1),PCIS(1),RHOT(1),RHOB(1)
     1 ,POIST(1),PCISB(1)
      SL=(8.15-5.70)/(3.33-2.67)
      BINT=5.70-SL*2.67
      N=1
2     PU(N)=VT
      PV(N)=VB
      IF (VST.LE.0.0001.AND.POISS.LT.0.00001) POISS=0.25
      IF (VSB.LE.0.0001) VSB=VST
      IF (VST.GT.0.0001) SU(N)=VST
      IF (VSB.GT.0.0001) SV(N)=VSB
      IF (VST.GT.0.0001) GO TO 3
      POIS(N)=POISS
      SQPS=SQRT((1.0-2.0*POISS)/(2.0*(1.0-POISS)))
      SU(N)=PU(N)*SQPS
      SV(N)=PV(N)*SQPS
3     CONTINUE
      ABT=PU(N)/SU(N)
      ABB=PV(N)/SV(N)
```

```
      ABSQT=ABT*ABT
      ABSQB=ABB*ABB
      POIST(N)=(2.0-ABSQT)/(2.0*(1.0-ABSQT))
      POISB(N)=(2.0-ABSQB)/(2.0*(1.0-ABSQB))
      IF (DENST.GT.0.0) GO TO 202
      DENST=(VT-PINT)/SL
      DENSB=(VB-PINT)/SL
202   CONTINUE
      RHOT(N)=DENST
      RHOB(N)=DENSB
      THK(N)=THICK
      RBOT=RTOP-THICK
      RTP(N)=RTOP
      RBT(N)=RBOT
      BS(N)=(ALOG(SV(N))-ALOG(SU(N)))/(ALOG(RTOP)-ALOG(RBOT))
      BP(N)=(ALOG(VB)-ALOG(VT))/(ALOG(RTOP)-ALOG(RBOT))
      BTTP(N)=RTOP/VT
      BTTS(N)=RTOP/SU(N)
      BBBP(N)=RBOT/VB
      BBBS(N)=RBOT/SV(N)
      RETURN
      END
      SUBROUTINE VELBOT (MB,NL,N,U,V,RADUS,RTP,B,P,IREL,SLOWN,VBOT,VBAR,
     1RBT,DBOT)
C     SUBROUTINE VELBOT WRITTEN BY R MEREU
C     THIS SUBROUTINE IS TO BE USED WITH PROGRAM XTAMP
C     THIS PROGRAM CALCULATES SLOWNESS APPARENT VELOCITY DEPTH
C     WHERE RAY BOTTOMS, VELOCITY AT THE BOTTOM,ETC AND RETURNS ANSWERS
C     TO XTAMP
      DIMENSION NL(20),U(20),V(20),RTP(20),B(20),RBT(20)
      DTR=3.14159265/180.0
      N=NL(MB)
      IF (IREL.EQ.1) GO TO 1
      RT=RTP(N)
      D=B(MB)
      VT=U(MB)
      G=1.0/(1.0+D)
      DG=D*G
      VTG=VT**G
      PG=P**G
      RTDG=RT**DG
      PMDG=P**(-DG)
      RBOT=PG*VTG*RTDG
      VBOT=VTG*RTDG*PMDG
      GO TO 2
1     VBOT=V(MB)
      RBOT=RBT(N)
2     SLOWN =P*DTR
      VBAR=RADUS/P
      DBOT=RADUS-RBOT
      RETURN
      END
      SUBROUTINE DELTA(P,PS,RT,RB,VT,VB,BB,RADUS,AI,DELT,BOD,AJ)
C     THIS PROGRAM CALCULATES DISTANCES FOR ANY RAY SEGMENT
C     FEED IN P,PS, RT,RB,VT,VB,BB,RADUS,
C     OMPUTES DELT AT AJ BOD
```

```
C       P= RAY PARAMETER
C       PS=P*P
C       RB=RADIUS AT BOTTOM OF LAYER
C       RT=RADIUS AT TOP OF LAYER
C       VB=VELOCITY AT BOTTOM OF LAYER
C       BB=VELOCITY INDEX
C       DELT=ANGULAR DISTANCE
C       AI= ANGLE RAY MAKES WITH RADIUS VECTOR AT TOP OF LAYE
C       AJ= ANGLE RAY MAKES WITH RADIUS VECTOR AT BOT OF LAYE
C       BOD =1  IF RAY BOTTOMS
C       BOD=0  IF IT DOES NOT
        DTR=3.14159265/180.0
        SAI=P*VT/RT
        SAJ=P*VB/RB
        IF (1.0-SAI)1,1,2
1       SAI=1.0
        SAJ=1.0
        AI=ARSIN(SAI)
        AJ=ARSIN(SAJ)
        SA=0.0
        GO TO 6
2       AI=ARSIN(SAI)
        IF (1.0-SAJ) 4,4,5
4       SAJ=1.0
        BOD=1.0
        AJ=ARSIN(SAJ)
        GO TO 3
5       AJ=ARSIN(SAJ)
        BOD=0.0
3       SA=(AJ-AI)/(1.0+BB)
6       CONTINUE
        DELT=SA
        RETURN
        END
        SUBROUTINE TIME (P,PS,RT,RB,VT,VB,BB,TM,BOT,RDPDL,DADP)
C       THIS PROGRAM CALCULATES THE TRAVEL TIME FOR ANY RAY SEGMENT
C       FEED IN P,PS,RB,RT,VT,VB,BB
C       CALCULATES TM,BOT,DADP,RDPDL
C       P=RAY PARAMETER
C       PS=P*P
C       RB=RADIUS AT BOTTOM OF LAYER
C       RT=RADIUS AT TOP OF LAYER
C       VB=VELOCITY AT BOTTOM OF LAYER
C       BB=VELOCITY INDEX
C       TM=TRAVEL TIME
C       BOT=1  IF RAY BOTTOMS
C       BOT=0  IF IT DOES NOT
C       DADP=RATE OF CHANGE OF ANGULAR DISTANCE WITH RAY PAR
C       RDPDL=RATE OF CHANGE OF DPDA WITH P
        QS=PS+10.0**(-7)
        QAI=RT*RT/(VT*VT)
        QAJ=RB*RB/(VB*VB)
        IF(QAI-QS) 1,1,2
1       TM=0.0
        GO TO 6
2       SQAI=SQRT(QAI-PS)
```

```
      IF (QAJ-QS) 4,4,5
4     SQAJ=0.0
      BOT=1.0
      GO TO 3
5     SQAJ=SQRT(QAJ-PS)
      BOT=0.0
      TM=(SQAI-SQAJ)/(1.0+BB)
      DADP=(1.0/SQAJ-1.0/SQAI)/(1.0+BB)
      RDPDL=P*(1.0/(SQAJ**3.0)-1.0/(SQAI**3.0))/(1.0+BB)
      GO TO 6
3     TM = (SQAI-SQAJ)/(1.0+BB)
      DADP=(-1.0/SQAI)/(1.0+BB)
      RDPDL=P*(-1.0/(SQAI**3.0))/(1.0+BB)
6     CONTINUE
      RETURN
      END
      SUBROUTINE ZCEP(V1,U1,RHO1,V2,U2,RHO2,AA,PW,SW,PR,PT,SR,ST,PHSPR,
     1PHSPT,PHSSR,PHSST,AMPV,AMPH,PHSAV,PHSAH,PAR,PAT,SAR,SAT,APEM,ID)
      DIMENSION F(4,4),A(4,4),B(4,4),ANB(4,4),BAB(4,4),EB(4,4),
     1 E(4,4),F(4,4),C(4),D(4),EC(4),FC(4),ED(4),FD(4),X(4),Y(4),AN(4,4)
      DTR=3.1415926S/180.0
      AAR=AA*DTR
      SNN=SIN(AAR)
      P=ABS(PW)*SNN/V1+ABS(SW)*SNN/U1
      PS=P*P
      SINA=P*V1
      SINB=P*U1
      SINE=P*V2
      SINF=P*U2
      DNRT=RHO2/RHO1
      Q1=1.0-SINA*SINA
      Q2=1.0-SINE*SINE
      S1=1.0-SINB*SINB
      S2=1.0-SINF*SINF
      COSB=SQRT(S1)
      SIN2B=2.0*SINB*COSB
      COS2B=2.0*S1-1.0
      IF(Q1) 2,1,1
2     COSA=SQRT(-Q1)
      G1=0.0
      GG1=1.0
      GO TO 3
1     COSA=SQRT(Q1)
      G1=1.0
      GG1=0.0
3     CONTINUE
      COS2A=2.0*COSA*COSA-1.0
      SIN2A=2.0*COSA*SINA
      IF(Q2) 12,11,11
12    COSE=-SQRT(-Q2)
      G2=0.0
      GG2=1.0
      GO TO 13
11    COSE=SQRT(Q2)
      G2=1.0
      GG2=0.0
```

```
 12   CONTINUE
      COS2F=2.0*COSF*COSF-1.0
      SIN2F=2.0*COSF*SINF
      IF(S2) 22,21,21
 22   COSF=-SQRT(-S2)
      H2=0.0
      HH2=1.0
      GO TO 23
 21   COSF=SQRT(S2)
      H2=1.0
      HH2=0.0
 23   CONTINUE
      COS2F=2.0*COSF*COSF-1.0
      SIN2F=2.0*COSF*SINF
      IF(PW) 8,10,7
  8   CONTINUE
      AF=-SIN2A
      BF=V1*COS2B/U1
      EF=SIN2A
      CF=COS2B
      DF=U1*SIN2B/V1
      FF=COS2B
      FU1=SINA
      FU2=-SINA
      FU3=COSB
      FW1=COSA
      FW2=COSA
      FW3=SINB
      GO TO 105
 10   IF(SW) 15,41,6
 15   CONTINUE
      AF=-U1*SIN2A/V1
      BF=COS2B
      EF=-BF
      CF=COS2B*V1/U1
      DF=SIN2B
      FF=SIN2B
      FU1=-COSB
      FU2=-SINA
      FU3=COSB
      FW1=SINB
      FW2=COSA
      FW3=SINB
      GO TO 105
105   CONTINUE
      DN=G1*(AF*DF-BF*CF)+GG1*(EF*BF*CF*CF+AF*AF*DF*DF)
      DAI=GG1*(AF*DF*EF*CF-AF*BF*CF*FF)/DN
      DA=G1*(AF*DF-EF*CF)/DN+GG1*(EF*BF*CF*CF+AF*AF*FF*DF)/DN
      CA=G1*(EF*DF-FF*BF)/DN+GG1*(FF*BF*BF*CF-EF*DF*BF*CF)/DN
      CAI=GG1*(AF*DF*(FF*EF-EF*CF))/DN
      EA=0.0000001
      FA=0.0000001
      EAI=0.0
      FAI=0.0
      AMPHR=FU1+FU2*CA+FU3*DA
      AMPHI=FU2*CAI+FU3*DAI
```

```
      AMPVR=FW1+FW2*CA*G1-FW2*CAI*GG1+FW3*DA
      AMPVI=GG1*FW2*CA+FW3*DAI
      AMPV=SQRT(AMPVR*AMPVR+AMPVI*AMPVI)
      AMPH=SQRT(AMPHR*AMPHR+AMPHI*AMPHI)
      AMPVR=AMPVR+0.00001
      AMPHR=AMPHR+0.00001
      PHSAV=ATAN2(AMPVI,AMPVR)
      PHSAH=ATAN2(AMPHI,AMPHR)
      APEM=ATAN2(AMPV,AMPH)
      APEM=APEM/DTR
      PHSAV=PHSAV/DTR
      PHSAH=PHSAH/DTR
      GO TO 102
    7 CONTINUE
      A(1,1)=-SINA
      B(1,1)=0.0
      A(1,2)=COSB
      B(1,2)=0.0
      A(1,3)=-SINE
      B(1,3)=0.0
      A(1,4)=COSF*F2
      B(1,4)=COSF*HH2
      A(2,1)=COSA
      B(2,1)=0.0
      A(2,2)=SINB
      B(2,2)=0.0
      A(2,3)=-COSE*G2
      B(2,3)=-COSE*GG2
      A(2,4)=-SINF
      B(2,4)=0.0
      A(3,1)=-2.0*SINA*COSA
      B(3,1)=0.0
      A(3,2)=V1*COS2B/U1
      B(3,2)=0.0
      A(3,3)=G2*DNRT*U2*U2*V1*SIN2E/(U1*U1*V2)
      B(3,3)=GG2*DNRT*U2*U2*V1*SIN2E/(U1*U1*V2)
      A(3,4)=-DNRT*U2*U2*V1*COS2F/(U1*U1*U2)
      B(3,4)=0.0
      A(4,1)=COS2B
      B(4,1)=0.0
      A(4,2)=U1*SIN2B/V1
      B(4,2)=0.0
      A(4,3)=DNRT*V2*COS2F/V1
      B(4,3)=0.0
      A(4,4)=H2*DNRT*U2*SIN2F/V1
      B(4,4)=HH2*DNRT*U2*SIN2F/V1
      C(1)=-SINA
      C(2)=G1*(-COSA)
      C(3)=G1*SIN2A
      C(4)=COS2B
      D(1)=0.0
      D(2)=GG1*(-COSA)
      D(3)=GG1*SIN2A
      D(4)=0.0
      GO TO 9
    6 CONTINUE
```

```
      A(1,1)=G1*COSA
      B(1,1)=GG1*COSA
      A(1,2)=SINB
      B(1,2)=0.0
      A(1,3)=-COSC*G2
      B(1,3)=-COSC*GG2
      A(1,4)=-SINF
      B(1,4)=0.0
      A(2,1)=SINA
      B(2,1)=0.0
      A(2,2)=-COSB
      B(2,2)=0.0
      A(2,3)=SINF
      B(2,3)=0.0
      A(2,4)=-COSF*H2
      B(2,4)=-COSF*HH2
      A(3,1)=-G1*U1*SIN2A/V1
      B(3,1)=-GG1*U1*SIN2A/V1
      A(3,2)=COS2B
      B(3,2)=0.0
      A(3,3)=G2*DNRT*U2*U2*SIN2E/(U1*V2)
      B(3,3)=GG2*DNRT*U2*U2*SIN2E/(U1*V2)
      A(3,4)=(-DNRT*U2*COS2F/U1)
      B(3,4)=0.0
      A(4,1)=V1*COS2B/U1
      B(4,1)=0.0
      A(4,2)=SIN2B
      B(4,2)=0.0
      A(4,3)=DNRT*V2*COS2F/U1
      B(4,3)=0.0
      A(4,4)=H2*DNRT*U2*SIN2F/U1
      B(4,4)=HH2*DNRT*U2*SIN2F/U1
      C(1)=-SINB
      C(2)=-COSB
      C(3)=-COS2B
      C(4)=SIN2B
      D(1)=0.0
      D(2)=0.0
      D(3)=0.0
      D(4)=0.0
    9 CONTINUE
      DO 60 I=1,4
      EC(I)=0.0
      FC(I)=0.0
      ED(I)=0.0
      FD(I)=0.0
      DO 61 J=1,4
      AN(I,J)=A(I,J)
      ANB(I,J)=0.0
      BAB(I,J)=0.0
      F(I,J)=0.0
   61 CONTINUE
   60 CONTINUE
      N=4
      NC=4
      EPS=10.0**(-8.0)
```

```
      DO 1000 J=1,N
      DO 1001 I=1,NC
 1001 R(I,J)=0.0
 1000 CONTINUE
      DO 1002 I=1,N
 1002 R(I,I)=1.0
      CALL GELG (R,AN,N,NC,EPS,IND)
      DO 1003 J=1,N
      DO 1004 I=1,NC
      AN(I,J)=R(I,J)
 1004 R(I,J)=0.0
 1003 CONTINUE
      DO 1007 I=1,N
 1007 R(I,I)=1.0
      INDA=IND
       DO 64 I=1,4
      DO 65 J=1,4
      DO 66 K=1,4
      ANB(I,J)=ANB(I,J)+AN(I,K)*B(K,J)
   66 CONTINUE
   65 CONTINUE
   64 CONTINUE
      DO 74 I=1,4
      DO 75 J=1,4
      DO 76 K=1,4
      BAB(I,J)=BAB(I,J)+B(I,K)*ANB(K,J)
   76 CONTINUE
      E(I,J)=A(I,J)+BAB(I,J)
      EB(I,J)=E(I,J)
   75 CONTINUE
   74 CONTINUE
      CALL GELG(R,E,N,NC,EPS,IND)
      DO 1005 J=1,N
      DO 1006 I=1,NC
 1006 E(I,J)=R(I,J)
 1005 CONTINUE
      INDB=IND
      INDP=INDA+INDB
      IF(INDP) 77,78,77
   77 CONTINUE
      WRITE(6,71) INDA,INDB
   71 FORMAT(1H ,4HIND=,2I4,37HMATRIX DID NOT INVERT    NOTE NOTE      )
   78 CONTINUE
      DO 72 I=1,4
      DO 73 J=1,4
      DO 70 K=1,4
      F(I,J) =F(I,J)-ANB(I,K)*E(K,J)
   70 CONTINUE
   73 CONTINUE
   72 CONTINUE
      IF(ID.NE.2) GO TO 602
   86 CONTINUE
      WRITE(6,85)
   85 FORMAT(1H ,15HMATRIX ELEMENTS)
      DO 80 I=1,4
      DO 81 J=1,4
```

```
      T1=A(I,J)
      T2=AN(I,J)
      T3=B(I,J)
      T4=AN3(I,J)
      T5=BAB(I,J)
      T6=FB(I,J)
      T7=E(I,J)
      T8=F(I,J)
  601 CONTINUE
      WRITE(6,82)I,J,T1,T2,T3,T4,T5,T6,T7,T8
   82 FORMAT(1H ,2I3,2X,8E10.3)
   81 CONTINUE
   80 CONTINUE
  602 CONTINUE
      DO 50 I=1,4
      DO 52 J=1,4
      EC(I)=EC(I)+E(I,J)*C(J)
      FD(I)=FD(I)+F(I,J)*D(J)
      FC(I)=FC(I)+F(I,J)*C(J)
      ED(I)=ED(I)+E(I,J)*D(J)
   52 CONTINUE
      X(I)=EC(I)-FC(I)
      Y(I)=FC(I)+ED(I)
   50 CONTINUE
      CA=X(1)
      CAI=Y(1)
      DA=X(2)
      DAI=Y(2)
      EA=X(3)
      EAI=Y(3)
       FA=X(4)
      FAI=Y(4)
  102 CONTINUE
      CAI=-CAI
      CA=-CA
      PAR=SQRT(CA*CA+CAI*CAI)
      CA=CA+0.00001
       PHSPR=ATAN2(CAI,CA)
      PHSPR=PHSPR/DTR
      PAT=SQRT(EA*EA+EAI*EAI)
      EA=EA+0.00001
      PHSPT=ATAN2(EAI,EA)
      PHSPT=PHSPT/DTR
      SAR=SQRT(DA*DA+DAI*DAI)
      DA=DA+0.00001
      PHSSR=ATAN2(DAI,DA)
      PHSSR=PHSSR/DTR
      SAT=SQRT(FA*FA+FAI*FAI)
      FA=FA+0.00001
      PHSST=ATAN2(FAI,FA)
      PHSST=PHSST/DTR
      IF(PW) 31,30,31
   30 AA=ARSIN(SINB)/DTR
      GO TO 32
   31 AA=ARSIN(SINA)/DTR
   32 CONTINUE
```

```
      SIN2AG=ABS(SW)*SIN2B+ABS(PW)*SIN2A
      PR=G1*SIN2A*PAR*PAR/SIN2AG
      PT=G2*RHO2*SIN2B*PAT*PAT/(PHO1*SIN2AG)
      SR=SIN2B*SAR*SAR/SIN2AG
      ST=H2*RHO2*SIN2B*SAT*SAT/(PHO1*SIN2AG)
      TOTEN=PR+PT+SR+ST
      IF(ID.EQ.0) GO TO 41
   40 CONTINUE
   51 FORMAT(1H ,F7.1,4X,3F7.3,4X,3F7.3,4X,3F7.3,4X,3F7.3,5X,F7.3)
      WRITE(6,51) AA,PR,PAR,PHSER,PT,PAT,PHSPT,SR,SAR,PHSSR,ST,SAT,PHSST
     1,TOTEN
   41 CONTINUE
      RETURN
      END
      SUBROUTINE GELG(R,A,M,N,EPS,IER)
      DIMENSION A(16),R(16)
      IF(M)23,23,1
C     SEARCH FOR GREATEST ELEMENT IN MATRIX A
    1 IER=0
      PIV=0.
      MM=M*M
      NM=N*M
      DO 3 L=1,MM
      TB=ABS(A(L))
      IF(TB-PIV)3,3,2
    2 PIV=TB
      I=L
    3 CONTINUE
      TOL=EPS*PIV
C     A(I) IS PIVOT ELEMENT. PIV CONTAINS THE ABSOLUTE VALUE OF A(I).
C
C
C     START ELIMINATION LOOP
      LST=1
      DO 17 K=1,M
C
C     TEST ON SINGULARITY
      IF (PIV)23,23,4
    4 IF(IER)7,5,7
    5 IF(PIV-TOL)6,6,7
    6 IER=K-1
    7 PIVI=1./A(I)
      J=(I-1)/M
      I=I-J*M-K
      J=J+1-K
C     I+K IS ROW-INDEX, J+K COLUMN-INDEX OF PIVOT ELEMENT
C
C     PIVOT ROW REDUCTION AND ROW INTERCHANGE IN RIGHT HAND SIDE R
      DO 8 L=K,NM,M
      LL=L+I
      TB=PIVI*R(LL)
      R(LL)=R(L)
    8 R(L)=TB
C
C     IS ELIMINATION TERMINATED
      IF(K-M)9,18,18
```

```
C
C       COLUMN INTERCHANGE IN MATRIX A
9       LEND=LST+M-K
        IF(J)12,12,10
10      II=J*M
        DO 11 L=LST,LEND
        TB=A(L)
        LL=L+II
        A(L)=A(LL)
11      A(LL)=TB
C
C       ROW INTERCHANGE AND PIVOT ROW REDUCTION IN MATRIX A
12      DO 13 L=LST,MM,M
        LL=L+I
        TB=PIVI*A(LL)
        A(LL)=A(L)
13      A(L)=TB
C
C       SAVE COLUMN INTERCHANGE INFORMATION
        A(LST)=J
C
C       ELEMENT REDUCTION AND NEXT PIVOT SEARCH
        PIV=0.
        LST=LST+1
        J=0
        DO 16 II=LST,LEND
        PIVI=-A(II)
        IST=II+M
        J=J+1
        DO 15 L=IST,MM,M
        LL=L-J
        A(L)=A(L)+PIVI*A(LL)
        TB=ABS(A(L))
        IF(TB-PIV)15,15,14
14      PIV=TB
        I=L
15      CONTINUE
        DO 16 L=K,NM,M
        LL=L+J
16      R(LL)=R(LL)+PIVI*R(L)
17      LST=LST+M
C       END OF ELIMINATION LOOP
C
C
C       BACK SUBSTITUTION AND BACK INTERCHANGE
18      IF(M-1)23,22,19
19      IST=MM+M
        LST=M+1
        DO 21 I=2,M
        II=LST-I
        IST=IST-LST
        L=IST-M
        L=A(L)+.5
        DO 21 J=II,NM,M
        TB=R(J)
        LL=J
```

```
      DO 20 K=IST,MM,M
      LL=LL+1
20    TB=TB-A(K)*R(LL)
      K=J+L
      R(J)=F(K)
21    R(K)=TB
22    RETURN
C
C
C     ERROR RETURN
23    IER=-1
      RETURN
      END
$ENTRY
    1                                        1
      1.00      200.0     800.00      20.00      7.900    6365.83     1

MDL -B
   16.05    6.05    18.90                                          6365.83
   26.85    6.85    15.20                                          6347.03
   37.90    7.90    16.0                                           6331.83
   48.40    8.40    200.0                                          6315.83

  P7                  4     8          1 11110222          12344321
31.82 34.29 36.65 38.97 41.33 43.75 46.09 48.45 50.82 53.18 55.54 57.91 60.27 6
60.27 62.63 64.98 67.36 69.73 72.08 74.44 76.81 79.16 81.54 83.89 86.25 88.61 9
88.61 90.98 93.34 95.68 98.06 100.42102.78
   37.90    7.90    18.25                                          6331.83
   48.40    8.40    200.0                                          6313.58

   37.90    7.90    18.35                                          6331.83
   48.40    8.40    200.0                                          6313.48

   37.90    7.90    18.45                                          6331.83
   48.40    8.40    200.0                                          6313.38

   37.90    7.90    18.55                                          6331.83
   48.40    8.40    200.0                                          6313.28

   37.90    7.90    18.65                                          6331.83
   48.40    8.40    200.0                                          6313.18

   37.90    7.90    18.75                                          6331.83
   48.40    8.40    200.0                                          6313.08

$IBSYS
$STOP
```

BIBLIOGRAPHY

Barr, K.G., 1969. Evidence for variations in upper mantle velocity in the Hudson Bay area. Can. Geol. Survey Paper 68-53, p. 365.

Bates, A.C., 1971. Upper mantle structure deduced from seismic records acquired during Project Edzoe in southern Saskatchewan and western Manitoba between distances of about 790 km. and 1285 km., unpublished M.Sc. thesis, Dept. of Earth Sciences, University of Manitoba.

Berry, M.J., 1971. Depth uncertainties from seismic first arrival refraction studies. J. Geophys. Res., vol. 76, p. 6464.

Berry, M.J., 1973. Structure of the crust and upper mantle in Canada. Tectonophysics, vol. 20, nos. 1-4, p. 183-201.

Berry, M.J. and G.F. West, 1966. A time-term interpretation of the first-arrival data of the 1963 Lake Superior Experiment. A.G.U. Geophys. Mon. Ser., pp. 166-180.

Borcherdt, R.D. and J.H. Healy, 1968. A method for estimating the uncertainty of seismic velocities measured by refraction techniques. B.S.S.A., vol. 58, No. 6, p. 1769.

Buldyrev, V.S. and A.I. Lanin, 1965. Interfering waves at surface of an ilastic inhomogereous sphere. Reviews of Geophys. and Space Phys. vol. 3, p. 49.

Buldyrev, V.S. and A.I. Lanin, 1966. On the investigation of the interference wave field at the surface of an elastic sphere. Numerical Methods for the Solution of Problems of Mathematical Physics, (Nauka, Moscow), pp. 131-143.

Bullen, K.E., 1961. Seismic ray theory. Geophys. J. Royal Astron. Soc., vol. 4, p. 93.

Bullen, K.E., 1963. Introduction to the Theory of Seismology, 3rd edition. University Press, Cambridge.

Cagniard, L., 1962. Reflection and Refraction of Progressive Seismic Waves. McGraw-Hill, New York.

Cerveny, V., 1967. The amplitude-distance curves for waves reflected at a plane interface for different frequency ranges. Geophys. J., vol. 4, p. 187.

Cerveny, V. and R. Ravindra, 1971. Theory of Seismic Head Waves. University of Toronto Press.

Dix, C.H., 1955. Seismic velocities from surface measurements. Geophysics, vol. 20, No. 1, pp. 68-86.

Dix, C.H., 1965. Reflection seismic crustal studies. Geophysics, vol. 30, No. 6, pp. 1068-1082.

Dobrin, B.M., 1960. Introduction to Geophysical Prospecting. McGraw-Hill.

Dowling, J.J., 1970. Uncertainties in velocities determined by seismic refraction. J. Geophys. Res., vol. 75, p. 6690.

Gettrust, J.F. and R.P. Meyer, 1971. Crust and upper mantle structure in a region of tectonism (abstract). Trans. Am. Geophys. Union, vol. 52, p. 281.

Green, R.W.E. and A.L. Hales, 1968. The travel times of P waves to 30° in the central United States and upper mantle structure. B.S.S.A., vol. 58, p. 267.

Gurbuz, B., 1969. Structure of the earth's crust and upper mantle under a portion of Canadian Shield deduced from travel-times and spectral amplitudes of body waves using data from Project Early Rise. Ph.D. Thesis, Dept. of Earth sciences, University of Manitoba.

Gurbuz, B., 1970. A study of the Earth's crust and upper mantle using travel times and spectrum characteristics of body waves. B.S.S.A, vol. 60, No. 6, p. 1921.

Gutenberg, B., 1944. Energy ratio of reflected and refracted seismic waves. B.S.S.A., vol. 34, p. 85.

Hajnal, Z., 1969. A two-layer model for the earth's crust under Hudson Bay. Geol. Surv. Can., Paper 68-53, p. 326.

Hajnal, Z., 1970. A continuous deep crustal seismic refraction and near-vertical reflection profile in the Canadian Shield interpreted by digital pro-

cessing techniques. Ph.D. Thesis, Dept. of Earth Sciences, University of Manitoba.

Hajnal, Z., 1971. Detailed seismic study of the earth's crust. Manit. Dept. Mines Nat. Resour., Mines Br. Publ. No. 71-1, pp. 417-425.

Hales, A.L., 1969. A seismic discontinuity in the lithosphere. Earth Plan. Sci. Lettr., vol. 7, p. 44.

Hales, A.L., 1972. The travel-times of P seismic waves and their relevance to the upper mantle velocity distribution. Tectonophysics, vol. 13, Nos. 1-4, pp. 447-482.

Hall, D.H. and W.C. Brisbin, 1961. Deep crustal seismic studies in vicinity of the Churchill Superior block boundary in Manitoba. Can. Mining and Metallurgical Bull., vol. 55, No. 599, PP. 199-200.

Hall, D.H. and W.C Brisbin, 1965. Crustal structure from converted head waves in central Western Manitoba. Geophysics, vol. 30,p. 1053.

Hall, D.H. and Z. Hajnal, 1969. Crustal structure of northwestern Ontario: Refraction Seismology. Can. J. Earth Sci., vol. 6, p. 81.

Hall, D.H. and Z. Hajnal, 1973. Deep crustal seismic studies in Manitoba. B.S.S.A., vol. 63, No. 3, p. 885.

Hunter, J.A. and R.F. Mereu, 1967. The crust of the Earth under Hudson Bay. Can. J. Earth Sci., vol. 4, No. 5, pp. 949-960.

Iyer, H.M., Pakiser, L.C., Stewart, D.J. and D.H. Warren, 1969. Project Early Rise: seismic probing in the upper mantle. J. Geophys. Res., vol. 74, p. 4409.

Julian, B.R. and D.L. Anderson, 1968. Travel times, apparent velocities and amplitudes of body waves. B.S.S.A., vol. 58, No. 1, p. 339.

Knott, C.G., 1899. Reflection and refraction of seismic waves with seismological applications. Phil. Mag., vol. 48, p. 64.

Lanin, A.I., 1966. Investigation of interference wave fields of diffraction by a transparent cylinder and an elastic sphere. Ph.D. Thesis, Leningrad University.

Lanin, A.I., 1968. Calculation of interference waves in problems of diffraction by a cylinder and a sphere. Mathematical Problems in the Theory of Propagation of Waves, ed. V.M. Babich, (Nauka, Leningrad Division, Leningrad), pp. 64-104.

Lewis, B.T. and R.P. Meyer, 1968. A seismic investigation of the upper mantle to the west of Lake Superior. B.S.S.A., vol. 58, No. 2, pp. 565-596.

Mereu, R.F., 1965. A study of apparent angles of emergence at Marathon, Ontario from the Lake Superior data. B.S.S.A., vol. 55, No. 2, pp. 405-416.

Mereu, R.F., 1968. Curvature corrections to upper mantle seismic refraction surveys. Earth Plan. Sci. Lett. vol.3, p. 469.

Mereu, R.F. and J.A. Hunter, 1968. Crustal and upper mantle structure under the Canadian Shield from Project Early Rise. B.S.S.A., vol. 59, No. 1, pp. 147-165.

Muskat, M., 1933. The theory of refraction shooting. Physics, vol. 4, pp. 14-38.

O'Brien, P.O., 1968. Problems of procedure in explosion seismology. Internat. Confer. on Explosion Seismology, 1st, Leningrad, 1968, trans: Kiev, Izdatel'stvo Nankova Dumka, pp. 228-229.

Pakiser, L.C. and J.S. Steinhart, 1964. Explosion seismology in the western hemisphere. Research in Geophysics, vol. 2, M.I.T. Press, p. 123.

Peacock, K.L. and S. Treitel, 1969. Predictive deconvolution; theory and practice. Geophysics, vol. 34, No. 2, p. 155.

Petrashen, G.I., 1964. On the modelling of the processes of seismic wave propagation. Voprosy dinam. raspro. seysmich. O.M.I.S., No. 7, p. 7-35.

Robinson, E.A. and S. Treitel, 1967. Principles of digital Weiner filtering. Geophys. Prosp., vol. 15, No. 3, p. 311.

Ruffman, A., 1969. Seismic investigation of the crust in the Hudson Bay region. Can. Geol. Survey Paper 68-53, pp. 307-314.

Scheid, F., 1968. Theory and Problems of Numerical Analysis. McGraw-Hill.

Stanton, R.G., 1961. Numerical Methods for Science and Engineering. Prentice-Hall.

Stewart, S.W., 1968. Crustal structure in Missouri by seismic refraction methods. B.S.S.A., vol. 58, p. 291.

Williams, P.W., 1972. Numerical Computations. Thomas, Nelson and Sons.

Zoppritz, K., 1919. Uber erdbebenwellen. VIIb, Gottingen Nachrichten, p. 66.